**SCHRIFTENREIHE**

**Institut für Pflanzenernährung und Bodenkunde**
**Universität Kiel**


**Nr. 91 (2011)**

**Christoph-Martin Geilfus**

# Expansin expression and apoplastic pH in expanding leaves under NaCl stress

**Herausgeber: R. Horn und K. H. Mühling**

**Gedruckt mit Genehmigung der Agrar- und Ernährungswissentschaftlichen Fakultät der Christian-Albrechts-Universität zu Kiel**
**Vertrieb: Institut für Pflanzenernährung und Bodenkunde**
**der Christian-Albrechts-Universität zu Kiel**
**Hermann Rodewald Str. 2**
**D - 24118 Kiel**
**(e-Mail: h.fleige@soils.uni-kiel.de)**

**ISSN 0933-680 X**
**Preis: Eur 15 (incl. Versandkosten)**

Aus dem Institut für Pflanzenernährung und Bodenkunde

der Christian-Albrechts-Universität zu Kiel

# Expansin expression and apoplastic pH in expanding leaves under NaCl stress

Dissertation

zur Erlangung des Doktorgrades

der Agrar- und Ernährungswissenschaftlichen Fakultät

der Christian-Albrechts-Universität zu Kiel

vorgelegt von

Christoph-Martin Geilfus, M. Sc.

aus Gießen

Kiel, 2011

---

Dekanin: Prof. Dr. Karin Schwarz

1. Berichterstatter: Prof. Dr. Karl H. Mühling

2. Berichterstatter: Prof. Dr. Christian Jung

3. Berichtserstatter: Prof. Dr. Urs Schmidhalter

Tag der mündlichen Prüfung:14. Juli 2011

Gedruckt mit der Genehmigung
der Agrar- und Ernährungswissenschaftlichen Fakultät
der Christian-Albrechts-Universität zu Kiel

*„Galilei:* Also werden wir an die Beobachtung der Sonne herangehen mit dem unerbittlichen Entschluß, den Stillstand der Erde nachzuweisen! Und erst wenn wir gescheitert sind, vollständig und hoffnungslos geschlagen und unsere Wunden leckend, in traurigster Verfassung, werden wir zu fragen anfangen, ob wir nicht doch recht gehabt haben und die Erde sich dreht! *Mit einem Zwinkern*: Sollte uns aber dann jede andere Annahme als diese unter den Händen zerronnen sein, dann keine Gnade mehr mit denen, die nicht geforscht haben und doch reden. Nehmt das Tuch vom Rohr und richtet es auf die Sonne!"

Bertolt Brecht, Leben des Galilei, 1938/39

# Contents

# Chapter 1

# General introduction

# 1. General introduction

Agricultural productivity is severely affected by soil salinity, with salt levels that are harmful to plant growth affecting large terrestrial areas of the world. This makes salinity a common agricultural problem throughout the world and, indeed, one that has influenced ancient and modern civilizations (Cramer, 1992; Yamaguchi and Blumwald, 2005). As summarized by Munns et al. (2002), about 7% of the world's total land area is affected by salt, as is a similar percentage of its arable land (Szabolcs, 1994).

The loss of farmable land to salinization is directly in conflict with the needs of the world population for food, because most of the suitable land has been cultivated, and any expansion into new areas to increase food production is rarely possible (Rangasamy, 2006). Moreover, global food production will need to increase by 38% by 2025 and by 57% by 2050 if food supply to the growing world population is to be maintained at current levels. Therefore, increasing the yield of crop plants in salinized lands is an absolute requirement for feeding the world population that is projected to increase by 1.5 billion over the next 20 years (Wild, 2003; Yamaguchi and Blumwald, 2005; Rangasamy, 2006).

## 1.1 Causes of soil salinity

Rahnama et al. (2011) defines salinization as the accumulation of water-soluble salts in the soil to a level that impacts on agricultural production, environmental health and economic welfare. A soil is considered saline if the electrical conductivity of its saturation extract (ECe) is above 4 dS $m^{-1}$ (Richards, 1954). Most of this salt-affected land has arisen from the accumulation of salts over long periods of time in arid and semi-arid zones (Rengasamy, 2002; Munns and Tester, 2008). Weathering is one dominant source of salts, because soils are derived from the chemical and physical weathering of rocks and other geological and organic materials that release salts such as chloride and sodium (Rengasamy, 2006; 2010). Other

cause of accumulation is the deposition of oceanic salts carried by wind and rain (Munns and Tester, 2008). Rainwater contains low amounts of salt but, over time, salt deposited by rain can accumulate in the landscape (Rengasamy, 2006). Wind-transported materials from the soil or lake surfaces further contribute to soil salinization. Seawater intrusion onto coastal lowlands, as in tsunami-affected regions or as occurs because of the rising water levels in many parts of the warming world, and capillary elevation of shallow saline groundwater can all deposit huge amounts of salts in the soil (Rozema and Flowers, 2008; Rengasamy, 2010). In addition to natural salinity, Munns and Tester (2008) report that cultivated agricultural land has become saline following land clearing or irrigation (secondary salinity), both of which cause water tables to rise and concentrate the salts within the root zone. For example, forest clearing allows salts present in the groundwater to reach the surface (Rengasamy, 2006; Flowers and Flowers, 2005). Irrigation has resulted in the accumulation of salt to above normal concentrations in the rooting zone of arable land, as high rates of evaporation and transpiration draw soluble salts from deep layers of the soil profile. Poor quality irrigation water exacerbates the problem of salt accumulation in irrigated soils (Rengasamy, 2006; Flowers and Flowers, 2008; Rozema and Flowers, 2008). As a result, 2% (32 million ha) of dry land-farmed areas and 20% (45 million ha) of irrigated land in the world are affected by secondary salinity (Munns and Tester, 2008).

## 1.2 Salinity inhibits leaf growth

The inhibition of leaf elongation growth is one of the primary effects of salt stress (Neves-Piestun and Bernstein, 2001). For this reason, salinity is directly related to yield constraints (Taleisnik et al., 2009). Munns (1993) has proposed the concept of the two-phase growth response in order to interpret the way that salt in the soil water inhibits plant growth.

In the first phase, viz. the osmotic stress phase, the rate of shoot growth falls significantly (Figure 1) immediately after the salt concentration around the roots increases to a threshold level of approximately 40 mM NaCl for most plants. This is largely attributable to the osmotic effect of the salt outside the roots, viz. a decrease in the soil water potential (Munns et al., 2006). This osmotic or water-deficit effect of salinity not only reduces the expansion of growing leaves, but also causes new leaves to emerge more slowly (Munns, 2002; Munns and Tester, 2008).

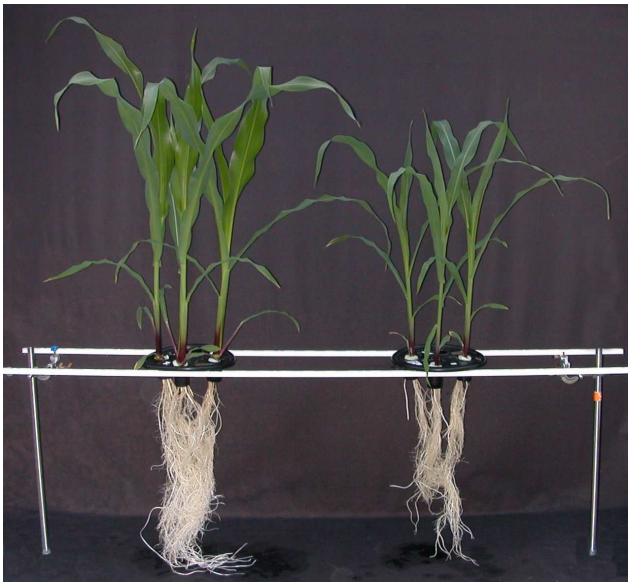

**Figure 1. The effect of the salt outside the roots, viz., the osmotic stress phase, on the plant growth.** Right plant: The presence of 100 mM NaCl at the roots over a period of 8 days decreases the growth of maize (*Zea mays* L). Left plant: Control-treated maize (no salt).

The physiological mechanisms underlying the leaf growth inhibition that occurs immediately in response to the salt outside the roots are not fully understood (Munns and Tester, 2008). Although the ability of the plant to take up water is reduced (Munns et al., 2006), the cell turgor is not the growth-limiting factor (De Costa et al., 2007). The treatment of maize (*Zea mays* L.) with 80 mM NaCl immediately reduces turgor and leaf elongation; however, 2.5 h after salinization, turgor has recovered but leaf elongation remains impaired (Cramer and Bowmann, 1991). Moreover, the salt that is taken up by the plant does not directly inhibit the growth of newly developed leaves in this first phase, because salt within the growing tissues does not reach concentrations that are known to inhibit growth (Munns et al., 2006). First

phase growth reduction is thought to be regulated by inhibitory hormonal signals coming from the roots in saline soil (Munns, 1993, 2005; Sauter et al., 2002; De Costa et al., 2007). Munns and Cramer (1996) suggest that the hormone abscisic acid might function as a chemical signal causing the reduction of leaf growth. However, this is not established as yet.

The second slower response phase results from the toxic effect of salt ions inside the plant (Schubert and Läuchli, 1986; Fortmeier and Schubert, 1995; Slabu et al., 2009). Munns (2005) has described that the continued salt uptake into transpiring leaves results in extremely high $Na^+$ and $Cl^-$ concentrations. As a result, vacuoles can no longer sequester incoming salts and, thus, salt concentrations in cell walls or cytoplasm rise and the leaves die. This is because salts probably accumulate in the cytoplasm and inhibit enzyme activity (Munns, 1993, 2005). Alternatively, they might build up in the cell walls and dehydrate the cell (Oertli, 1968). If leaves die at a rate greater than new leaves are produced, the photosynthetic capacity of the plant is no longer able to supply the carbohydrate requirement of the young leaves, which further reduces their growth rate (Munns, 1993, 2005; Munns and Tester 2008).

## 1.3 Significance of cell wall-loosening agents for growth processes

The salinity-induced reduction of leaf growth that occurs in the osmotic stress phase is probably induced by a decrease in the soil water potential outside the roots. This growth depletion might be controlled by hormonal signals (Munns et al., 2006). However, the growth-related processes that are altered by this putative signal are not precisely known.

Bernstein et al. (1993) have reported that salinity reduces the leaf growth rate by shortening the length of the leaf elongating zone and decreasing its growth intensity. This has led to the assumption that the leaf growth inhibition observed under salt stress might occur via an effect on this region (Lazof and Bernstein, 1998). A modified capacity of cell walls to expand irreversibly has been suggested to be the major growth-limiting factor causing growth

inhibition under salt stress (Cramer and Bowman, 1991). Cell-wall enlargement begins with wall stress relaxation, allowing the cells physically to enlarge. Following the acid growth theory, an auxin-mediated acidification of the leaf apoplast is the major requirement for an increase in wall extensibility (Hager et al., 1971). Auxin is assumed to activate the proton pump of the plasma membrane (PM-$H^+$-ATPases) to pump protons from the cytosol into the apoplast, resulting in wall-loosening and cell expansion (Figure 2) (Moriau et al., 1999). In accordance with this, increasing growth rates have been found to be associated with increasing acidification rates of the apoplast in the leaves of maize (*Zea mays* L.) (Van Volkenburgh and Boyer, 1985).

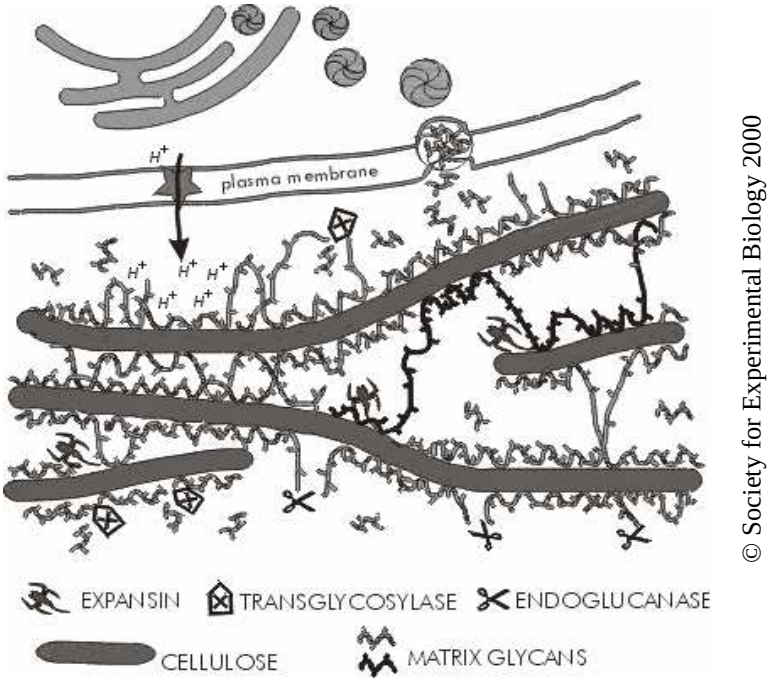




**Figure 2. Model of the cell wall and some of the activities that might alter cell wall extensibility.** Cellulose microfibrils are coated with matrix glycans such as xyloglucan and are embedded in a pectin/hemicellulose matrix. Expansins are thought to loosen the adhesion of the matrix to the microfibrils, allowing slippage of the microfibrils and extension of the cell wall in response to the tensile forces generated by cell turgor pressure. $H^+$-ATPases (star) in the plasma membrane can lower wall pH and thereby activate expansins. Transglycosylases, such as XET, can cut and ligate matrix glycans to one another, whereas endoglucanases can cut the xyloglucan backbone, making the wall more sensitive to expansin-induced wall extension. Cross-linking enzymes (not shown) could have the opposite effect. Figure according to Wu and Cosgrove (2000; as modified from Cosgrove, 1997). Figure legend according to Wu and Cosgrove (2000). © Society for Experimental Biology 2000.

The pH of the apoplast of growing cells is typically in a range in which acidification activates expansin activity (Cosgrove, 2005). Expansins are a group of non-enzymatic cell-wall proteins that are thought to mediate acid- induced growth. The precise way in which expansins mediate wall enlargement remains unclear. However, experimental evidence supports the idea that expansins intercalate within carbohydrate matrices in the cell wall, leading to a transient loosening of non-covalent interactions (Figure 3), and thus enhance the ability of these matrices to move relative to each other (Cosgrove, 2000; 2005). Strong correlations between the presence of expansins, wall extensibility and cell elongation have been demonstrated (Cho and Kende, 1997, Cosgrove, 2005). Interestingly, Pitann et al. (2009) have revealed that β-expansins are down-regulated in shoots of salt-affected maize plants in response to salinity.

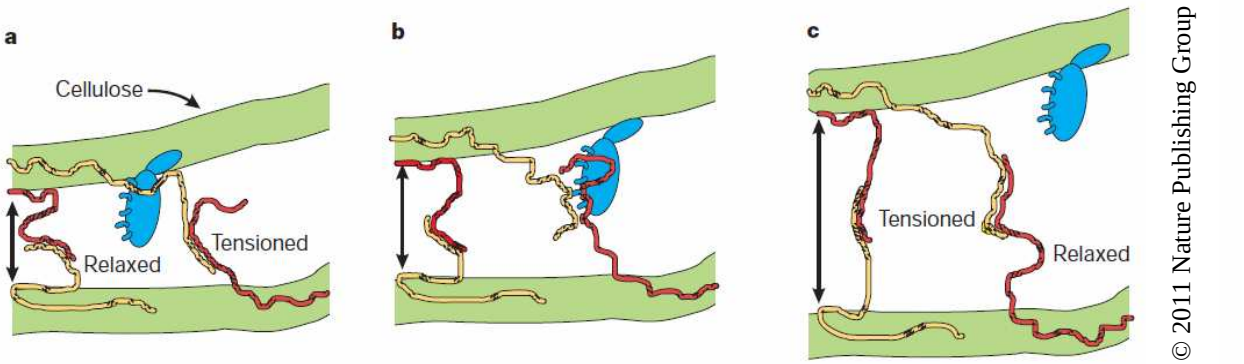


**Figure 3. A model of the wall-loosening action of expansin.** Cellulose microfibrils are connected to each other by glycans (thin yellow and red strands) that can stick to the microfibril surface and to each other. The expansin protein (blue) is hypothesized to disrupt the bonding of the glycans to the microfibril surface (a) or to each other (b). Under the mechanical stress arising from turgor, expansin action results in a displacement of the wall polymers (c) and slippage at the points of polymer adhesion (compare a and c). Figure and figure legend according to Cosgrove (2000). © 2011 Nature Publishing Group.

In addition to expansin, other candidate wall-loosening proteins are assumed to contribute to cell elongation. For example, an enzymatic modification of load-bearing xyloglucan tethers of the cell wall must occur, because this is a prerequisite in cell-wall loosening (Fry 1989). Xyloglucan-metabolizing enzymes therefore represent potentially important agents in the

control of wall extensibility. In this context, the involvement of endo-1,4-β-D-glucanases (EGases) and xyloglucan endotransglucosylase/hydrolase (XTH) has been suggested in xyloglucan metabolism during cell elongation (Fry 1989; Nishitani, 1995). EGases are thought to cause the release of xyloglucans that are trapped in cellulose microfibrils, whereby this cleavage of load-bearing xyloglucan results in increased wall extensibility relevant for cell growth (Cosgrove, 2005). In accordance, EGase enzyme activity is known to be involved in auxin-stimulated cell enlargement (Fan and Maclachlan, 1966).

The enzyme XTH is a wall-loosening factor (Vissenberg et al., 2005) that is weakly bound to the cell wall where it possibly alters the architecture of the cell wall by modifying polymer cross-links (Genovesi et al., 2008). XTH can function in a transglucosylase (XET) mode, whereby XET catalyzes the transfer of a load-bearing xyloglucan molecules fragment to another xyloglucan (Figure 4). This action is thought to allow incremental slippage of adjacent microfibrils by facilitating hydrostatic pressure of the protoplasm against this weakened wall. This results in the creep of cellulose microfibrils (Nishitani, 1995; Catalá et al., 1997; Vissenberg et al., 2005).

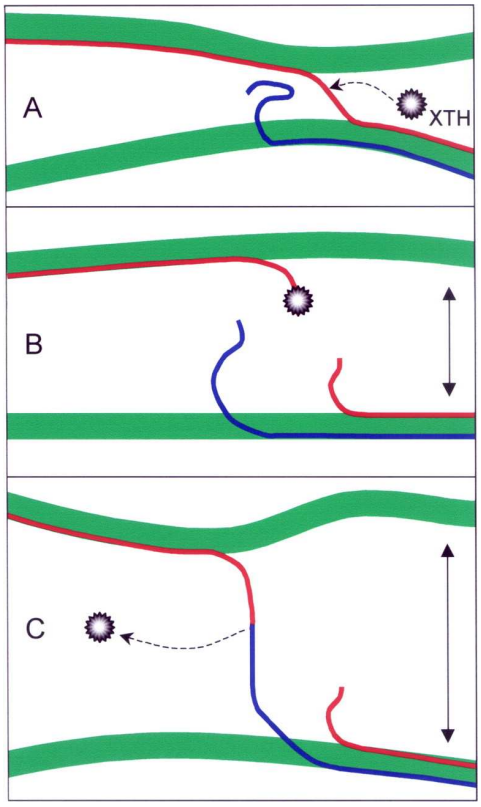




**Figure 4. Polysaccharide-to-polysaccharide transglucosylation of xyloglucan in the cell wall.** (Step 1; A-B) XTH cleaves a xyloglucan chain (red line), which acts as a tether between two neighbouring microfibrils (green). This xyloglucan chain is broken and a xyloglucan–XTH complex is formed. If the cell is turgid, the microfibrils can now move further apart, as indicated by the unbroken arrows. (Step 2; B-C). The xyloglucan–XTH complex is now out of reach of the new non-reducing terminus but within reach of the non-reducing terminus of an adjacent xyloglucan chain (blue line). The latter acts as an acceptor substrate and a tether is thereby re-formed between the two microfibrils. Rose et al. (2002; revised from Thompson and Fry, 2001). Figure legend changed according to Rose et al. (2002). 

## 1.4 Objectives

Salintiy inhibits the growth of young expanding leaves because of the osmotic effect caused by the salt outside the roots. A reduction of the water potential is predicted to reduce the cell wall yielding properties (Epstein et al., 1980; Cramer and Bowmann 1991; Munns and Tester, 2008). However, the mechanisms that down-regulate growth are not precisely known (Munns, 1993).

This thesis provides a broad analysis of the impact of an 8-day 100 mM NaCl stress treatment on shoot growth-related factors of the cell wall of expanding leaves. A comparative approach by using two *Zea mays* L. hybrids that differ markedly in their salt resistance has been conducted in order to contrast features of physiological function that may bear a causal relation to the differences in the leaf growth responses to salt stress.

In this thesis, it has been answered if an 8-day 100 mM NaCl stress treatment differentially affect …

- the transcript abundance (mRNA) of wall-loosening factors
- the abundance of growth-mediating β-expansin proteins
- the growth-related apoplastic pH

… in expanding leaves of two different maize hybrids that contrast markedly in the intensity of the NaCl-induced shoot growth reduction.

In order to answer the questions raised above, a method that has enabled the ratiometric quantitation of leaf apoplastic pH in intact plants has been developed. Furthermore, the 2D Western blotting procedure has been improved in order to yield more reliable data.

## References

Bernstein, N., Silk, W.K., Läuchli, A. (1993) Growth and development of sorghum leaves under conditions of NaCl stress: spatial and temporal aspects of leaf growth inhibition. *Planta.* 191, 433-439.

Catalá, C., Rose, J.K.C., Bennett, A.B. (1997) Auxin regulation and spatial localization of an endo-1,4-β-D-glucanase and a xyloglucan endotransglycosylase in expanding tomato hypocotyls. *Plant J.* 12, 417-426.

Cho, H.T., Kende, H. (1997) Expression of expansin genes is correlated with growth in deepwater rice. *Plant Cell.* 9, 1661-1671.

Cosgrove, D.J. (1997) Relaxation in a high-stress environment: the molecular bases of extensible cell walls and cell enlargement. *Plant Cell*. 9, 1031-1041.

Cosgrove, D.J. (2000) Loosening of plant cell walls by expansins. *Nature.* 407, 321-326.

Cosgrove, D.J. (2005) Growth of the plant cell wall. *Nat Rev Mol Cell Biol*. 6, 850-861.

Cramer, G.R., Bowman, D.C. (1991) Kinetics of maize leaf elongation. I: Increased yield threshold limits short-term, steady-state elongation rates after exposure to salinity. *J Exp Bot.* 42, 1417-1426.

Cramer, G.R. (1992) Kinetics of maize leaf elongation. II: Responses of a Na-excluding cultivar and a Na-including cultivar to varying Na/Ca salinities. *J Exp Bot.* 251, 857-864.

De Costa, W., Zörb, C., Hartung, W., Schubert, S. (2007) Salt resistance is determined by osmotic adjustment and abscisic acid in newly developed maize hybrids in the first phase of salt stress. *Physiol Plantarum*. 131, 311-321.

Epstein, E., Norlyn, J.D., Rush, D.W., Kingsbury, R.W., Kelley, D.B., Cunningham, G.A., Wrona, A.F. (1980) Saline culture of crops: a genetic approach. *Science*. 210, 399-404.

Fan, D.F., Maclachlan, G.A. (1966) Control of cellulase activity by indoleacetic acid. *Can J Bot*. 44, 1025-1034.

Flowers, T.J., Flowers, S.A. (2005) Why does salinity pose such a difficult problem for plant breeders? *Agricult Water Manag*. 75, 15-24.

Fortmeier, R., Schubert, S. (1995): Salt tolerance of maize (*Zea mays* L.): The role of sodium exclusion. *Plant Cell Environ*. 18, 1041-1047.

Fry, S.C. (1989) Cellulases, hemicelluloses and auxin-stimulated growth: a possible relationship. *Physiol Plant*. 75, 532-536.

Genovesi, V., Fornalé, S., Fry, S.C., Ruel, K., Ferrer, P., Encina, A., Sonbol, F.M., Bosch, J., Puigdomènech, P., Rigau, J., Caparrós-Ruiz, D. (2008) ZmXTH1, a new xyloglucan endotransglucosylase/hydrolase in maize, affects cell wall structure and composition in *Arabidopsis thaliana*. *J Exp Bot*. 59, 875-889.

Hager, A., Menzel, H., Krauss, A. (1971) Versuche und Hypothese zur Primärwirkung des Auxins beim Streckungswachstum. *Planta*. 100, 47-75.

Lazof, D., Bernstein, N. (1998) The NaCl-induced inhibition of shoot growth: the case for disturbed nutrition with special consideration of calcium nutrition. *Adv Bot Res.* 29, 113-189.

Moriau, L., Michelet, B., Bogaerts, P., Lambert, L., Oufattole, M., Boutry, M. (1999) Expression analysis of two gene subfamilies encoding the plasma membrane $H^+$-ATPase in *Nicotiana plumbaginifolia* reveals the major transport functions of this enzyme. *Plant J.* 19, 31-41.

Munns, R. (1993) Physiological processes limiting plant growth in saline soils: some dogmas and hypotheses. *Plant Cell Environ.* 16, 15-24.

Munns, R., Cramer, G.R. (1996) Is coordination of leaf and root growth mediated by abscisic acid? *Plant Soil*. 185, 33-49.

Munns, R. (2002) Comparative physiology of salt and water stress. *Plant Cell Environ.* 25, 239-250.

Munns, R., Husain, S., Rivelli, A.R., James, R.A., Condon, A.G., Lindsay, M.P., Lagudah, E.S., Schachtman, D.P., Hare, R.A. (2002) Avenues for increasing salt tolerance of crops, and the role of physiologically based selection traits. *Plant Soil*. 247, 93-105.

Munns, R. (2005) Tansley review: genes and salt tolerance: bringing them together. *New Phytol*. 167, 645-663.

Munns, R., James, R.A., Läuchli, A. (2006) Approaches to increasing the salt tolerance of wheat and other cereals. *J Exp Bot.* 57, 1025-1043.

Munns, R., Tester, M. (2008) Mechanism of salinity tolerance. *Annu Rev Plant Biol.* 59, 651-681.

Neves-Piestun, B.G., Bernstein, N. (2001) Salinity-induced inhibition of leaf elongation in maize is not mediated by changes in cell wall acidification capacity. *Plant Physiol*. 125, 1419-1428.

Nishitani, K. (1995) Endo-xyloglucan transferase, a new class of transferase involved in cell wall construction. *J Plant Res*. 108, 2105-2117.

Oertli, J.J., (1968) Extracellular salt accumulation, a possible mechanism of salt injury in plants. *Agrochimica*. 12, 461-469.

Pitann, B., Zörb, C., Mühling, K.H. (2009) Comparative proteome analysis of maize (*Zea mays* L.) expansins under salinity. *J. Plant Nutr Soil Sci*. 172, 75-78.

Rahnama, A.R., Munns, R., Poustini, K., Watt, M. (2011) A screening method to identify genetic variation in root growth response to a salinity gradient. *J Exp Bot*. 62, 69-77.

Rengasamy, P. (2002) Transient salinity and subsoil constraints to dryland farming in Australian sodic soils: an overview. *Aust J Exp Agric*. 42, 351-61.

Rengasamy, P. (2006) World salinization with emphasis on Australia. *J Exp Bot*. 57, 1017-1023.

Rengasamy, P. (2010) Soil processes affecting crop production in salt-affected soils. *Funct Plant Biol.* 37, 613-620.

Richards, L.A. (1954) Diagnosis and improvements of saline and alkali soils. *Agriculture Handbook No. 60.* U.S.D.A, Washington, D.C.

Rose, J.K.C., Braam, J., Fry, S.C., Nishitani, K. (2002) The XTH family of enzymes involved in xyloglucan endotransglucosylation and endohydrolysis: current perspectives and a new unifying nomenclature. *Plant Cell Physiol.* 43, 1421-1435.

Rozema, L., Flowers, T. (2008) Crops for a salinized world. *Science*. 322, 1478-1480.

Sauter, A., Dietz, K.J., Hartung, W. (2002) A possible stress physiological role of abscisic acid conjugates in root-to-shoot signalling. *Plant Cell Physiol.* 25, 223-228.

Schubert, S., Läuchli, A. (1986) $Na^+$ exclusion, $H^+$ release, and growth of two different maize cultivars under NaCl salinity. *J Plant Physiol.* 126: 145-154

Slabu, C., Zörb, C., Steffens, D., Schubert, S. (2009) Is salt stress of faba bean (*Vicia faba*) caused by $Na^+$ or $Cl^-$ toxicity? *J Plant Nutr Soil Sci.* 172, 644-650.

Szabolcs, I. (1994) Soils and salinisation. In *Handbook of Plant and Crop Stress*. Ed. M Pessarakali. p 3-11. Marcel Dekker, New York.

Taleisnik, E., Rodríguez, A.A., Bustos, D., Erdei, L., Ortega, L., Senn, M.E. (2009) Leaf expansion in grasses under salt stress. *J Plant Physiol*. 166, 1123-1140.

Thompson, J.E., Fry, S.C. (2001) Restructuring of wall-bound xyloglucan by transglycosylation in living plant cells. *Plant J*. 26, 23-34.

Van Volkenburgh, E., Boyer, J.S. (1985) Inhibitory effects of water deficit on maize leaf elongation. *Plant Physiol*. 77, 190-194.

Vissenberg, K., Fry, S.C., Pauly, M., Hofte, H., Verbelen, J.P. (2005) XTH acts at the microfibril-matrix interface during cell elongation. *J Exp Bot*. 56, 673-683.

Wild, A. (2003) *Soils, land and food: managing the land during the twenty-first century*. Cambridge University Press, Cambridge.

Wu, Y., Cosgrove, D.J. (2000) Adaptation of roots to low water potentials by changes in cell wall extensibility and cell wall proteins. *J Exp Bot*. 51(350), 1543-1553.

Yamaguchi, T., Blumwald, E. (2005) Developing salt-tolerant crop plants: challenges and opportunities. *Trends Plant Sci.* 10, 615-620.

# Chapter 2

## Salt stress differentially affects growth-mediating β-expansins in resistant and sensitive maize (*Zea mays* L.)

Christoph-Martin Geilfus, Christian Zörb and Karl H. Mühling

Plant Physiology and Biochemistry 48 (2010) 993-998

Plant Physiology and Biochemistry 48 (2010) 993–998

Contents lists available at ScienceDirect

Plant Physiology and Biochemistry

journal homepage: www.elsevier.com/locate/plaphy

Research article

# Salt stress differentially affects growth-mediating β-expansins in resistant and sensitive maize (*Zea mays* L.)

Christoph-Martin Geilfus*, Christian Zörb, Karl H. Mühling

*Institute of Plant Nutrition and Soil Science, Christian Albrechts University, Hermann-Rodewald-Str. 2, 24118 Kiel, Germany*

ARTICLE INFO

*Article history:*
Received 16 February 2010
Accepted 22 September 2010
Available online 1 October 2010

*Keywords:*
Salt stress
β-Expansin
Growth inhibition
*Zea mays* L.
Apoplast

ABSTRACT

Salinity mainly reduces shoot growth by the inhibition of cell division and elongation. Expansins loosen plant cell walls. Moreover, the expression of some isoforms is clearly correlated with growth. Effects of salinity on β-expansin transcripts protein abundance were recently reported for different crop species. This study provides a broad analysis of the impact of an 8-day 100 mM NaCl stress treatment on the mRNA expression of different maize (*Zea mays* L.) β-Expansin isoforms using real-time quantitative RT-PCR. The composite β-expansin protein expression was analyzed by western blotting using an anti-peptide antibody raised against a conserved 15-amino-acid region shared by vegetatively expressed β-expansin isoforms. For the first time, changes in β-expansin transcript and protein abundance have been analyzed together with the salinity-induced inhibition of shoot growth. A salt-resistant and a salt-sensitive cultivar were compared in order to elucidate physiological changes. Genotypic differences in the relative concentration of six β-expansin transcripts together with differences in the abundance β-expansin protein are shown in response NaCl stress. In salt-sensitive Lector, reduced β-expansin protein expression was found to correlate positively with reduced shoot growth under stress. A down-regulation of *ZmExpB2*, *ZmExpB6*, and *ZmExpB8* transcripts possibly contribute to this decrease in protein abundance. In contrast, the maintenance of shoot growth in salt-resistant SR03 might be related to an unaffected abundance of growth-mediating β-expansin proteins in the shoot. Our data suggest that the up-regulation of *ZmExpB2*, *ZmExpB6*, and *ZmExpB8* may sustain the stable expression of β-expansin protein under conditions of salt stress.



## 1. Introduction

Soil salinity is a major environmental constraint limiting agricultural production worldwide. Up to 20% of the world's arable land and up to 50% of all irrigated land is adversely affected by salinity mainly attributable to non-adapted irrigation practices [1–3]. The mechanisms by which plants cope with salt is a subject of increasing interest as the global problem of salinity increases [4]. Soil salinity stresses plants in two ways. The high concentration of salts in the soil makes it harder for roots to extract water, and high concentrations of salts within the plant can be toxic [5]. Immediately after the salt concentration around roots increases to a threshold level, the rate of shoot growth falls significantly [6]. Thus, high concentration of salts in the soil are seen as a rapid inhibition of the expansion rate of young leaves caused by an inhibition of cell division and cell elongation. This effect is largely caused by the osmotic effect of the salt outside the roots [7–10].

Plants differ in their resistance against salinity, whereas maize (*Zea mays* L.) is classified as a salt-sensitive glycophyte plant [11–14]. Phenotypic variation in salt resistance amongst glycophytes was described [15], whereas the sensitivity of glycophytes and the mechanism that decreases leaf growth and shoot development under such stress is not precisely known [16]. Genes controlling cell growth and leaf function genes that could increase the growth rate of plants in saline soil would influence the rate of production of new leaves and roots by controlling the rate of cell division, the development of new primordia for shoot or root branching, the rate of cell wall expansion, or the dimensions of differentiated cells [17].

Salinity may restrict cell expansion by affecting the uptake rates of water or osmolytes, turgor generation, and/or cell wall properties [18]. However, numerous studies report changes in tissue growth rate during stress, whereas turgor remains unaffected (reviewed by Fricke [19]; [16]). Additionally, Munns [9] suggests that turgor does not control growth but acts as an extending force on the cell wall

*Abbreviation:* Real-time quantitative RT-PCR, real-time quantitative reverse transcriptase-polymerase chain reaction.

* Corresponding author. Tel.: +49 431 8803359; fax: +49 431 8801625.
*E-mail address:* cmgeilfus@plantnutrition.uni-kiel.de (C.-M. Geilfus).

0981-9428/$ – see front matter © 2010 Elsevier Masson SAS. All rights reserved.
doi:10.1016/j.plaphy.2010.09.011

and thereby is essential for growth. Moreover it was reviewed by Cosgrove [20] that turgor-driven cell expansion is ultimately controlled by stress relaxation in the cell wall. However, changes in wall properties must occur, although their exact nature remains unknown [6].

The precise molecular basis of wall properties is not known, but increasing evidence indicates that wall properties are under enzymatic, protein-biochemical, or chemical control. Vegetatively expressed growth-mediating expansins are one important component of the protein-biochemical activity. It is assumed that expansins regulate cell wall enlargement in growing cells and have been directly implicated in cell wall-loosening processes [21–23]. The expression of some expansin isoforms is clearly correlated with growth and the external application of expansins can stimulate cell expansion in vivo in several systems [23,24]. Changes in expansin transcript level were shown to correlate with the maintenance of root growth and increase in wall extensibility at low water potentials [25,26]. Furthermore, regulation of expansin mRNA pools likely contributes to fast adjustment of cell wall-loosening in maize under conditions of water deficit [27].

How expansins catalyse wall enlargement remains unclear. One interpretation is that expansins intercalate within carbohydrate matrices in the cell wall, leading to the transient loosening of non-covalent interactions, and thus enhance the ability of these matrices to move relative to each other [23].

Expansins are the primary mediators of acid-induced growth [23]. The acid growth theory explains growth by auxin-mediated cell wall elongation [28,29]. According to this theory, the acidification of the leaf apoplast is the major requirement for increasing cell wall extensibility, which then controls extension growth [30]. The theory is supported by the finding that auxin mediates the acidification of the apoplast below a pH of 5.0 [31], thus stimulating cell elongation in maize, *Avena* coleoptiles, and pea [29,32]. Moreover, the pH of the apoplast of growing cells typically spans 4.7–6 [33], which is the range in which acidification activates expansin activity Moreover, it was shown that isolated cell walls exhibit acid growth, which results from the action of pH-dependent wall-loosening expansin proteins [23,34].

However, only a few reports have evaluated the effects of salinity on the abundance of these growth-mediating proteins. Buchanan et al. [35] report a salinity-induced increase in β-expansin transcript abundance for *Sorghum bicolor*. Recently, Pitann et al. [36] have shown results derived from two-dimensional proteome analyses indicating a decrease in β-expansin protein in a salt-sensitive maize cultivar, whereas β-expansin protein level in a resistant cultivar is less affected by salinity.

In general, β-expansins are more numerous and more abundantly expressed in maize tissue compared to α-expansins and are hypothesized to function in cell enlargement and other processes in which wall loosening is required [37]. β-Expansins are assumed to have evolved specialized functions in conjunction with the evolution of the grass cell wall, which has a distinctive set of matrix polysaccharides and structural proteins compared with other land plants [37,38]. Furthermore it is suggested that that β-expansins might have supplanted or replaced α-expansin function in grasses [39].

An understanding of the growth responses of maize shoot to salinity is of great importance on the one hand for a better comprehension of plant resistance and, on the other hand, for the eventual screening or smart breeding of stress-adapted crop plants. This study addresses the question as to whether salt stress differentially affects growth-mediating β-expansin in resistant and sensitive maize cultivars. For the first time, changes in β-expansin transcript and protein abundance have been analyzed together with the salinity-induced inhibition of shoot growth. Moreover, we have shown genotypic differences relevant to this effect within maize.

## 2. Results

### 2.1. Shoot growth reduction

Salinity affects shoot growth and leaf development [9]. Compared with control plants (1 mM NaCl), a significant decrease of 65% in shoot growth was measured in salt-sensitive cultivar Lector in response to a 100 mM NaCl treatment (Fig. 1). However, in salt-resistant SR03 plants, the decrease in shoot growth was only 11%, which was not significantly different from the control (Fig. 1). These incremental measurements were based on expanding shoot material of plants grown entirely under the influence of an 8-day 100 mM NaCl treatment.

### 2.2. Protein abundance of β-expansin

The effect of 100 mM NaCl treatment on vegetatively expressed β-expansin protein in shoot material was investigated by using a polyclonal rabbit antibody (anti-ZmExpB; see Material section). The loading control of the PAGE gels indicated equivalent levels of proteins in all lanes (Fig. 2A). Western blot analysis revealed the presence of a strong signal band at ca. 25 kDa in the salt-treated plants and corresponding controls (Fig. 2B). Signal was obtained in both maize genotypes. For salt-sensitive hybrid Lector, a significant decrease of 50% in β-expansin protein abundance was detected densiometrically in response to the salt treatment (Fig. 2C). In contrast to the salt-sensitive hybrid Lector, no significant difference in protein abundance was detected for SR03. The negative control with preimmune serum did not detect any specific bands (data not shown).

### 2.3. Relative β-expansin transcript abundance

The effect of salt treatment on the relative transcript abundance of six vegetatively expressed *Z. mays* β-expansin isoforms (*ZmExpB2*, *ZmExpB3*, *ZmExpB5*, *ZmExpB6*, *ZmExpB7*, *ZmExpB8*; Fig. 3) was studied on the basis of purified poly(A)$^+$ RNA by using real-time quantitative RT-PCR. In comparison with various reference genes, ubiquitin-conjugating enzyme was validated as the most

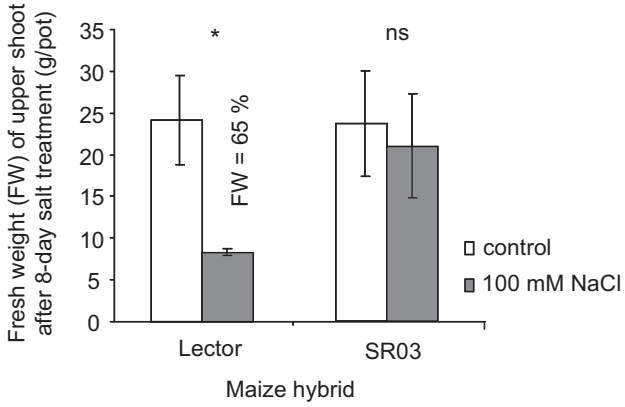


**Fig. 1.** Growth inhibition analyses of plants grown in hydroponics. Biomass reduction of young expanding maize shoot (*Zea mays* L.) under conditions of salt stress. Plants were treated with 100 mM NaCl for 8 days (corresponding control plants with 1 mM NaCl). For the evaluation of growth inhibition in response to salt stress, only fresh weights (FW) of young expanding leaves entirely grown under the influence of an 8-day NaCl treatment (and corresponding controls) were studied. The remaining older shoot material was not considered. Sensitive maize hybrid, Lector; resistant hybrid, SR03. ΔFW indicates treatment-induced shoot growth inhibition in %. The data are means of three biological replicates, each run being carried out in triplicate ± SE. Asterisks indicate significant differences between genotypes ($p \leq 0.05$%; ns, not significant).

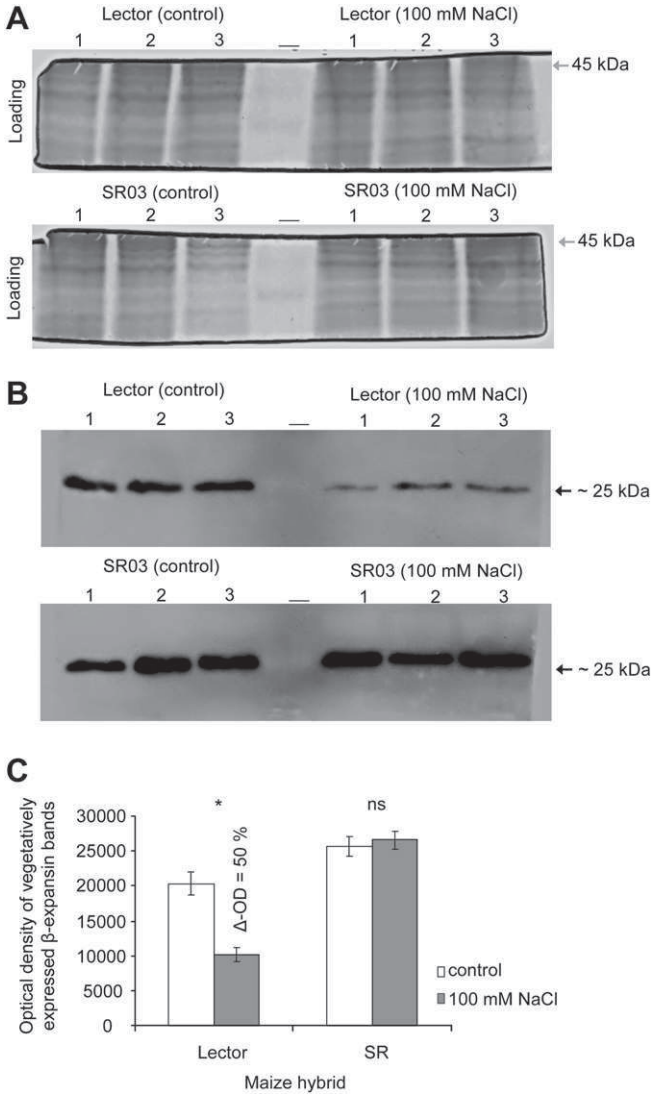


**Fig. 2.** Western blot analysis of vegetatively expressed β-expansin. (A) Loading controls of Western blots shown in (B) indicate equivalent protein levels in all lanes. 30 μg proteins per lane were separated on 15% SDS-PAGE. Gels were Coomassie-stained (for details of the Western blot procedure, see Material section). Numbers 1–3 indicate the three biological replicates used. (B) Detection of vegetatively expressed β-expansin in shoot material of salt-treated (100 mM NaCl) and control-treated (1 mM NaCl) Lector and SR03 hybrids of maize. β-expansin bands appear at 25 kDa. Numbers 1–3 indicate the three biological replicates. (C) Densitometric analysis (TINA 2.08) of Western blot bands shown in (B). Bands were plotted as the average of the optical density (OD). ΔOD indicates the decrease in signal intensity in response to salt treatment (%). The data are means of three biological replicates ± SE. Asterisks indicate significant differences between genotypes ($p \leq 0.05\%$; ns, not significant).

stable reference gene for salt stress [40]. Because this report was also based on a monocot grass species (*Brachypodium distachyon*), we also used ubiquitin-conjugating enzyme as the reference gene.

The β-expansin isoforms *ZmExpB2*, *ZmExpB6*, *ZmExpB7*, and *ZmExpB8* of the sensitive hybrid Lector were down-regulated in response to salt treatment. Within these isoforms, *ZmExpB2* was highly down-regulated (−850%). The other transcripts *ZmExpB3* and *ZmExpB5* were up-regulated in the same genotype. However, the resistant hybrid SR03 showed increased relative transcript abundance of the isoforms *ZmExpB2*, *ZmExpB3*, *ZmExpB5*, *ZmExpB6*, and *ZmExpB8*. Within this group *ZmExpB2* exhibited the highest up-regulation. In contrast, only *ZmExpB7* was down-regulated in SR03 after salt stress was applied (Fig. 3).

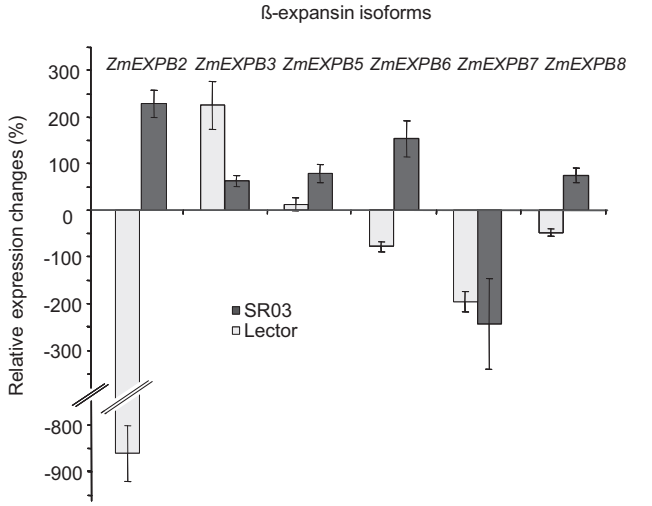


**Fig. 3.** Real-time quantitative RT-PCR analyses of vegetatively expressed β-expansin isoforms. Relative changes in expression of six vegetatively expressed β-expansin isoforms (*ZmExpB2*, *ZmExpB3*, *ZmExpB5*, *ZmExpB6*, *ZmExpB7*, and *ZmExpB8*) in response to an 8-day 100 mM NaCl treatment. SYBR-green-based real-time quantitative RT-PCR analysis was carried out with reverse-transcribed highly purified maize poly(A)$^+$ RNA. The gene for ubiquitin-conjugating enzyme was used as the endogenous control in an Applied Biosystems 7300 real-rime PCR system. Data show effect of salt treatment on relative transcript abundance with the control (1 mM NaCl) as a calibrator sample (+100% rel. expression changes = 2-fold up-regulation). Grouped bars show salt-sensitive Lector (grey) and salt-resistant SR03 (black) cultivars. Expression data correspond to means of three biological replicates, each being run in triplicate ± SE.

No adequate primer pairs were found for the vegetative isoform *ZmExp4*. Generally, in this study, only those β-expansin isoforms expressed in vegetative tissue were included in this study; others such as *ZmExpB1* had a different origin, such as pollen.

## 3. Discussion

In this study, only young expanding shoot material entirely grown under the influence of exogenously added 100 mM NaCl was taken into account. Shoot material that had started developing when full-strength NaCl concentration had not yet been applied to the hydroponic culture was rejected. Thus, the shoot increments measured in this study adequately reveal the effect of an 8-day 100 mM NaCl treatment. The maize hybrid Lector shows a significant shoot growth reduction of 65% under salt stress (Fig. 1), which is more marked than previously reported findings for maize [14,41,42]. This is because the measurements have only been carried out on young shoot material solely developing under saline conditions. On the contrary, the highly salt-resistant SR03 hybrid shows no significant effect on shoot growth (Fig. 1). This indicates differences in salt resistance mechanisms related to the shoot growth within the two maize cultivars. This is remarkable because an inhibition of shoot growth in response to salt treatment is broadly described in literature [6,10,13]. The SR03 hybrid, which was developed and characterised as being highly salt resistant, shows no harvest deficits under 10 dS m$^{-1}$ soil salinity [43], whereas conductivity of 6 dS m$^{-1}$ usually leads to 50% reduced harvest of almost all recent maize genotypes [44]. Thus, the salt-resistant SR03 hybrid exhibits a good tool for researching on physiological changes. Besides this genotypic differences manifested in shoot growth, a specific stress response in terms of expression of growth-mediating vegetatively expressed β-expansin protein was observed in the shoots of both cultivars: The salt-sensitive cultivar Lector exhibits a significant decline in composite

β-expansin protein expression (Fig. 2B), whereas β-expansin expression in the salt-resistant cultivar SR03 is not affected by the exogenously added 100 mM NaCl.

Since previous work on expansins had shown a strong correlation between the presence of some isoforms, wall extensibility and cell elongation [23,24], it can be assumed that these effects on shoot growth are related to the expansin protein expression. In salt-sensitive Lector the reduced β-expansin protein abundance (Fig. 2B) was found to correlate positively with the reduced shoot growth (Fig. 1) under salinity stress conditions. In contrast, for salt-resistant SR03 no stress effect on β-expansin abundance was observed. Interestingly this genotype did not show an effect of the salt treatment on the shoot growth.

In the shoot of salt-sensitive maize Lector, vegetative β-expansin protein expression significantly decreases in response to exogenously added 100 mM NaCl. Consequently, it can be suggested that fewer β-expansin proteins act as softening factors on the wall, thus, the decrease in protein abundance may damp wall-softening processes in the sensitive maize Lector. This might hamper turgor-driven cell wall elongation, possibly resulting in both reduced wall expansion and reduced shoot growth as shown for the salt-sensitive Lector under conditions of salt stress (Fig. 1). Reduced wall extensibility can probably account for the observed effects on growth, as cell elongation is highly dependent on extensibility [20]. In contrast, the expression of vegetative growth-mediating β-expansin proteins is not affected in the salt-resistant SR03 cultivar. Western signals obtained from control and salt treatment do not differ (Fig. 2B). It can be suggested, that in response to salt treatment β-expansin proteins remain acting as a wall-softening factor, thus, enabling turgor-driven cell expansion. This probably explains why no significant shoot growth inhibition had been measured for the salt-resistant cultivar under 100 mM NaCl (Fig. 1), representing a high level of salt stress for maize [43]. The maintenance of shoot growth in salt-resistant SR03 might be related to an unaffected abundance of growth-mediating β-expansin proteins in the shoot.

Besides expansin, enzymes like xyloglucan endotransglycosylase (XET) and endo-1,4-β-D-glucanase (EG) have been proposed to act as cell wall-loosening agents by cleaving the xyloglucans that hypothetically knit cellulose microfibrils together [45]. However, this function has not yet been proved neither for XET nor for EG. As reviewed by Cosgrove [23] despite assertions in the literature that XTH causes wall loosening, there is little direct evidence in support of XTH as a primary wall-loosening agent. Furthermore, potential function of EG for cell wall loosening have drawn surprisingly little experimental attention, indicating that role EG in wall loosening is not yet fully understood [23]. For this reasons, this study is specifically focused on expansins, which regulate cell wall enlargement in growing cells and are the primary mediators of acid-induced growth [23,46].

Observations on expansins strongly suggest an important role of expansins in the control of growth [22]. But which vegetatively expressed β-expansin transcript isoforms contribute to salinity-induced genotypic differences in the protein abundance? As far as we know, specific functions for the vegetatively expressed *Z. mays* β-expansin isoforms *ZmExpB2*, *ZmExpB3*, *ZmExpB5*, *ZmExpB6*, *ZmExpB7*, and *ZmExpB8* have not yet been reported. Only the function for the generatively expressed *Z. mays* β-expansin 1 (*ZmExpB1*) is known. *ZmExpB1* loosens maternal cell walls to aid penetration of the stigma by the pollen tube [34]. In order to elucidate the effect of salt treatment on six vegetatively expressed transcript isoforms, we have employed the real-time quantitative RT-PCR technique. Moreover, this study demonstrates genotypic responses leading to a different expression of vegetatively expressed β-expansin isoforms in the shoot of maize in response to exogenously added 100 mM NaCl.

A predominant decrease of *ZmExpB2* transcripts (Fig. 3) has been observed for salt-sensitive Lector. This confirms previous results derived from two-dimensional proteome analyses, reporting about a down-regulation of this particular isoforms in a sensitive maize cultivar after salt stress [47]. As this isoform is down-regulated in response to salt treatment, at both the transcript and protein levels, it can reasonably be considered to have an impact on shoot growth under conditions of salt stress. Moreover, this isoform experiences the strongest down-regulation (−850%). Beside *ZmExpB2*, two further transcripts, viz., *ZmExpB6* and *ZmExpB8* are down-regulated in the salt-sensitive maize cultivar Lector (Fig. 3). This down-regulation of these three β-expansin transcripts may contribute to the decreased abundance of growth-mediating β-expansin protein in salt-sensitive Lector in response to salt stress (Fig. 2B). In contrast, the resistant SR03 hybrid is able to up-regulate these particular β-expansin transcripts, viz., *ZmExpB2*, *ZmExpB6*, and *ZmExpB8*, in response to salt treatment (Fig. 3). This up-regulation of transcripts may sustain the expression of β-expansin protein under conditions of salt stress in SR03 cultivar (Fig. 2B). An up-regulation of *ZmExpB5* in SR03 may also contribute to the stable level of this protein (Fig. 3). Transcripts of isoform *ZmExpB7* were equally down-regulated in both genotypes, thus, this isoform might not contribute to the genotypic differences at the protein level. Transcript levels of *ZmExpB3* were up-regulated in both genotypes (Fig. 3), with a higher increase in the salt-sensitive Lector. Nevertheless, this up-regulation of *ZmExpB3* transcripts is not able to compensate for the decrease of β-expansin protein in the salt-sensitive cultivar.

In conclusion, genotypic differences in the relative concentration of six β-expansin transcripts together with genotypic differences in the abundance of vegetatively expressed β-expansin protein are shown in response to salinity using real-time qRT-PCR and western blotting with an anti-peptide antibody. In shoot of salt-sensitive Lector, reduced β-expansin protein expression was found to correlate positively with reduced shoot growth under salinity stress conditions. Since expansins regulate cell wall enlargement in growing cells and expansins are the primary mediators of acid-induced growth [23,46], the decrease of β-expansin protein in the shoot possibly accounts to the inhibition of shoot growth. A down-regulation of *ZmExpB2*, *ZmExpB6*, and *ZmExpB8* transcripts may contribute to this decrease of protein. In contrast, the maintenance of shoot growth in salt-resistant SR03 might be related to an unaffected abundance of growth-mediating β-expansin proteins in the shoot. Our data suggest that the up-regulation of *ZmExpB2*, *ZmExpB6*, and *ZmExpB8* may sustain the stable expression of β-expansin protein in shoot under conditions of salt stress. Thus, indicating a function of these individual isomers, viz., *ZmExpB2*, *ZmExpB6*, and *ZmExpB8* in response to the 8-day 100 mM NaCl treatment.

## 4. Materials and methods

### 4.1. Plant cultivation

A salt-sensitive maize hybrid Lector and a salt-resistant maize hybrid SR03 (*Z. mays* L.; [43]) were grown in the greenhouse under hydroponic culture conditions. The experimental set-up consisted of three independent replicates of the salt-treated plants (100 mM NaCl) and the corresponding control plants (1 mM NaCl). Each biological replicate was run in triplicate in a completely randomized design. Seedlings were imbedded in 1 mM $CaSO_4$ in an aerated solution at 25 °C for 1 day and placed between filter papers moistened with 1 mM $CaSO_4$ for a period of 3 days. Subsequently, the seedlings were transferred to 4.5 l plastic pots (3 plants per pot) containing one quarter-strength nutrient solution. After 2 days

cultivation, the concentration of nutrients was increased to half-strength and after 4 days cultivation to full-strength, respectively. The full-strength nutrient solution had the following concentration (in mM): $Ca(NO_3)_2$ 2.5; $K_2SO_4$ 1.0; $KH_2PO_4$ 0.2; $MgSO_4$ 0.6; $CaCl_2$ 5.0; and (in μM), $H_3BO_4$ 1.0; $MnSO_4$ 2.0; $ZnSO_4$ 0.5; $CuSO_4$ 0.3; $(NH_4)_6Mo_7O_{24}$ 0.005; Fe-EDTA 200. The solution was changed every 2nd day to avoid nutrient depletion. NaCl treatment was started 2 days after the full-nutrient concentration had been reached and was increased stepwise by 25 mM increments every 2nd day. Temperature was kept constant at 26 °C for the light period and at 18 °C for the dark period; relative humidity was ca. 70%. In this study, only young expanding shoot material that developed entirely under the full influence of the 8-day 100 mM NaCl treatment was harvested for investigation. The remaining older shoot material that had started to develop when full-strength NaCl concentration had not yet been reached was rejected. After measurement of fresh weights of this young shoot material, leaves were ground in liquid nitrogen and stored at −80 °C for Western blot and real-time quantitative reverse transcriptase (RT)-PCR (real-time quantitative RT-PCR) analysis.

### 4.2. Isolation of expansin protein

Aliquots of 100 mg ground shoot material were extracted with 1 ml PBST buffer (0.1% v/v Tween 20; 10 mM PMSF; pH 7.4) and incubated for 2 h at 4 °C with agitation. After removal of cell wall fragments by centrifugation (14,000 *g*, 3 min), proteins were precipitated by the addition of 390 g $l^{-1}$ $(NH_4)_2SO_4$ [48] and resuspended in 15 mM MES (pH 6.5). Protein concentrations were determined by the method of Bradford [49].

### 4.3. Antibodies and Western blot

For reporting on the composite maize β-expansin protein expression an anti-peptide antibody raised against a conserved 15-amino-acid region shared by seven different, vegetatively expressed, beta-expansin isoforms was used. The synthetic 15-amino-acid peptide used for antibody production was designed according to the amino-acid sequence L152-LVARNVIPANWRPN-T166 of ZmExp2. This is the region with highest sequence homology of all vegetatively expressed *Z. mays* β-expansin isoforms, thus providing the highest probability for detecting them simultaneously (Table I; see Supplementary data). Since this peptide represents the specific antibody binding site within the expansin protein, this conserved 15-amino-acid sequence was checked by BLASTP against a *Z. mays* non-redundant protein sequences (nr) for its specific appearance in the vegetatively expressed β-expansin protein sequence. According to an alignment with an X-ray-based three-dimensional structure of ZmExpB1 [50], the newly generated antibody, viz., anti-ZmExpB, is predicted to bind at the surface of the β-expansin (data not shown). The antibody was produced commercially (BioTrend, Cologne, Germany). Preimmune serum was taken before booster injections. For Western blots, 30 μg proteins were separated by 15% SDS-PAGE and transferred to a PVDF transfer membrane (BioTrace, PALL Life Sciences, Pensacola, USA) by using a semi-dry transfer system (SemiPhor, Hoefer Pharmacia Biotech, San Francisco, USA; Towbin buffer: 25 mM TRIS-base, 192 mM glycine, 20% v/v methanol, 0.01% w/v SDS, pH 8.3). Proteins from each maize cultivar, viz., Lector and SR03, were separated by using two different SDS gels, which were then blotted together onto the same PVDF membrane. Subsequently, the membrane was saturated in a solution of milk powder in TBST (2.5% w/v bovine skimmed milk; 0.1% v/v Tween) for 2 h. The membrane was then incubated with the antibody (ZmExpB, 1:250) in the same buffer for 2 h and washed three times with TBST (0.1% v/v). Subsequently the second antibody was applied for 1 h (1:38,000, goat anti-rabbit IgG conjugated to horseradish peroxidase; Sigma–Aldrich, St. Louis, USA). Finally, the membrane was washed once in TBST buffer (0.1% v/v Tween) containing 0.1 M NaCl, two times in TBST (0.1% v/v Tween), and finally in TBS. Proteins were detected by using chemiluminescent peroxidase subtrate-3 on Kodak BioMax light film (Sigma, Munich, Germany).

### 4.4. RNA extraction and cDNA synthesis

Aliquots of 100 mg ground shoot material were used for RNA extraction. Total maize RNA was isolated according to a modified method of Cox and Goldberg [51]. The quality and quantity of RNA was checked by $OD_{260}$. Poly(A)$^+$ RNA purification was carried out with oligo(dT)$_{25}$-coupled paramagnetic particles (Dynabeads® mRNA Purification Kit, Invitrogen GmbH, Karlsruhe, Germany) by using 75 μg total RNA according the instructions of the manufacturer. Highly purified maize poly(A)$^+$ RNA (3 μg) was reverse-transcribed in a 10 μl cDNA reaction with a first-strand cDNA synthesis system following the manufacturer's instructions (SuperScript® VILO cDNA synthesis kit, Invitrogen, Karlsruhe, Germany). Single-stranded cDNA was diluted at a concentration depending on the level of expression of the studied gene; cDNA was aliquoted to avoid discrepancy in the data attributable to the repetition of freezing-thawing cycles.

### 4.5. Real-time quantitative reverse transcriptase-polymerase chain reaction

The SYBR-Green-based real-time quantitative RT-PCR technique was performed on an Applied Biosystems 7300 real-time PCR system. For each reaction, 2 μl diluted single-stranded cDNA were used in a total volume of 20 μl (forward and reverse gene-specific primer, 0.8 pM each; dNTP mix, 0.82 mM; SYBR-Green, 0.1×; ROX, 1×; *Taq* DNA polymerase 0.6 U,Invitek, Berlin, Germany). After an initial denaturation step (92 °C, 2 min), real-time quantitative RT-PCR was carried out over 40 cycles (denaturation: 92 °C, 30 s; amplification and quantification: 40 s [for primer-pair-specific temperatures see Table II; Supplementary data], elongation: 72 °C, 20 s). To check the specificity of annealing of the oligonucleotides, dissociation kinetics was performed by the real-time PCR system at the end of the experiment (60–95 °C, continuous fluorescence measurement). In a study exploring reference genes for real-time PCR gene expression studies in a grass species ([40]; *B. distachyon*), the gene for the ubiquitin-conjugating enzyme was validated as the most stable reference gene, being particularly useful for the analysis of genes in high-salt- and drought-treated samples.

The comparative Ct method of relative quantification was used to analyze the real-time quantitative RT-PCR data (threshold cycles; Ct). With this method, the Ct values were normalized by comparison to the endogenous reference gene, viz., ubiquitin-conjugating enzyme. The normalized Ct values were then used to compare NaCl-treated plants and corresponding controls. Data were expressed as the relative change in transcript expression (+100% rel. expression changes = 2-fold up-regulation). Threshold cycles were calculated by the internal software of the real-time PCR system and were means of three biological replicates each run in triplicate. The sizes of amplified products were confirmed by gel electrophoresis. Negative controls with no templates were carried out concurrently.

### 4.6. PCR primer design

Specific primer pairs for six vegetatively expressed β-expansins (*ZmExpB2*, *ZmExpB3*, *ZmExpB5*, *ZmExpB6*, *ZmExpB7*, and

*ZmExpB*8;Table I; see Supplementary data) were designed on the basis of nucleotide alignments (ClustalW, http://www.clustal.org). The primer pair for the ubiquitin-conjugating enzyme (*ZmUbc*) was designed by using Primer3Plus and Primer-BLAST software (http://bioinformatics.nl/cgi-bin/primer3plus/primer3plus.cgi; http://www.ncbi.nlm.nih.gov/). Primers were prepared commercially by Eurofins MWG Operon (Ebersberg, Germany). Additionally, for the prevention of false priming sites, all primer pairs were checked *in silico* by BLASTN against a *Z. mays* nucleotide collection (nr/nt) and *Z. mays* reference mRNA sequences (refseq_rna). In order to avoid primer–dimer formation and the formation of hairpin structures, primers were evaluated *in silico* by using Primer-BLAST and Primer3Plus.

## Acknowledgment

We are grateful to Prof. Dr. Sven Schubert for providing the SR03 hybrids and to Prof. Dr. D. Ober for discussing various details in the manuscript. CMG receives a grant from the Friedrich-Ebert-Foundation, which is gratefully acknowledged. M. Shazhad is kindly acknowledged for his help with plant cultivation. This work was supported by a DFG research grant (ZO118/6) which is gratefully acknowledged.

## Appendix. Supplementary data

Supplementary data associated with this article can be found in the online version, at doi:10.1016/j.plaphy.2010.09.011.

## References

[1] T.J. Flowers, P.F. Troke, A.R. Yeo, Mechanisms of salt tolerance in halophytes, Annu. Rev. Plant Physiol. 28 (1977) 89–121.
[2] E. Epstein, J.D. Norlyn, D.W. Rush, R.W. Kingsbury, D.B. Kelly, Saline culture of crops: a genetic approach, Science 210 (1980) 399–404.
[3] T.J. Flowers, Salinisation and horticultural production, Sci. Hortic. 78 (1999) 1–4.
[4] R. Munns, Prophylactively parking sodium in the plant, New Phytol. 176 (2007) 501–504.
[5] R. Munns, Comparative physiology of salt and water stress, Plant Cell Environ. 25 (2002) 239–250.
[6] R. Munns, M. Tester, Mechanism of salinity tolerance, Annu. Rev. Plant Biol. 59 (2008) 651–681.
[7] H.M. Rawson, R. Munns, Leaf expansion in sunflower as influenced by salinity and short-term changes in carbon fixation, Plant Cell Environ. 7 (1984) 207–213.
[8] R. Munns, A. Termaat, Whole-plant responses to salinity, Aust. J. Plant Physiol. 13 (1986) 143–160.
[9] R. Munns, Physiological processes limiting plant growth in saline soils: some dogmas and hypotheses, Plant Cell Environ. 16 (1993) 15–24.
[10] M. Tester, R. Davenport, $Na^+$ tolerance and $Na^+$ transport in higher plants, Ann. Bot. 91 (2003) 503–527.
[11] E.V. Maas, Salt tolerance of plants, Appl. Agric. Res. 1 (1986) 12–25.
[12] G.R. Cramer, D.C. Bowmann, Kinetics of maize leaf elongation, J. Exp. Bot. 42 (1991) 1417–1426.
[13] K.H. Mühling, A. Läuchli, Effect of salt stress on growth and cation compartmentation in leaves of two plant species differing in salt tolerance, J. Plant Physiol. 159 (2002) 137–146.
[14] C. Zörb, S. Schmitt, A. Neeb, S. Karl, M. Linder, S. Schubert, The biochemical reaction of maize (*Zea mays* L.) to salt stress is characterized by a mitigation of symptoms and not by a specific adaptation, Plant Sci. 167 (2004) 91–100.
[15] B.A. Hajibagheri, D.M.R. Harvey, T.J. Flowers, Quantitative ion distribution within root cells of salt-sensitive and salt-tolerant maize varieties, New Phytol. 105 (1987) 367–379.
[16] C.S. Byrt, R. Munns, Living with salinity, New Phytol. 179 (2008) 903–905.
[17] R. Munns, Genes and salt tolerance: bringing them together, New Phytol. 167 (2005) 645–663.
[18] E. Taleisnik, A.A. Rodríguez, D. Bustos, L.E.L. Ortega, M.E. Senn, Leaf expansion in grasses under salt stress, J. Plant Physiol. 166 (2009) 1123–1140.
[19] W. Fricke, Biophysical limitation of cell elongation in cereal leaves, Ann. Bot. 90 (2002) 157–167.
[20] D.J. Cosgrove, Water uptake by growing cells: an assessment of the controlling roles of wall relaxation, solute uptake, and hydraulic conductance, Int. J. Plant Sci. 154 (1993) 10–21.
[21] S. McQueen-Mason, D. Cosgrove, Expansin mode of action on cell walls: analysis of wall hydrolysis, stress relaxation, and binding, Plant Physiol. 107 (1995) 87–100.
[22] S.F. Rochange, C.L. Wenzel, S.J. McQueen-Mason, Impaired growth in transgenic plants over-expressing an expansin isoform, Plant Mol. Biol. 46 (2001) 581–589.
[23] D.J. Cosgrove, Growth of the plant cell wall, Nat. Rev. Mol. Cell Biol. 6 (2005) 850–861.
[24] H.T. Cho, H. Kende, Expression of expansin genes is correlated with growth in deepwater rice, Plant Cell 9 (1997) 1661–1671.
[25] Y. Wu, R.E. Sharp, D.M. Durachko, D.J. Cosgrove, Growth maintenance of the maize primary root at low water potentials involves increases in cell-wall extension properties, expansin activity, and wall susceptibility to expansins, Plant Physiol. Biochem. 111 (1996) 765–772.
[26] Y. Wu, D.J. Cosgrove, Adaptation of roots to low water potentials by changes in cell wall extensibility and cell wall proteins, J. Exp. Bot. 51 (2000) 1543–1553.
[27] I.B. Sabirzhanova, B.E. Sabirzhanov, A.V. Chemeris, D.S. Veselov, G.R. Kudoyarova, Fast changes in expression of expansin gene and leaf extensibility in osmotically stressed maize plants, Plant Physiol. Biochem. 43 (2005) 419–422.
[28] D.L. Rayle, R.E. Cleland, Enhancement of wall loosening and elongation by acid solutions, Plant Physiol. 46 (1970) 250–253.
[29] A. Hager, H. Menzel, A. Krauss, Versuche und Hypothese zur Primärwirkung des Auxins beim Streckungswachstum, Planta 100 (1971) 47–75.
[30] A. Hager, Role of the plasma membrane $H^+$-ATPase in auxin-induced elongation growth: historical and new aspects, J. Plant Res. 116 (2003) 483–505.
[31] W.S. Peters, H. Felle, Control of apoplast pH in corn coleoptile segments. I: the endogenous regulation of cell wall pH, J. Plant Physiol. 137 (1991) 655–661.
[32] M. Jacobs, P.M. Ray, Rapid auxin-induced decrease in free space pH and its relationship to auxin-induced growth in maize and pea, Plant Physiol. 58 (1976) 203–209.
[33] K.H. Mühling, C. Plieth, U.P. Hansen, B. Sattelmacher, Apoplastic pH of intact leaves of *Vicia faba* as influenced by light, J. Exp. Bot. 46 (1995) 377–382.
[34] D.J. Cosgrove, Loosening of plant cell walls by expansins, Nature 407 (2000a) 321–326.
[35] C.D. Buchanan, S. Lim, R.A. Salzman, I. Kagiampakis, D.T. Morishige, B.D. Weers, *Sorghum bicolor*'s transcriptome response to dehydration, high salinity and ABA, Plant Mol. Biol. 58 (2005) 699–720.
[36] B. Pitann, C. Zörb, K.H. Mühling, Comparative proteome analysis of maize (*Zea mays* L.) expansins under salinity, J. Plant Nutr. Soil Sci. 172 (2009a) 75–77.
[37] Y. Wu, R.B. Meeley, D.J. Cosgrove, Analysis and expression of the α-expansin and β-expansin gene families in maize, Plant Physiol. 126 (2001) 222–232.
[38] N.C. Carpita, Structure and biogenesis of the cell walls of grasses, Annu. Rev. Plant Physiol. Plant Mol. Biol. 47 (1996) 445–476.
[39] B. Reidly, S.J. McQueen-Mason, J. Nösberger, A.J. Fleming, Differential expression of α- and β-expansin genes in the elongating leaf of *Festuca pratensis*, Plant Mol. Biol. 46 (2001) 491–504.
[40] S.Y. Hong, P.J. Seo, M.S. Yang, F. Xiang, C.M. Park, Exploring valid reference genes for gene expression studies in *Brachypodium distachyon* by real-time PCR, BMC Plant Biol. 8 (2008) 112–122.
[41] A. Sümer, C. Zörb, F. Yan, S. Schubert, Evidence of sodium toxicity for the vegetative growth of maize (*Zea mays* L.) during the first phase of salt stress, J. Appl. Bot. 78 (2004) 135–139.
[42] W. De Costa, C. Zörb, W. Hartung, S. Schubert, Salt resistance is determined by osmotic adjustment and abscisic acid in newly developed maize hybrids in the first phase of salt stress, Physiol. Plant. 131 (2007) 311–321.
[43] S. Schubert, A. Neubert, A. Schierholt, A. Sümer, C. Zörb, Development of salt resistant maize hybrids: the combination of physiological strategies using conventional breeding methods, Plant Sci. 177 (2009) 196–202.
[44] J. Doorenbos, A.H. Kassam, Yield response to water. in: FAO (Ed.), FAO Irrigation and Drainage Paper, FAO (1979), p. 160 Rome.
[45] D.J. Cosgrove, Expansive growth of plant cell walls, Plant Physiol. Biochem. 38 (1/2) (2000b) 109–124.
[46] S. McQueen-Mason, Expansins and cell wall expansion, J. Exp. Bot. 46 (1995) 1639–1650.
[47] B. Pitann, T. Kranz, K.H. Mühling, The apoplastic pH and its significance in adaptation to salinity in maize (*Zea mays* L.): comparison of fluorescence microscopy and pH-sensitive microelectrodes, Plant Sci. 176 (2009b) 497–504.
[48] S. McQueen-Mason, D.M. Durachko, D.J. Cosgrove, Two endogenous proteins that induce cell wall expansion in plants, Plant Cell 4 (1992) 1425–1433.
[49] M.M. Bradford, A rapid and sensitive method for the quantitation of microgram quantities of protein using the method of protein dye bonding, Anal. Biochem. 72 (1976) 248–254.
[50] N.H. Yennawar, L.C. Li, D.M. Dudzinksi, A. Tabuchi, D.J. Cosgrove, Crystal structure and activities of EXPB1 (Zea m 1), β-expansin and group-1 pollen allergen from maize, Proc. Natl. Acad. Sci. U. S. A. 103 (2006) 14664–14671.
[51] K.H. Cox, R.B. Goldberg, Isolation of total RNA. in: C.H. Shaw (Ed.), Plant Molecular Biology. IRL Press, Oxford, 1988, pp. 2–8.

# Supplementary data

**Table I Synthetic peptide used for production of vegetative β-expansin antibody in rabbit**

| | Region of highest sequence homology | | |
|---|---|---|---|
| **Gene (Genbank Acc. No.)** | **Position of amino-acid residue** | **Detail with highest sequence homology (grey shadow)** | **Homology to synthetic peptide (%)** |
| ZmExpB2 **AF332175** | L152-T166 | LVARNVIPANWRPNT | 100 |
| ZmExpB8 **AF332176** | L163-T177 | LVANNVIPANWRPNT | 93.4 |
| ZmExpB5 **AF332177** | L193-N207 | LVATRVIPANWAPNT | 80.0 |
| ZmExpB7 **AF332178** | L254-V268 | LVADHVIPANWVPNT | 80.0 |
| ZmExpB3 **AF332179** | L154-T168 | LVADQVIPADWQPDN | 60.0 |
| ZmExpB6 **AF332180** | L246-T160 | LVAKNVIPANYIPDV | 66.7 |
| ZmExpB4 **AF332181** | L175-K189 | LVANNAIPAAWKPGK | 60.0 |

**Legend table I**

An antibody (anti-ZmExpB) was generated for detecting simultaneously seven vegetatively expressed β-expansin isoforms in maize (*Zea may* L.). For this reason, amino-acid sequences of all seven isoforms (1st column) were compared by multiple sequence alignment in order to find a peptide with the highest sequence homology within all isoforms (CLUSTAL 2.0.12 detail with highest sequence homology of all isoforms shown in 3rd column; grey shadow means that the residues in that column are identical in all sequences in the alignment). The 15-amino-acid oligopeptide LVARNVIPANWRPNT, which represents the sequence with highest homology within all seven β-expansin isoforms, was synthesized and used for rabbit immunization. This synthetic peptide is equivalent to the amino-acid residue L152-T166 of ZmExp2. The homology of all seven vegetative β-expansin isoforms to the synthetic peptide is given in 4th column (shown in %). Gene bank numbers are according to http://www.ncbi.nlm.nih.gov/.

**Table II Parameters for real-time quantitative RT-PCR primers**

| Gene (Genbank Acc. No.) | | Sequence (5'->3') | Length [bp] | $T_m$ [°C] | GC-content [%] | Specific annealing temp. [°C] | Product length [bp] |
|---|---|---|---|---|---|---|---|
| *ZmExpB2* | sense | CTACCGCTCCTTCGTCCAGT | 20 | 62 | 60 | 64.6 | 225 |
| (**AF332175**) | antisense | GCAACGACTCAAAGGACCAT | 20 | 60 | 50 | | |
| *ZmExpB3* | sense | ACTACTACCCGGTGGCCCCC | 20 | 66 | 70 | 63.3 | 105 |
| (**AF332176**) | antisense | CGATGATTCCTGCGTGCCTT | 20 | 66 | 55 | | |
| *ZmExpB5* | sense | TCCATCTGGAGGCTGGACG | 19 | 65 | 63 | 56.0 | 107 |
| (**AF332178**) | antisense | TTGGCAGGGATGACCCGAG | 19 | 67 | 63 | | |
| *ZmExpB6* | sense | GCTCCGGCGTGGCTCAG | 17 | 67 | 76 | 53.9 | 337 |
| (**AF332179**) | antisense | ATGGAGCCCCAGGACTCGT | 19 | 64 | 63 | | |
| *ZmExpB7* | sense | CAACCTTGTCCTCCACAGTAG | 21 | 57 | 52 | 63.3 | 109 |
| (**AF332180**) | antisense | GTGAGGTCGGAGGCGTTAAA | 20 | 62 | 55 | | |
| *ZmExpB8* | sense | TTCAAGCACACCAACCAG TA | 20 | 58 | 45 | 63.3 | 106 |
| (**AF332181**) | antisense | TGCACCGAATCTTGTAGCAG | 20 | 60 | 50 | | |
| *ZmUBC* | sense | GTCCTGCTCTCCATCTGCTC | 20 | 61 | 60 | 52-65 | 113 |
| (**AF034946.1**) | antisense | CGGGCCGTCGACTCGTACTT | 20 | 64 | 65 | | |

**Legend table II**

Table of primer pairs for the detection of vegetatively expressed β-expansins of maize as used in real-time quantitative RT-PCR experiments. Gene bank numbers are according to http://www.ncbi.nlm.nih.gov/. Specific annealing temperature for the sense and antisense primer pair used are shown in 7$^{th}$ column. *ZmUBC* primer pairs have excellent annealing quality in a range between 52°C to 68°C. The predicted length of all PCR-product is given in 8$^{th}$ column.

# Chapter 3

## Differential transcript expression of wall-loosening candidates in leaves of maize cultivars differing in salt resistance

Christoph-Martin Geilfus, Christian Zörb, Christina Neuhaus, Tim Hansen, Hartwig Lüthen

and Karl H. Mühling

Journal of Plant Growth Regulation DOI 10.1007/s00344-011-9201-4

J Plant Growth Regul
DOI 10.1007/s00344-011-9201-4

# Differential Transcript Expression of Wall-loosening Candidates in Leaves of Maize Cultivars Differing in Salt Resistance

**Christoph-Martin Geilfus · Christian Zörb · Christina Neuhaus · Tim Hansen · Hartwig Lüthen · Karl H. Mühling**

Received: 3 November 2010 / Accepted: 17 January 2011


**Abstract** Salt-sensitive crop plants such as maize (*Zea mays* L.) exhibit a strong and rapid growth reduction in response to NaCl stress. The unique salt-resistant maize hybrid SR03 and the salt-sensitive maize hybrid Lector provide good tools to characterize various genotypic responses to salinity in terms of shoot growth, shoot extensibility, and the expression pattern of wall-loosening candidates. The mRNA transcript levels of wall-loosening candidates such as xyloglucan endotransglucosylase (XET), endo-1,4-$\beta$-D-endoglucanase (EGase), $\alpha$-expansins (EXPA), and the plasma membrane proton pump (PM-$H^+$-ATPase) are correlated with cell-wall extensibility and with shoot growth under NaCl stress. We have found for the salt-sensitive maize that a decrease in the relative transcript abundance of ZmXET1, ZmEXPA1, and the composite PM-$H^+$-ATPase mRNAs correlates with a decrease in wall extensibility and shoot growth. We suggest that this downregulation of wall-loosening candidates contributes to a reduction in extensibility and consequently in growth. In contrast, the decrease in wall extensibility is less strong in the salt-sensitive hybrid SR03. In the salt-resistant maize genotype, an upregulation of ZmXET1, ZmEXPA1 and PM-$H^{+-}$ATPase transcripts possibly mitigates the salinity-induced decrease in wall extensibility and thus in shoot growth.

**Keywords** Salinity · Growth inhibition · Wall extensibility · XET · EGase · PM-$H^+$-ATPases · $\alpha$-expansins · Real-time quantitative RT-PCR

## Introduction

Plant growth responds to salinity in two phases: a first rapid osmotic phase that decreases the growth rate of young leaves and a second ionic-toxic phase in which the senescence of mature leaves accelerates. The mechanism that downregulates the growth of young leaves under salt stress is not precisely known. Changes in the mechanical properties of the cell wall have been demonstrated to control elongation-type growth in most systems studied so far and are predicted to be involved in salinity-related growth adaptations (Cramer and Bowmann 1991; Munns 1993; Munns and Tester 2008).

The primary cell wall of plants is a complex polymeric network that must provide a rigid constraint to cell turgor and yet be sufficiently compliant to allow controlled cell expansion. The cell-wall framework is composed primarily of cellulose microfibrils embedded in matrices of hemicellulosic and pectic polymers, with additional minor components such as structural proteins (Carpita and Gibeaut 1993; Catalá and others 1997; Cosgrove 1997). According to

**Electronic supplementary material** The online version of this article (doi:10.1007/s00344-011-9201-4) contains supplementary material, which is available to authorized users.

C.-M. Geilfus (✉) · C. Zörb · C. Neuhaus · K. H. Mühling
Institute of Plant Nutrition and Soil Science, Christian Albrechts University, Hermann-Rodewald-Str. 2, 24118 Kiel, Germany
e-mail: cmgeilfus@plantnutrition.uni-kiel.de

C. Zörb
e-mail: czoerb@plantnutrition.uni-kiel.de

C. Neuhaus
e-mail: cneuhaus@plantnutrition.uni-kiel.de

K. H. Mühling
e-mail: khmuehling@plantnutrition.uni-kiel.de

T. Hansen · H. Lüthen
Biozentrum Flottbek, University of Hamburg, Ohnhorststr. 18, 22609 Hamburg, Germany
e-mail: timhansenbc@live.de

H. Lüthen
e-mail: h.luthen@botanik.uni-hamburg.de

Published online: 25 February 2011

current models of primary walls (Carpita and Gibeaut 1993), cellulose microfibrils interact with matrix components such as hemicelluloses and form a complex network. Xyloglucan, an extremely abundant hemicellulosic compound in primary cell walls, binds noncovalently to cellulose microfibrils and thus coats and crosslinks adjacent microfibrils. This results in an extensive xyloglucan-cellulose network that is thought to act as the major tension-bearing structure in the primary wall (Hayashi 1989; McCann and others 1990; Rose and others 2002). However, the primary cell wall is also capable of expanding, indicating that the interactions between wall polymers can be modified to make walls extensible for elongation (Wu and others 2001; Cosgrove 2005). Nevertheless, cellulose microfibrils are neither extensible nor degradable during cell elongation; they can only move apart. This explains why the network between microfibrils is crucial for determining cell-wall yielding behavior (Wu and others 2001).

Cell-wall enlargement begins with wall stress relaxation, allowing the cells physically to enlarge. According to the acid growth theory, an auxin-mediated acidification of the leaf apoplast is the major requirement for increasing wall extensibility (Hager and others 1971; Hager 2003). This theory is supported by the finding that the fungal toxin fusicoccin and, at least in part, the plant hormone auxin mediate the acidification of the apoplast below a pH of 5.0, thus stimulating cell elongation in maize and pea (Jacobs and Ray 1976; Peters and others 1998). Auxin is assumed to cause the plasma-membrane proton pump (PM-$H^+$-ATPase) to actively pump protons from the cytosol into the apoplast, resulting in wall-loosening and cell expansion (Moriau and others 1999). The pH of the apoplast of growing cells typically lies between 4.7 and 6 (Mühling and others 1995), which is the range in which acidification activates expansin activity (Cosgrove 2005). Expansins are a group of nonenzymatic cell-wall proteins that are thought to mediate acid-induced growth. In this context, isolated cell walls have been shown to exhibit acid growth resulting from the action of these pH-dependent wall-loosening proteins (Cho and Kende 1997). However, the precise way in which expansins mediate wall enlargement remains unclear. One interpretation is that expansins intercalate within carbohydrate matrices in the cell wall, leading to the transient loosening of noncovalent interactions, and thus enhance the ability of these matrices to move relative to each other (Cosgrove 2000, 2005). In addition to expansin, other candidate wall-loosening proteins are assumed to contribute to cell elongation. Catalá and others (1997) have summarized that xyloglucan undergoes substantial depolymerization and solubilization during auxin-induced cell elongation, suggesting that xyloglucan turnover is integral to auxin-induced cell-wall loosening. An enzymatic modification of load-bearing xyloglucan tethers, resulting in cell-wall loosening, is considered a key process necessary for cell expansion (Fry 1989). Xyloglucan-metabolizing enzymes therefore represent potentially important agents in controlling wall strength and extensibility. The basis of xyloglucan metabolism during cell elongation is not precisely known, but the involvement of endo-1,4-$\beta$-D-glucanases (EGases) and xyloglucan endotransglucosylase/hydrolase (XTH) has been suggested (Fry 1989; Nishitani 1995).

It has been proposed that EGases act primarily on the $\beta$-1,4-linked glucan backbone of xyloglucan in the plant cell wall (Hayashi 1989; Catalá and others 1997). The enzyme is thought to digest the noncrystalline regions of cellulose microfibrils and to release trapped xyloglucans, whereby this cleavage of load-bearing xyloglucan allows cell growth (Cosgrove 2005). Moreover, increased EGase enzyme activity is associated with auxin-stimulated cell enlargement. The enzyme xyloglucan endotransglucosylase/hydrolase (XTH) is involved in the modification of cell-wall structure by acting on the xyloglucans attached to cellulose microfibrils. One action of XTH proteins is referred to enzymologically as xyloglucan endotransglucosylase (XET) activity (Rose and others 2002; Vissenberg and others 2005; Genovesi and others 2008). XETs cleave and rejoin xyloglucan chains or suitable xyloglucan-derived oligosaccharides and are therefore candidates for wall-loosening. XET-mediated transglucosylation between two potentially load-bearing xyloglucan molecules is thought to allow incremental slippage of adjacent microfibrils by facilitating hydrostatic pressure of the protoplasm against this weakened wall. This results in a "creep" of cellulose microfibrils (Nishitani 1995; Catalá and others 1997; Vissenberg and others 2005).

Because salinity inhibits cell elongation in young leaves and because proteins such as xyloglucan endotransglucosylases, endo-1,4-$\beta$-D-glucanases, PM-$H^+$-ATPases, and expansins are believed to play key roles in cell-wall extension, the transcript expression patterns of these wall-loosening candidates have been correlated with the wall extensibility and growth of maize shoots under conditions of salt stress.

## Materials and Methods

### Plant Cultivation

The salt-sensitive maize hybrid Lector and the highly salt-resistant maize hybrid SR03 (*Zea mays* L.; Schubert and others 2009) were grown in greenhouses under hydroponic culture conditions. The experimental setup consisted of three independent replicates of the salt-treated plants (100 mM NaCl) and the corresponding control plants (1 mM NaCl). Each biological replicate was run in triplicate in a completely randomized design. The roots of seedlings were embedded in

1 mM $CaSO_4$ in an aerated solution at 25°C for 1 day and placed between filter papers moistened with 1 mM $CaSO_4$ for a period of 3 days. Subsequently, the seedlings were transferred to 4.5-L plastic pots (3 plants per pot) containing one-quarter-strength nutrient solution. After 2 days of cultivation, the concentration of nutrients was increased to half-strength and, after 4 days of cultivation, to full-strength. The nutrient solution had the following composition: 2.5 mM $Ca(NO_3)_2$, 1.0 mM $K_2SO_4$, 0.2 mM $KH_2PO_4$, 0.6 mM $MgSO_4$, 5.0 mM $CaCl_2$, 1.0 μM $H_3BO_4$, 2.0 μM $MnSO_4$, 0.5 μM $ZnSO_4$, 0.3 μM $CuSO_4$, 0.005 μM $(NH_4)_6Mo_7O_{24}$, and 200 μM Fe-EDTA. The solution was changed every second day to avoid nutrient depletion. NaCl treatment was started 2 days after the full-nutrient concentration had been reached and was increased stepwise by 25-mM increments every second day. Temperature was kept constant at 26°C for the light period and at 18°C for the dark period; relative humidity was set to about 70%.

In this study, only young expanding shoot material that had developed entirely under the full influence of the 8-day 100-mM NaCl treatment was harvested. Any remaining older shoot material that had started to develop before the full-strength NaCl concentration had been reached was not taken into account. After the measurement of fresh weight, leaf material was immediately frozen in liquid nitrogen. Tissues used for extensibility measurements were then stored at −20°C. For RNA analysis, leaves were ground in liquid nitrogen and stored at −80°C.

### $N_{creep}$ Measurement

Measurement of cell-wall extensibility was carried out as described previously (Büntemeyer and others 1998). Briefly, frozen-thawed basal sections of leaves were clamped between the tips of an extensiometer and incubated in a 10-mM K-phosphate buffer, pH 7.2. Extension was measured by using a positional angular transducer (TWK Instruments, Düsseldorf, Germany), which could be equilibrated with a counterweight. Further weights could be placed on the counterweight axis to induce extension. For inducing creep, we used a weight of 20 g. Time courses of creep were found to be excellently represented by a logarithmic function of the type

$$L = L_0 + N_{\mathrm{Creep}} * \log t$$

with $t$ being the time that had elapsed since the application of the weight. $N_{creep}$ is a measure of the slope of the cell-wall creep; this has previously been shown to represent growth-relevant changes in the cell-wall rheology of maize root cell walls (Büntemeyer and others 1998). $L_0$ reflects the initial change in length once the weight had been added. The extensiometer software and the data regression software were developed in house by HL.

### Primer Design for Polymerase Chain Reaction

For analyzing the mRNA transcript level of wall-loosening candidates, group-specific, that is, degenerated, and isoform-specific polymerase chain reaction (PCR) primer pairs were designed (Table 1). Primer pairs for amplifying *Zea mays* xyloglucan endotransglucosylase homolog 1 (*ZmXET1*) and *Zea mays* ubiquitin-conjugating enzyme (*ZmUBC*; used as reference gene for real-time quantitative reverse transcription [qRT]-PCR) were designed by means of Primer3Plus and Primer-BLAST software (http://bioinformatics.nl/cgi-bin/primer3plus/primer3plus.cgi; http://www.ncbi.nlm.nih.gov/). Primer pairs for analyzing three *Zea mays* α-expansin-isoforms (*ZmEXPA1*, *ZmEXPA3*, and *ZmEXPA4*; Table 1) were designed on the basis of nucleotide alignments (ClustalW, http://www.clustal.org). To measure the transcript level of four composite *Zea mays* membrane-$H^+$-ATPases (*ZmMHA1*, *ZmMHA2*, *ZmMHA3*, and *ZmMHA4*), we created a degenerated, that is, group-specific, primer that was designed by first generating a multiple alignment and then manually identifying the most conservative regions for primer design. Henceforth, this degenerated primer pair is referred to as primer pair *ZmMHA_fam* (Table 1). A degenerated, that is, group-specific, primer pair for *Zea mays* endoglucanases was designed on the basis of three sequences available at the NCBI GenBank (http://www.ncbi.nlm.nih.gov; *Zea mays* endoglucanase 1 LOC100285069, *Zea mays* endoglucanase 1 LOC100285091, and *Zea mays* endoglucanase cl6880_1; see Table 1 for GenBank accession numbers). This group-specific primer pair (*ZmEGases*; Table 1) allows the quantitation of the composite transcript level and was designed as described for *ZmMHA_fam.* All primer pairs were purchased from Eurofins MWG Operon (Ebersberg, Germany). For the prevention of false priming sites, all primer pairs were checked *in silico* by BLASTN against a *Zea mays* nucleotide collection (nr/nt) and *Zea mays* reference mRNA sequences (refseq_rna). To avoid primer-dimer formation and the formation of hairpin structures, primers were evaluated *in silico* by using Primer-BLAST and Primer3Plus.

For demonstrating the specificity of the degenerated primer/template interactions, and for proving that no cross-amplifications bias the measurements, the real-time qRT-PCR products were sequenced (MWG Eurofins, Munich, Germany). DNA sequencing of the amplicons that were generated with the degenerated primer pairs (*ZmMHA_fam* or *ZmEGases*) revealed correct products. No undesired PCR products were generated (Supplementary Table 1). Moreover, dissociation curve analysis (data not shown) gave no suggestion of erroneous amplification of templates during real-time qRT-PCR. Furthermore, after real-time qRT-PCR measurements, agarose gels were run to ensure that only a PCR product with the correct length was amplified (Supplementary Fig. 1).

**Table 1** Real-time quantitative RT-PCR primer pairs for maize (*Zea mays* L.)

| Primer name | GenBank accession No. | Sequence of forward (f) and reverse (r) primers (5′–3′) | | Annealing temp (°C) | Product size (bp) |
|---|---|---|---|---|---|
| *ZmXET1* | NM_001111897.1 | f | CTACCAGGACGTGGACATCA | 63.3 | 208 |
| | | r | ACCCTGCGACGAAAGATAGA | | |
| *ZmEGases* | NM_001157986 | f | SMGSVVGCAGRTGGACTAC | 60.0 | 200 |
| | NM_001157964 | r | CGRYGAGCWSGTTGGGRTT | | |
| | NM_001158465 | | | | |
| *ZmMHA_fam* | NM_001111890 | f | AGCCAGGCYCTKATCTTCGT | 64.0 | 195 |
| | NM_001112000 | | | | |
| | AJ441084 | r | SACGATGYTGTASAGCCAGA | | |
| | AJ539534 | | | | |
| *ZmEXPA1* | AAK56119 | f | ATGGCGGCAGCTGCTAGTG | 65.9 | 100 |
| | | r | CGCTCTGCCACGAGCCGTA | | |
| *ZmEXPA3* | AAK56121 | f | CGCCACCTTCTATGGCGGTA | 633 | 171 |
| | | r | GCCTGGTAGTCGCAGGAGAT | | |
| *ZmEXPA4* | AAK56122 | f | GTGCCGTGCCGCAAGTCC | 65.5 | 126 |
| | | r | GCTGGCCGCCTTGACGCT | | |
| *ZmUBC* | AF034946.1 | f | GTCCTGCTCTCCATCTGCTC | 52.0–65.0 | 113 |
| | | r | CGGGCCGTCGACTCGTACTT | | |

XET = xyloglucan endotransglucosylase; EGases = endoglucanases; MHA = plasma membrane (PM) proton pump ($H^+$)-ATPase; EXPA = α-expansins; UBC = ubiquitin-conjugating enzyme

The letter code Y, K, S, R, or M within the primer sequences represents abbreviations for nucleotide combinations following IUPAC recommendations (Nomenclature Committee of NC-IUB and IUPAC-IUB Joint Commission on Biochemical Nomenclature)

No adequate primer pairs were found for the α-expansin isoforms *ZmEXP2* and *ZmEXP5*.

## RNA Extraction and cDNA Synthesis

Aliquots of 100 mg ground shoot material were used for RNA extraction. Total maize RNA was isolated according to a modified method of Cox and Goldberg (1988). The quality and quantity of RNA was checked by $OD_{260}$. Poly(A)$^+$ RNA purification was carried out with oligo(dT)$_{25}$-coupled paramagnetic particles (Dynabeads® mRNA Purification Kit, Invitrogen GmbH, Karlsruhe, Germany) by using 75 µg total RNA according the instructions of the manufacturer. Highly purified maize poly(A)$^+$ RNA (3 µg) was reverse-transcribed in a 10-µl cDNA reaction with a first-strand cDNA synthesis system following the manufacturer's instructions (SuperScript® VILO cDNA synthesis kit, Invitrogen). Single-stranded cDNA was diluted to a concentration dependent on the level of expression of the studied gene; cDNA was aliquoted to avoid discrepancy in the data attributable to the repetition of freezing-thawing cycles.

## Real-time Quantitative RT-PCR

The SYBR® Green-based real-time qRT-PCR technique was performed on an Applied Biosystems 7300 real-time PCR system. For each reaction, 2 µl diluted single-stranded cDNA was used in a total volume of 20 µl (0.8 pM each forward and reverse primer, 0.82 mM dNTP mix, 0.1 × SYBR Green, 1 × ROX, 0.6 U *Taq* DNA polymerase; Invitek, Berlin, Germany). After an initial denaturation step (92°C, 2 min), real-time qRT-PCR was carried out over 40 cycles [denaturation: 92°C, 30 s; amplification and quantification: 40 s (for primer-pair-specific temperatures, see Table 1), elongation: 72°C, 20 s]. To check the specificity of the annealing of the oligonucleotides, dissociation kinetics were performed by the real-time PCR system at the end of the experiment (60–95°C, continuous fluorescence measurement). The comparative $C_t$ (threshold cycles) method of relative quantification was used to analyze the real-time qRT-PCR data. With this method, the $C_t$ values were normalized by comparison with the endogenous reference gene, that is, the ubiquitin-conjugating enzyme. The normalized $C_t$ values were then used to compare NaCl-treated plants and corresponding controls. Data were expressed as the relative change in transcript expression (+100 relative expression = 2-fold upregulation; −100 relative expression = 2-fold downregulation). Threshold cycles were calculated by the internal software of the real-time PCR system and were the means of three biological replicates of each run in triplicate. The sizes of amplified products were confirmed by gel electrophoresis.

Negative controls with no templates were carried out concurrently.

## Results

### Shoot Growth and Wall Extensibility

All measurements were based on expanding leaf material derived from plants grown entirely under the influence of an 8-day 100-mM NaCl treatment. In response to the salt treatment, a significant decrease in shoot fresh weight of about 60% was measured for the salt-sensitive cultivar Lector when compared with control plants (Fig. 1). In contrast, only a slight decrease in shoot fresh weight was measured for the salt-resistant SR03. This was not significant. Creep activity ($N_{creep}$) was used as a rheological parameter to monitor wall extensibility in shoots (Table 2). Under conditions of salt stress, $N_{creep}$ decreased in both genotypes. The percentage of $N_{creep}$(100 mM NaCl) on $N_{creep}$(control) was about 80% for Lector and 90% for SR03. Thus, in response to salt treatment, $N_{creep}$ decreased about 20% in the salt-sensitive hybrid Lector and about 10% in the salt-resistant hybrid SR03.

### Relative Transcript Expression

The effect of salt treatment on the relative transcript abundance of wall-loosening candidates was studied on the basis of purified poly(A)$^+$ RNA by using the real-time qRT-PCR technique. In comparison with various reference genes, the ubiquitin-conjugating enzyme was validated as the most stable reference gene, being particularly useful for the analysis of genes in salt-treated samples (Hong and others 2008). Because the report of Hong and others (2008) was based also on a monocot grass species (*Brachypodium distachyon*), we used ubiquitin-conjugating enzyme as the reference gene. In response to the 8-day 100-mM NaCl treatment, *ZmXET1* was downregulated in the salt-sensitive hybrid Lector but upregulated in the salt-resistant hybrid SR03 (Fig. 2a). The composite transcript abundance of *ZmEGases* was downregulated in both genotypes, whereas this downregulation was not noticeably different between the two genotypes (Fig. 2b). *ZmEXPA1* was downregulated

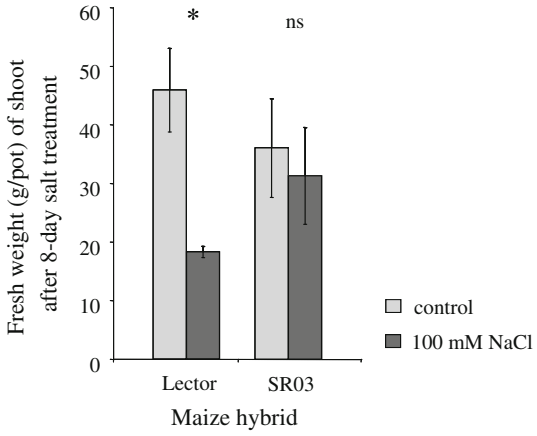


**Fig. 1** Effect of salt treatment on shoot growth. Biomass reduction of expanding maize shoots (*Zea mays* L.) under conditions of salinity. Plants were treated with 100 mM NaCl for 8 days. Only expanding leaves grown entirely under the influence of the 8-day NaCl treatment and corresponding controls were studied. The remaining older shoot material was not considered. Control (*light gray*); 100 mM NaCl (*dark gray*). Data are means of three biological replicates ± SE. Each measurement was carried out in triplicate. Asterisk indicates significant differences between treatments ($p \leq 0.05\%$; ns, not significant)

**Table 2** Effect of 8-day 100-mM NaCl treatment on $N_{creep}$ activity

| Hybrid | Treatment | $N_{creep}$ | | | |
|---|---|---|---|---|---|
| | | Mean | *n* | SE | % $N_{creep}$(100 mM NaCl) on $N_{creep}$(control) |
| Lector | Control | 3.91 | 30 | 0.77 | 80.8 |
| | 100 mM NaCl | 3.16 | 29 | 0.43 | |
| SR03 | Control | 2.55 | 36 | 0.33 | 90.1 |
| | 100 mM NaCl | 2.30 | 34 | 0.19 | |

*SE* standard error of the mean, *n* number of replicates

Maize genotypes: Lector, salt-sensitive; SR03, salt-resistant

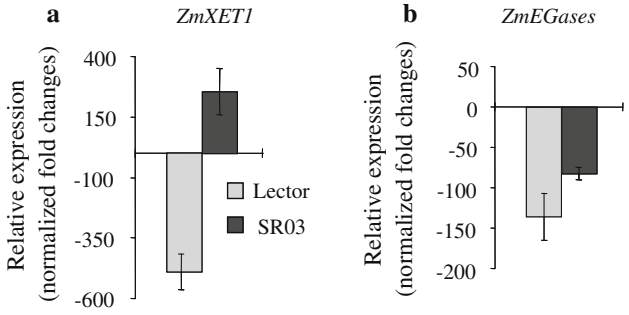


**Fig. 2** Effect of salt treatment on relative XET1 and EGases transcript abundance as measured by SYBR Green-based real-time quantitative RT-PCR. Relative expression changes in response to an 8-day 100-mM NaCl treatment of (**a**) xyloglucan endotransglucosylase homolog 1 (*ZmXET1*) and (**b**) endoglucanases (*ZmEGases*). Isoforms of three endoglucanases were detected simultaneously by using a degenerated, that is, family-specific, primer pair (see Materials and Methods section). The transcript for ubiquitin-conjugating enzyme was used as the endogenous control in an Applied Biosystems 7300 real-time PCR system. Data show the effect of salt treatment on the relative transcript abundance, with the control as the calibrator sample (+100 relative expression = 2-fold upregulation, −100 relative expression = 2-fold downregulation). Salt-sensitive Lector (*light gray*); salt-resistant SR03 (*dark gray*). Expression data correspond to means of three biological replicates, each being run in triplicate, ±SE

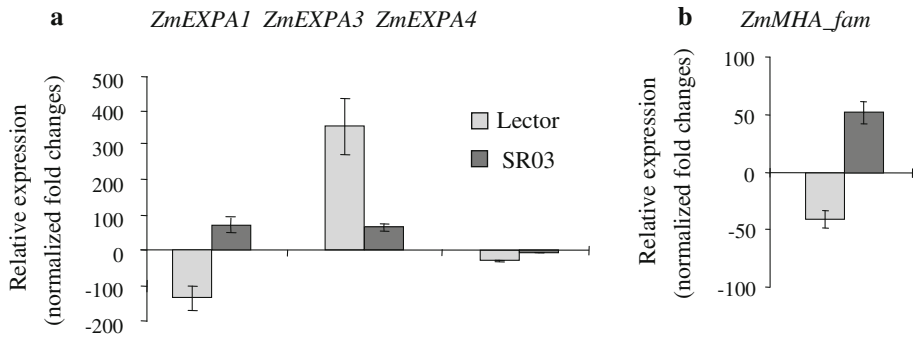


**Fig. 3** Effect of salt treatment on the relative transcript abundance of EXPA1, EXPA2, EXPA3, and MHA1-4 as measured by SYBR Green-based real-time quantitative RT-PCR. Relative expression changes in response to an 8-day 100-mM NaCl treatment of (**a**) α-expansin-isoforms (*ZmEXPA1*, *ZmEXPA3*, and *ZmEXPA4*) and (**b**) four plasma membrane $H^+$-ATPase isoforms (*ZmMHA1*, *ZmMHA2*, *ZmMHA3*, and *ZmMHA4*). Isoforms of four plasma membrane $H^+$-ATPases were detected simultaneously by using a degenerated, that is, family-specific, primer pair *ZmMHA_fam* (see Materials and Methods section). The transcript for ubiquitin-conjugating enzyme was used as the endogenous control in an Applied Biosystems 7300 real-time PCR system. Data show the effect of salt treatment on the relative transcript abundance with the control as the calibrator sample (+100 relative expression = 2-fold upregulation, −100 relative expression = 2-fold downregulation). Salt-sensitive Lector (*light gray*); salt-resistant SR03 (*dark gray*). Expression data correspond to means of three biological replicates, each being run in triplicate, ±SE

in the salt-sensitive hybrid Lector but upregulated in the salt-resistant hybrid SR03 (Fig. 3a). The isoform *ZmEXPA3* was upregulated in both genotypes, whereas *ZmEXPA4* was not affected under conditions of salt stress (Fig. 3a). The composite relative transcript expression of all four PM-$H^+$-ATPase isoforms was downregulated in the salt-sensitive hybrid Lector but upregulated in the salt-resistant hybrid SR03 (Fig. 3b).

## Discussion

This study was based on the use of young expanding leaf material (*Zea mays* L.) grown entirely under the influence of exogenously added 100 mM NaCl. For this reason, the tissue adequately reveals the effect of the 8-day salt treatment on growth. The salt-sensitive maize hybrid Lector showed a significant shoot growth reduction of 60%, whereas the highly salt-resistant SR03 hybrid exhibited no significant growth reduction under conditions of salinity (Fig. 1). These findings are in line with previously reported results describing the effect of salinity on shoot growth for these two genotypes (Geilfus and others 2010). The ability of the salt-resistant hybrid SR03 to maintain growth under condition of salt stress is remarkable, because salinity has been widely described in the literature as inhibiting the growth of young leaves via an inhibition of cell division and cell elongation (Mühling and Läuchli 2002; Munns and Tester 2008). SR03 maize was originally developed and characterized as being highly salt-resistant; it shows no harvest deficits under 10 dS $m^{-1}$ soil salinity (Schubert and others 2009), whereas a soil conductivity of 6 dS $m^{-1}$ usually leads to a 50% reduced harvest of almost all recent maize genotypes (Doorenbos and Kassam 1976).

Taking into account that the mechanisms that downregulate leaf growth under salt stress are not precisely known, the unique, highly salt-resistant maize genotype SR03 and the salt-sensitive genotype Lector provide good tools to characterize differences in wall extensibility and growth and, thus, differences in the expression patterns of wall-loosening candidates.

### Cell-wall Extensibility of Maize Shoots in Response to Salinity

Under salinity, rheological changes are predicted to occur in cell-wall properties, although their nature remains unknown (Cramer and Bowmann 1991; Munns and Tester 2008). In the current study, the salinity-induced rheological properties of the wall have been monitored by measuring creep activity ($N_{creep}$). $N_{creep}$ has been shown to follow changes in the volumetric extensibility parameter from the Lockhart equation, which cannot be directly determined. Thus, creep activity is an adequate parameter for measuring growth-relevant processes in the cell wall of maize (Büntemeyer and others 1998). In response to salt treatment, creep activity decreases more strongly in the shoot of the salt-sensitive hybrid Lector as compared with the salt-resistant hybrid SR03 (Table 2). Because creep activity reflects changes in the volumetric extensibility (Büntemeyer and others 1998), these results show that the decrease in wall extensibility is more pronounced for the salt-sensitive hybrid Lector than for the salt-resistant SR03. This probably contributes to the remarkable genotypic differences in terms of shoot growth, with reduction being greater in the salt-sensitive Lector (Fig. 1).

These detected changes in wall extensibility strongly suggest an effect of salinity on elements that alter the rheological properties of the cell wall. In favor of this assumption, we have detected a genotype-specific stress response in terms of *ZmXET1* transcript expression (Fig. 2a).

### Genotype-specific XET1 and EGases Transcript Abundances in Response to Salinity

Genovesi and others (2008) have suggested that ZmXET1 is bound to the cell wall, thereby encouraging the idea that ZmXET action affects the physical properties of the cell wall. Moreover, Saab and Sachs (1995) have assumed an involvement of ZmXET in cell-wall metabolism during processes leading to structural wall modifications. Furthermore, XET is proposed to play a role in wall-loosening during cell expansion, thereby allowing molecular grafting between polysaccharide chains that crosslink cellulose microfibrils (Fry and others 1992; Nishitani and Tominaga 1992). A decrease of *ZmXET1* mRNA as detected in the salt-sensitive Lector (Fig. 2a) probably contributes to the lower abundance of this enzyme in the cell wall of salinity-affected shoots. On the other hand, an increase of *ZmXET1* mRNA in the salt-resistant SR03 (Fig. 2a) indicates the higher abundance of this protein under salinity. This higher abundance probably improves wall extensibility by facilitating the creep of cellulose microfibrils as described by Vissenberg and others (2005). In agreement with this assumption, creep activity is strongly reduced when *ZmXET1* is downregulated (Table 2), whereas creep activity is only weakly reduced when *ZmXET1* is upregulated. This is supported by the findings that XET activity is correlated with an increasing growth rate (Nishitani and Tominaga 1992; Fry and others 1992). Thus, an increase in *XET* transcript abundance seems to counteract the salinity-induced decrease in creep activity in salt-resistant plants.

In addition to the involvement of XETs, a contribution of EGases has been assumed in xyloglucan metabolism during cell elongation (Catalá and others 1997). EGases are thought to cause the release of xyloglucans trapped in cellulose microfibrils, resulting in increased wall extensibility and cell growth (Cosgrove 2005). In this study, the composite transcript abundance of *ZmEGases* is equally downregulated in both genotypes (Fig. 2b); thus, EGases are unlikely to contribute to the genotypic differences in creep activity described in response to salinity (Table 2).

### α-Expansin and Total PM-$H^+$-ATPase Transcript Abundance and Apoplastic pH

XETs are considered to be directly involved in xyloglucan metabolism during cell elongation, whereas expansin proteins are thought to act at the interface between cellulose microfibrils and hemicelluloses, making them obvious candidates for mediating cell-wall enlargement in growing cells (Cosgrove 2000). Expansins are grouped into α- and β-expansins. The β-expansins appear to have specialized roles in the loosening of the cell walls of grasses, whereas the α-expansins have been found to promote cell-wall growth in many species, including monocots and dicots (Cho and Kende 1997; Brummell and others 1999).

After an 8-day 100-mM salt treatment, the reduced β-expansin transcript and protein expression correlated positively with reduced shoot growth in the salt-sensitive hybrid Lector. On the other hand, an unaffected abundance of growth-mediating β-expansin protein in the salt-resistant hybrid SR03 was related to the maintenance of shoot growth under salinity (Geilfus and others 2010). In the present study, a genotype-specific stress response in terms of *ZmEXPA1* transcript expression has been detected in the shoots of both cultivars. A decrease of *ZmEXPA1* transcripts in the salt-sensitive Lector (Fig. 3a) indicates a decrease in ZmEXPA1 protein abundance in the walls of the salinity-affected leaves. Consequently, fewer ZmEXPA1 proteins seem to act as softening factors on the wall, thus mitigating wall-loosening processes in the salt-sensitive hybrid Lector. This is supported by the reduced creep activity (Table 2), reflecting a decrease in wall extensibility. On the other hand, the increased *ZmEXPA1* expression in the wall of the salt-resistant cultivar SR03 can be suggested to counteract these decreases in creep activity, explaining the less pronounced creep reduction in the salt-resistant cultivar under salinity. In favor of this assumption, Veselov and others (2007) have proposed a rapid increase of *ZmEXPA1* expression as a mechanism contributing to rapid cell wall-loosening and the maintenance of elongation-type growth in maize leaves under conditions of salinity-induced water deficit. In addition, *ZmEXPA1* has been reported to increase leaf extensibility and growth resumption after osmotic stress (Sabirzhanova and others 2005). Moreover, *ZmEXPA1* was expressed specifically in the growing region in maize roots at low water potentials (Wu and others 2001).

The upregulation of *ZmEXPA3* transcripts in Lector (Fig. 3a) is obviously not able to compensate for the decrease in salinity-induced growth reduction. Thus, this expression pattern is not consistent with a role in wall-loosening for shoot cell elongation under conditions of salinity, indicating the different physiological function of this isoform. For instance, in *Zinnia elegans*, *ZeEXPA3* was xylem cell-specific and possibly involved in the intrusive growth of the primary walls of differentiating xylem cells (Im and others 2000). In *Cicer arietinum*, *CaEXPA3* transcripts are related to radicle development (Sánchez and others 2004). The expression of the α-expansin isoform

*ZmEXPA4* is not affected by salinity, in either Lector or SR03 (Fig. 3a), indicating that this isoform does not participate in salinity-induced differences in terms of shoot expansion growth. Muller and others (2007) have demonstrated the high correlation between *ZmEXPA4* transcript expression and the relative widening rate of the maize leaf, whereas a poor correlation has been observed between *ZmEXPA4* and the relative leaf elongation rate. In deepwater rice internodes, the transcript levels of *OsEXPA4* were induced by submergence (Cho and Kende 1997).

Expansin protein isoforms have an acidic pH optimum (Cosgrove 2000). This observation gains in importance because Pitann and others (2009) have reported apoplastic alkalinization in the shoots of a salt-sensitive maize genotype. Moreover, Zörb and others (2005) have demonstrated that salt stress decreases PM-$H^+$-ATPase pumping activity in a salt-sensitive maize hybrid, whereas hydrolytic activity is not affected. Apoplastic alkalization has been suggested to inactivate expansin activity, causing growth reduction under salinity (Pitann and others 2009). In the present study, a decrease in the transcript expression of the four PM-$H^+$-ATPase isoforms has been detected in the salt-sensitive hybrid Lector (Fig. 3b). This decrease probably contributes to the lower abundance of this enzyme in the plasma membrane of the sensitive genotype, possibly explaining the alkalization of the apoplast as detected by Pitann and others (2009). In contrast, Pitann and others (2009) have reported that the apoplastic pH is not affected in the salt-resistant SR03. In the current study, the transcript expression of the four PM-$H^+$-ATPases was determined to be upregulated in the salt-resistant hybrid SR03 (Fig. 3b). A higher PM-$H^+$-ATPases protein abundance might impede apoplastic alkalization by pumping protons from the cytosol into the apoplast. In both genotypes, the total mRNA of the composite PM-$H^+$-ATPases transcript correlates positively with changes in the apoplastic pH under salinity. In salt-resistant SR03, an upregulation of PM-$H^+$-ATPase transcripts possibly contributes to the maintenance of the apoplastic pH within a range in which the pH activates expansin activity, thus promoting wall-loosening and cell expansion.

## Conclusion

In conclusion, salinity has been shown to change the transcript expression of wall-loosening candidates such as ZmXET1, ZmEGases, α-expansins, and PM-$H^+$-ATPases in the shoot of maize. For the first time, genotypic differences in the expression patterns of *ZmXET1*, *ZmEXPA1*, and the composite PM-$H^+$-ATPase transcripts have been demonstrated between a salt-sensitive and a highly salt-resistant maize hybrid in response to salinity, together with genotypic differences in wall extensibility and growth. A decrease in the relative transcript expression of *ZmXET1*, *ZmEXPA1*, and the composite PM-$H^+$-ATPase mRNAs has been detected in the salt-sensitive hybrid Lector. This downregulation of wall-loosening candidates correlates positively with a decreased wall extensibility and with decreased shoot growth. In contrast, the decrease in wall extensibility is less strong in the salt-sensitive hybrid SR03. An upregulation of *ZmXET1*, *ZmEXPA1*, and PM-$H^{+-}$ATPase transcripts possibly mitigates the salinity-induced decrease in wall extensibility and thus the decrease in shoot growth in the salt-resistant maize genotype.

**Acknowledgments** Christoph-Martin Geilfus is in receipt of a grant from the Friedrich-Ebert-Foundation, which is gratefully acknowledged. We are grateful to Prof. Dr. Sven Schubert for providing the SR03 hybrids. This work was supported by a DFG research grant (ZO118/6), which is gratefully acknowledged.

## References

Brummell DA, Harpster MH, Civello PM, Palys JM, Bennett AB, Dunsmuir P (1999) Modification of expansin protein abundance in tomato fruit alters softening and cell wall polymer metabolism during ripening. Plant Cell 11:2203–2216

Büntemeyer K, Lüthen H, Böttger M (1998) Auxin-induced changes in cell wall extensibility of maize roots. Planta 204:515–519

Carpita NC, Gibeaut DM (1993) Structural models of the primary cell walls of flowering plants. Consistency of structure with the physical and biochemical changes during growth. Plant J 3:1–30

Catalá C, Rose JKC, Bennett AB (1997) Auxin regulation and spatial localization of an endo-1,4-β-D-glucanase and a xyloglucan endotransglycosylase in expanding tomato hypocotyls. Plant J 12:417–426

Cho HT, Kende H (1997) Expression of expansin genes is correlated with growth in deepwater rice. Plant Cell 9:1661–1671

Cosgrove DJ (1997) Assembly and enlargement of the primary cell wall in plants. Annu Rev Cell Dev Biol 13:171–201

Cosgrove DJ (2000) Loosening of plant cell walls by expansins. Nature 407:321–326

Cosgrove DJ (2005) Growth of the plant cell wall. Nat Rev Mol Cell Biol 6:850–861

Cox KH, Goldberg RB (1988) Isolation of total RNA. In: Shaw CH (ed) Plant Molecular Biology. IRL Press, Oxford, pp 2–8

Cramer GR, Bowmann DC (1991) Kinetics of maize leaf elongation. J Exp Bot 42:1417–1426

Doorenbos J, Kassam AH (1976) Yield response to water. In: FAO irrigation and drainage paper. Food and Agriculture Organization, Rome, p 160

Fry SC (1989) Cellulases, hemicelluloses and auxin-stimulated growth: a possible relationship. Physiol Plant 75:532–536

Fry SC, Smith RC, Renwick KF, Martin DJ, Hodge SK, Matthews KJ (1992) Xyloglucan-endotransglycosylase, a new wall-loosening enzyme activity from plants. Biochem J 282:821–828

Geilfus CM, Zörb C, Mühling KH (2010) Salt stress differentially affects growth-mediating β-expansins in resistant and sensitive maize (*Zea mays* L.). Plant Physiol Biochem 48:993–998

Genovesi V, Fornalé S, Fry SC, Ruel K, Ferrer P, Encina A, Sonbol FM, Bosch J, Puigdomènech P, Rigau J, Caparrós-Ruiz D (2008) ZmXTH1, a new xyloglucan endotransglucosylase/hydrolase in

maize, affects cell wall structure and composition in *Arabidopsis thaliana*. J Exp Bot 59:875–889

Hager A (2003) Role of the plasma membrane $H^+$-ATPase in auxin-induced elongation growth: historical and new aspects. J Plant Res 116:483–505

Hager A, Menzel H, Krauss A (1971) Versuche und Hypothese zur Primärwirkung des Auxins beim Streckungswachstum. Planta 100:47–75

Hayashi T (1989) Xyloglucans in the primary-cell wall. Ann Rev Plant Physiol Plant Mol Biol 40:139–168

Hong SY, Seo PJ, Yang MS, Xiang F, Park CM (2008) Exploring valid reference genes for gene expression studies in *Brachypodium distachyon* by real-time PCR. BMC Plant Biol 8:112–122

Im KH, Cosgrove DJ, Jones AM (2000) Subcellular localization of expansin mRNA in xylem cells. Plant Physiol 123:463–470

Jacobs M, Ray PM (1976) Rapid auxin-induced decrease in free space pH and its relationship to auxin-induced growth in maize and pea. Plant Physiol 58:203–209

McCann MC, Wells B, Roberts K (1990) Direct visualization of cross-links in the primary plant cell wall. J Cell Sci 96:323–334

Moriau L, Michelet B, Bogaerts P, Lambert L, Oufattole M, Boutry M (1999) Expression analysis of two gene subfamilies encoding the plasma membrane $H^+$-ATPase in *Nicotiana plumbaginifolia* reveals the major transport functions of this enzyme. Plant J 19:31–41

Mühling KH, Läuchli A (2002) Effect of salt stress on growth and cation compartmentation in leaves of two plant species differing in salt tolerance. J Plant Physiol 159:137–146

Mühling KH, Plieth C, Hansen UP, Sattelmacher B (1995) Apoplastic pH of intact leaves of *Vicia faba* as influenced by light. J Exp Bot 46:377–382

Muller B, Bourdais G, Reidy B, Bencivenni C, Massonneau A, Condamine P, Rolland G, Conejero G, Rogowsky P, Tardieu F (2007) Association of specific expansins with growth in maize leaves is maintained under environmental, genetic, and developmental sources of variation. Plant Physiol 143:278–290

Munns R (1993) Physiological processes limiting plant growth in saline soils: some dogmas and hypotheses. Plant Cell Environ 16:15–24

Munns R, Tester M (2008) Mechanism of salinity tolerance. Annu Rev Plant Biol 59:651–681

Nishitani K (1995) Endo-xyloglucan transferase, a new class of transferase involved in cell wall construction. J Plant Res 108:2105–2117

Nishitani K, Tominaga R (1992) Endo-xyloglucan transferase, a novel class of glycosyltransferase that catalyzes transfer of a segment of xyloglucan molecule to another xyloglucan molecule. J Biol Chem 267:21058–21064

Peters WS, Lüthen H, Böttger M, Felle H (1998) The temporal correlation in apoplast pH and growth rate in maize coleoptile segments. Aust J Plant Physiol 25:21–25

Pitann B, Kranz T, Mühling KH (2009) The apoplastic pH and its significance in adaptation to salinity in maize (*Zea mays* L.): comparison of fluorescence microscopy and pH-sensitive microelectrodes. Plant Sci 176:497–504

Rose JKC, Braam J, Fry SC, Nishitani K (2002) The XTH family of enzymes involved in xyloglucan endotransglucosylation and endohydrolysis: current perspectives and a new unifying nomenclature. Plant Cell Physiol 43:1421–1435

Saab IN, Sachs MM (1995) Complete cDNA and genomic sequence encoding a flooding responsive gene from maize (*Zea mays L.*) homologous to xyloglucan endotransglycosylase. Plant Physiol 108:439–440

Sabirzhanova IB, Sabirzhanov BE, Chemeris AV, Veselov DS, Kudoyarova GR (2005) Fast changes in expression of expansin gene and leaf extensibility in osmotically stressed maize plants. Plant Phsiol Biochem 43:419–422

Sánchez MA, Mateos I, Labrador E, Dopico B (2004) Brassinolides and IAA induce the transcription of four a-expansin genes related to development in *Cicer arietinum*. Plant Physiol Biochem 42:709–716

Schubert S, Neubert A, Schierholt A, Sümer A, Zörb C (2009) Development of salt-resistant maize hybrids: the combination of physiological strategies using conventional breeding methods. Plant Sci 177:196–202

Veselov DS, Sabirzhanova IB, Chemeris AV (2007) Changes in expansin gene expression, IAA content, and extension growth of leaf cells in maize plants subjected to salinity. Russ J Plant Physiol 55:101–106

Vissenberg K, Fry SC, Pauly M, Hofte H, Verbelen JP (2005) XTH acts at the microfibril-matrix interface during cell elongation. J Exp Bot 56:673–683

Wu Y, Meeley RB, Cosgrove DJ (2001) Analysis and expression of the alpha-expansin and beta-expansin gene families in maize. Plant Physiol 126:222–232

Zörb C, Stracke B, Tramnitz B, Denter D, Sümer A, Mühling KH, Yan F, Schubert S (2005) Does H+ pumping by plasmalemma ATPase limit leaf growth of maize (*Zea mays*) during the first phase of salt stress? J Plant Nutr Soil Sci 168:550–557

# Supplementary data

### Supplementary Material 1

The specificity of degenerated primer pairs used for this study was demonstrated by DNA sequencing of the real-time quantitative RT-PCR products. The degenerated primer pair used for the amplification is shown in column 1 (for more details see material section). The corresponding DNA sequencing results are presented in column 2. The sequences were alignment against NCBI's reference mRNA sequences (refseq_rna; blastn). Search was limited to *Zea mays* L. (taxid:4577). Blast hits are presented in column 3 together with the respective Genbank accession numbers. Column 4 shows the resulting description of the Blast hits. Parameters for statistical quality of the hit were presented in columns 5 - 7.

| **Degenerated primer pair used for real-time quantitative RT-PCR** | **Sequencing summary of real-time quantitative RT-PCR products** (using IUPAC base calls for wobbles) | **Significant alignments of sequences** (NCBI blastn on *Zea mays* L. [taxid:4577]; database: refseq_rna) | | | | |
|---|---|---|---|---|---|---|
| | | **Genbank accession number** | **Description** | **Max score/ Total score** | **Query coverag. (%)/ Max ident (%)** | **E value** |
| *ZmMHA_fam* | ACGCCTGGTCTGCTCCTGGTCACCGCGTTCC TGCTCGCTCAACTTGTTGCCACCTTCCTC GCTGTCTACGCCAACTGGGGCTTCGCCAGGA TCAAGGGTATCGGCTGGGGCTGGGCAGGT GTGGTCTGGCTCTACAGCATCGTCSAT | NM_001112000.1<br><br>No other Blast hits found | Zea mays plasma-membrane H+ATPase2 (mha2), mRNA >emb\|X85805.1\| Z.mays mRNA for plasma membrane H+ ATPase | 207/ 207 | 95/ 93 | 1e-53 |
| *ZmEGases* | TCKAGCCTGCGTGCAGCCGATGACTCCTTGC TGTGCTTGTACGGCACGATGGACGCGGCG CGGTGGTGCACCCGGCTGGGGTACTTGGGGC CGTAGCCGACGAGGTAGCTGACGCCCCTG GGGTTGGTGCCGAGCACGTAGTCCACCTGC | NM_001157964.1<br><br>No other Blast hits found | Zea mays endoglucanase 1 (LOC100285069), mRNA >gb\|EU970755.1\| Zea mays clone 350091 endoglucanase 1 precursor, mRNA, complete cds | 263/ 263 | 93/ 99 | 2e-70 |

**Supplementary Material 2**

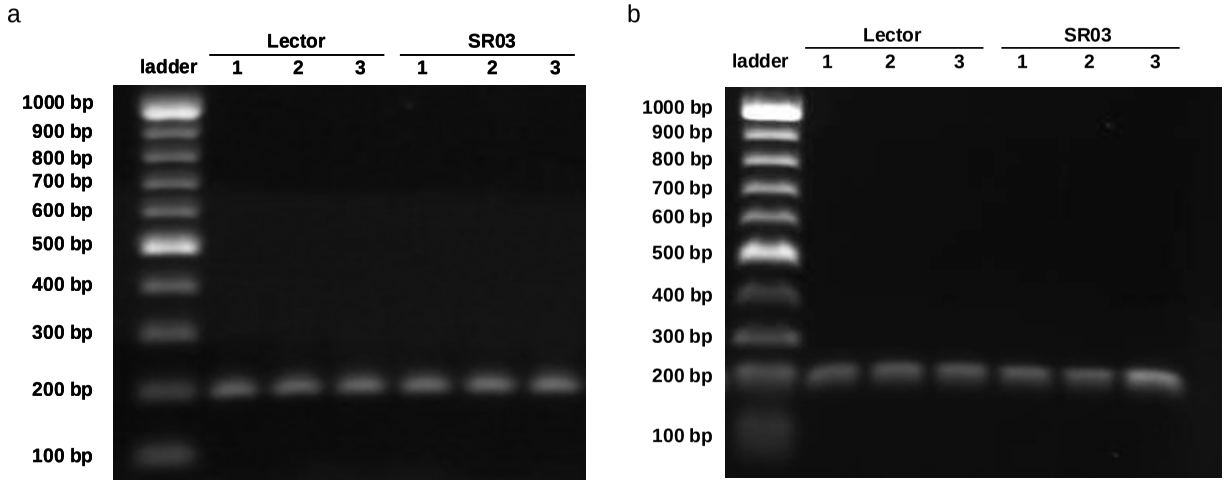


Demonstration of the specificity of the degenerated primer pairs *ZmMHA_fam* and *ZmEGases*. After real-time quantitative RT-PCR measurement, PCR products from both maize varieties were run on agarose gels. (a) By the use of the degenerated primer pair *ZmMHA_fam* for template amplification, only one single DNA band was visualized. This band appeared at the molecular size that was predicted by *in-silico* analysis (expected size of PCR product of plasma membrane proton pump ($H^+$)–ATPase genes = 195 bp). (b) By the use of the degenerated primer pair *ZmEGases*, only one single DNA band was visualized. This band appeared at the molecular size that was expected by *in-silico* analysis (predicted size of PCR product of endoglucanase genes = 200 bp). PCR conditions were as described in Materials and Methods. Numbers 1-3, biological replicates of the real-time quantitative RT-PCR amplifications of Lector and SR03.Gels contain 1% agarose, Tris-borate-EDTA, 0.4 µg of ethidium bromide per ml.

# Chapter 4

## A methodical approach for improving the reliability of quantifiable two-dimensional Western blots

Christoph-Martin Geilfus, Karl H. Mühling and Christian Zörb

Journal of Immunological Methods 362 (2010) 89–94

Journal of Immunological Methods 362 (2010) 89–94

Contents lists available at ScienceDirect

Journal of Immunological Methods

journal homepage: www.elsevier.com/locate/jim

Research paper

# A methodical approach for improving the reliability of quantifiable two-dimensional Western blots

Christoph-Martin Geilfus, Karl H. Mühling, Christian Zörb *

*Institute of Plant Nutrition and Soil Science, Christian Albrechts University, Hermann-Rodewald-Str. 2, 24118 Kiel, Germany*

ARTICLE INFO

*Article history:*
Received 14 May 2010
Received in revised form 23 August 2010
Accepted 1 September 2010
Available online 15 September 2010

*Keywords:*
2D Western blotting
2D-SDS-PAGE
Protein isoform
Quantitation
Reliability
Improve

ABSTRACT

Western transfer after the electrophoretic separation of proteins onto an adsorbent membrane, with subsequent immunodetection, is a powerful tool for detecting and characterizing a multitude of proteins. An important aspect of the study of proteins is that they often exist as isoforms with structural microheterogeneity giving rise to differences in biological activity. Western blotting (WB) in combination with two-dimensional SDS-polyacrylamide gel electrophoresis (2D-SDS-PAGE) allows the specific quantification of single isoforms of a protein. We have investigated whether a methodical modification of 2D-SDS-PAGE improves the quality of quantifiable 2D-WB data. The effect of a combined separation of three previously electrofocused protein extracts lying side by side on a single SDS-gel in parallel has been tested against the traditional procedure, viz., the separation of one protein extract per SDS-gel. The modified procedure results in a more reliable and better quality data than the traditional procedure, which seems to be prone to producing systematic or random errors. Our simple practical procedure improves immunoblotting accuracy by excluding numerous sources of errors and saves time, immunoblotting reagents and costly antibodies.



## 1. Introduction

Western transfer of proteins separated by SDS-polyacrylamide gel electrophoresis (PAGE) onto an adsorbent membrane, with subsequent immunodetection, has found wide application in the field of life sciences and biochemistry. It is a powerful tool for detecting and characterizing a multitude of proteins, especially those that are of low abundance (Kurien and Scoflied, 2006). In combination with two-dimensional electrophoretic (2-DE) gels, Western blotting (WB) allows the subsequent immunodetection of relevant antigens among several thousand individual proteins separated by using 2-DE (Canelle et al., 2005). 2D-blotting includes the separation of proteins according to their molecular characteristics (i.e., molecular weight and isoelectric point) before immobilization onto a membrane for immunostaining (Towbin et al., 1979). This enables the specific quantitation of single isoforms, even when the antibody itself does not differentiate between them (Zellner et al., 2008). This feature is of special importance, as a determination of the various isoforms directly with conventional immunoassay methods is rarely possible, because of the difficulty of making high-affinity non-crossreacting antibodies directed against all the epitopes of interest (Lönnberg and Carlsson, 2000).

The structural microheterogeneity of protein isoforms often gives rise to differences in their biological activity. Such changes have functional significance and therefore need to be studied. The most common microheterogeneities result from variations in the carbohydrate structures of glycoproteins. Other examples include the changed functional groups in the side chain of one or several amino acids or missing amino acids following degradation processes occurring *in vivo* (Lönnberg and Carlsson, 2000).

The combination of 2-DE with WB represents a suitable technique for qualitative and quantitative measurements of isoform abundance and modification states and might

*Abbreviation:* (TCA), trichloroacetic acid.

* Corresponding author. Tel.: +49 0431 8803359; fax: +49 0431 8801625.
*E-mail address:* cmgeilfus@plantnutrition.uni-kiel.de (C. Zörb).

0022-1759/$ – see front matter © 2010 Elsevier B.V. All rights reserved.
doi:10.1016/j.jim.2010.09.006

provide information to aid the understanding of their role in diverse physiological processes. Accurate quantitation of the data is essential for the interpretation of these experimental results. A large amount of reproducible and quantitative high-quality data with low variance is required. The processing of such data is a costly time-consuming multi-step procedure prone to systematic or random errors (Aksamitiene et al., 2007).

We propose a simple modification of the 2D-WB procedure that improves the reliability of quantifiable data, thus decreasing variance. Additionally, the procedure increases throughput and saves time, immunoblotting reagents and costly antibodies.

## 2. Materials and methods

### 2.1. Plant material and cultivation

*Zea mays* L. hybrid Lector (Limagrain, Rilland, NL) was grown in the greenhouse under hydroponic culture conditions. The nutrient solution had the following composition: 2.5 mM Ca $(NO_3)_2$, 1.0 mM $K_2SO_4$, 0.2 mM $KH_2PO_4$, 0.6 mM $MgSO_4$, 5.0 mM $CaCl_2$, 1.0 μM $H_3BO_4$ 2.0 μM $MnSO_4$, 0.5 μM $ZnSO_4$, 0.3 μM $CuSO_4$, 0.005 μM $(NH_4)_6Mo_7O_{24}$, 200 μM Fe-EDTA. Temperature was kept constant at 26 °C for the light period and at 18 °C for the dark period; relative humidity was ca. 70%. Plant material was ground in liquid nitrogen and stored at −80 ° C.

### 2.2. Protein extraction

Proteins for isoelectric focusing (IEF) were prepared by using a dithiothreitole (DTT)–trichloroacetic acid (TCA)–acetone precipitation method adopted from Zörb et al. (2004). Protease activity was kept low by maintaining the cell material at 4 °C and addition of 6 M urea plus 2 M thiourea to the protein sample buffer supplemented by protease inhibitors (Pefabloc; Roche, Freiburg, Germany). A total of 1.8 mL lysis solution (10% TCA in acetone) was added to 100 mg ground plant material. After vigorous shaking, samples were incubated for 10 min in an ice-cold ultrasonic bath and subsequently incubated for at least 1 h at −20 °C before centrifugation (20 000 × *g*; 15 min; 4 °C). The precipitant was resuspended in 1 mL ice-cold solution (50 mM DTT; 2 mM EDTA in acetone). Samples were incubated for 5 min in an ice-cold ultrasonic bath. The procedure was repeated and precipitated proteins were lyophilized under $N_2$. The pellets were then resuspended in 1 mL protein sample buffer (8 M urea; 2 M thiourea; 0.5% v/v pharmalyte buffer, pH 3–10; 4% w/v CHAPS; 30 mM DTT; 20 mM TRIS, pH 8.8; 5 mM Pefablock). For protein solubilization, samples were incubated for 2 h at 33 °C, followed by a 10-min incubation in an ultrasonic bath. Samples were centrifuged (18 000 × *g;* 30 min) and the resulting supernatant was subjected to IEF. Protein concentrations were determined by using a 2D QUANT protein determination kit (GE-Healthcare, München, Germany).

**Table 1**
Coefficient of variation of densiometric 2D-Western blotting data.

| | Coefficient of variation (n = 3) | |
|---|---|---|
| | Two-dimensional separation procedure | |
| | Traditional | Modified |
| Isoform I | 48.8% | 3.7% |
| Isoform II | 6.5% | 1.5% |
| Isoform III | 8.2% | 1.0% |

### 2.3. IEF and 2D PAGE

First-dimension IEF was carried out on a Protean IEF Cell system, with a focusing tray accommodating up to 12 immobilized pH gradient (IPG) strips (Biorad, Munich, Germany). Proteins (60 μg) were diluted in a total volume of 125 μL IPG sample buffer. The sample was loaded on pre-cast IPG strips (70 × 3.0 × 0.5 mm, pH 3–11, non-linear, GE-Healthcare, Munich, Germany). This was repeated six times and, thus, six technical replicates of this protein extract were conducted in parallel. All IPG gel strips were covered with paraffin oil to prevent evaporation. Gels were rehydrated for 12 h at 50 V and 20 °C. IEF was performed for 11 831 Vh with the initial voltage set to 250 V for 30 min, then a gradient up to 500 V for 30 min, followed by a gradient up to 3000 V for 30 min, and finally separation at 3000 V for 4 h. The system temperature was 20 °C. To run the second dimension, strips were placed in equilibration buffer (50 mM TRIS–HCl, pH 8.8; 6 mM urea; 30% v/v glycerol; 2% w/v SDS; and 0.001% w/v bromophenol blue containing 1% w/v DTT) and gently agitated for 10 min. Strips were incubated again for 10 min in equilibration buffer containing 4% w/v iodoacetamide instead of DTT, under gentle agitation, and rinsed with SDS-PAGE running buffer (25 mM TRIS; 192 mM glycine; 0.1% w/v SDS). Up to this point, all six replicates were treated in parallel.

For the 2D-PAGE, the six electrofocused protein extracts were divided into two experimental groups. The experimental setup was as follows: three of six IPG gel strips were separated each on a different 20 cm × 20 cm SDS-gel (control, Fig. 1). The remaining three gel strips were combined together side by side onto a single 20 cm × 20 cm SDS-gel, thus being separated on the same gel in parallel (modified procedure). However, three 7-cm long IPG gel strips were too long to be embedded side by side on a common 20 cm SDS-gel. Moreover, contact between the adjoined gel strips had to be avoided in order to avoid any diffusion of protein from one strip to another. Hence, the length of each of the three IPG gels had to be reduced, allowing us to combine them on a single 20 cm × 20 cm SDS-gel (Fig. 1). Before reducing the length of the equilibrated gel strips, attention had to be paid to ensure that the isoforms of interest were not located on the outermost region of the gel strip, as this region was discarded during length reduction. For this, pilot WB experiments and an *in-silico* calculation of the pI were carried out to determine the position of the dedicated isoforms on the IPG gel strip (data not shown). In this work, 0.5 cm of both gel ends was cut off, reducing the gel length from 7 cm to 6 cm. In order to avoid contact between gel strips, molten agarose was use to fill in the gaps between the gel strips. In total, four SDS-gels, viz., three single SDS-gels loaded with one protein extract replicate (traditional) and one SDS-gel loaded with three protein extract replicates (modified procedure), were run (Fig. 1).

Two-dimensional separation was carried out with a multi-gel electrophoresis unit that enabled all four gels to be run in parallel (Protean 2 Multi Cell, Biorad, Munich, Germany) and

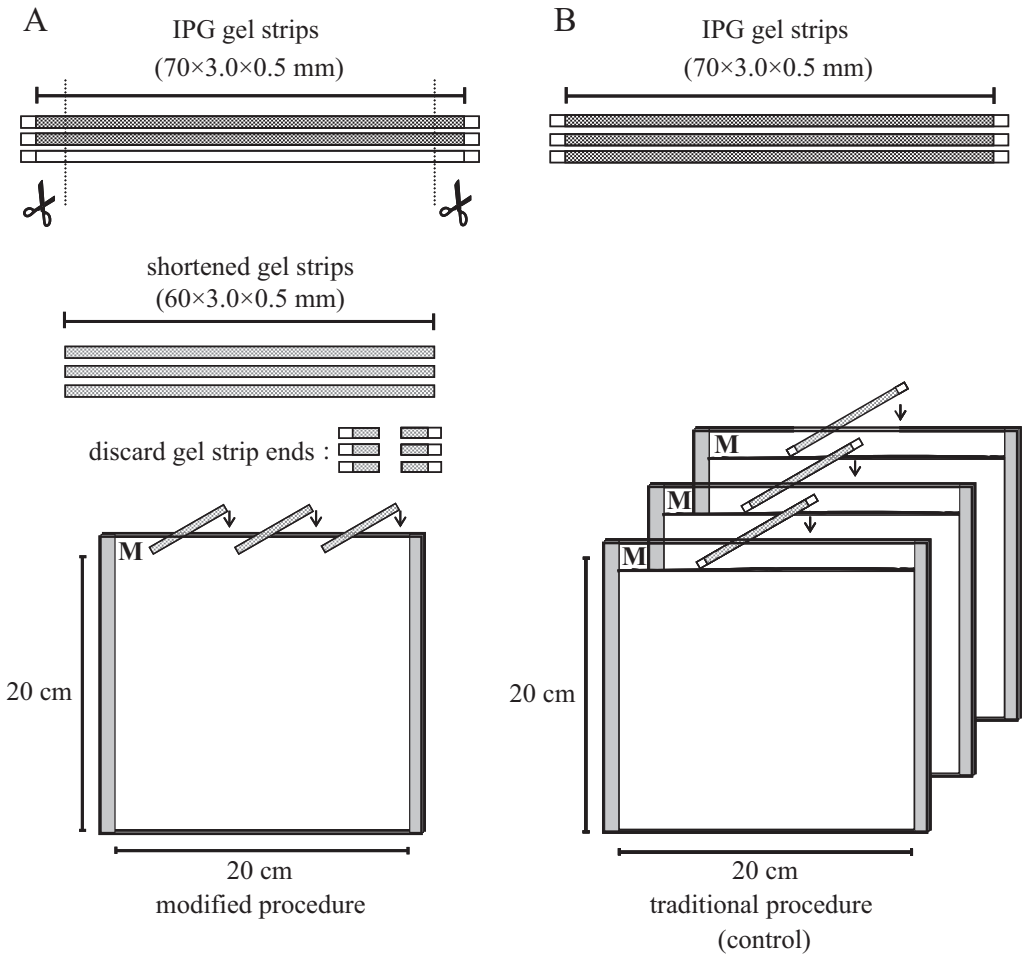


**Fig. 1.** Representation showing 2D-SDS-PAGE preparation. All six IPG gel strips were loaded with identical protein samples (technical replicates). The gel strips were rehydrated, electrofocused and equilibrated in parallel and then split into two groups, viz., the modified versus traditional procedure. Modified procedure: in order to separate three previously electrofocused protein extracts side by side onto a single 20 cm × 20 cm SDS-gel, the strips were shortened (A). Traditional procedure (control): the remaining three protein extracts were embedded each onto a different SDS-gel (B). M, pre-stained protein marker.

that was equipped with a continuous flow cooling system. The equilibrated IPG gel strips were embedded at the top of 12% w/v acrylamide (20 cm × 20 cm) gels in molten agarose (1% w/v in running buffer). All four SDS-gels were run at 30 mA/gel for 6.5 h (120 W) at 15 °C. The apparent molecular mass of proteins was determined by co-electrophoresis of protein markers (pre-stained molecular weight standards from 8 to 210 kDa; Sigma, Hamburg, Germany).

### 2.4. 2D-blotting procedures

Proteins in cropped SDS-gel fragments derived from both procedures, viz., traditional and modified, were electroblotted together onto the same polyvinylidene difluoride (PVDF) membrane (Fig. 2; PVDV-membrane: pore size 45 µm, BioTrace, PALL Life Sciences, Pensacola, USA) by using a semi-dry transfer system (SemiPhor, Hoefer Pharmacia Biotech, San Francisco, USA).The gel fragments with the isoforms could be cropped, as the molecular size of the isoform of interest was known. The region of interest could easily be located with the help of the visible pre-stained marker. In this study, gel fragments with markers of less than 35 kDa were used for the blotting procedure. The SDS-gel fragment above this level was used as a loading control. For electroblotting, SDS-gel fragments were equilibrated in Towbin buffer (25 mM TRIS-base; 192 mM glycine; 20% v/v methanol; 0.01% w/v SDS; pH 8.3) for 15 min. At the same time, the PVDF membrane was hydrated initially in methanol for 10 s and then equilibrated in Towbin buffer for 15 min. For protein transfer, the transfer stack was assembled as follows. Three sheets of filter paper (Whatman gelblot paper; 1.2 mm, Sigma, Munich, Germany) soaked in Towbin buffer were placed on the horizontal anode plate followed by the hydrated PVDF membrane. The equilibrated gel fragments were placed on top and covered with three sheets of gelblot paper soaked in Towbin buffer (Fig. 2). Transfer was conducted for 75 min at 40 to 50 V, 0.8 mA/cm$^2$. Transfer efficiency was checked with the pre-stained protein marker.

### 2.5. Immunodetection

For immunostaining, the 2D-blot membrane was saturated in a solution of milk powder in TRIS-buffered saline (TBS) with

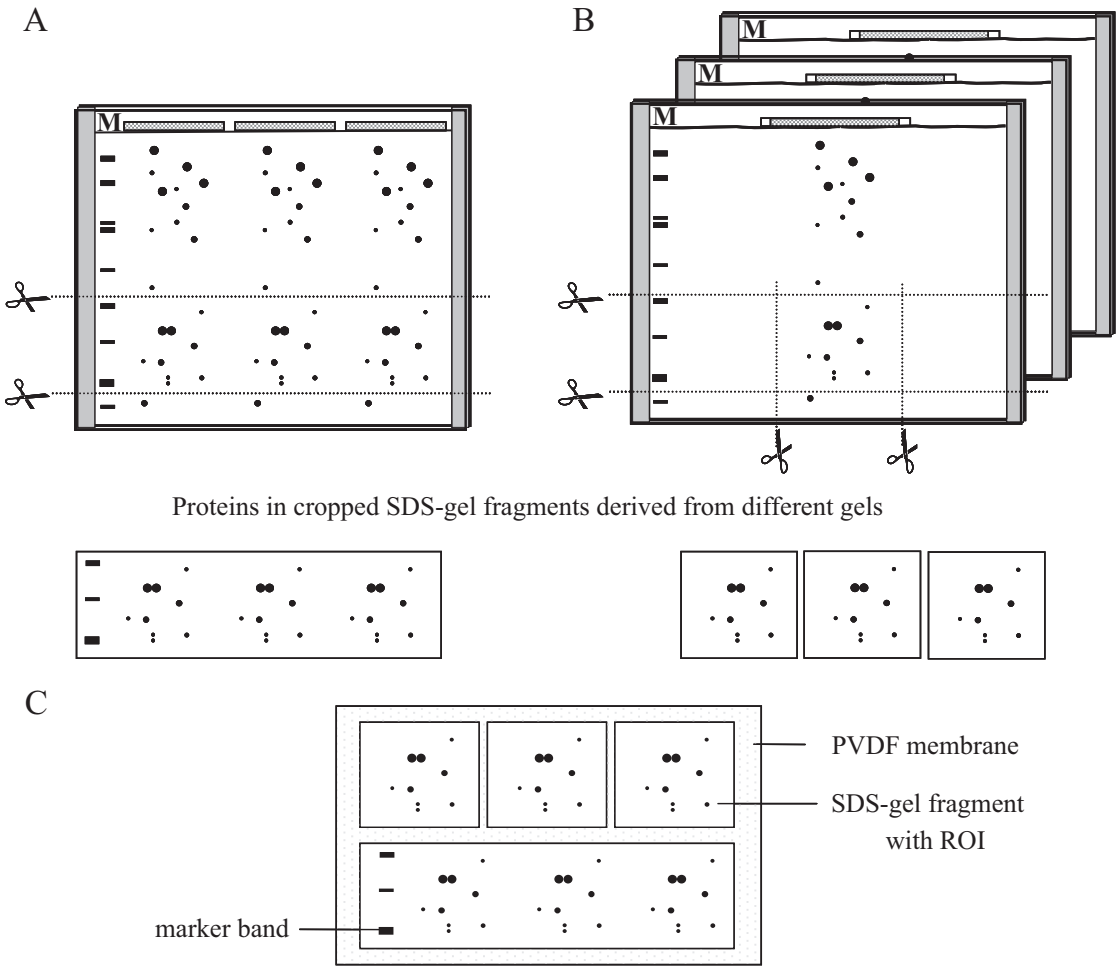


**Fig. 2.** Representation showing transfer stack preparation. The spots shown are hypothetical. Modified procedure: three technical replications on one SDS-gel (A). Traditional procedure (control): three technical replications on three different SDS-gels (B). The preparation of transfer stack was done by combining proteins in cropped SDS-gel fragments (region of interest, ROI) derived from different gels onto the same PVDF membrane. The pre-stained molecular weight marker (M) reveals the position of isoforms on the SDS-gel (C).

Tween (TBS-T; 2.5% w/v bovine skimmed milk; 0.1% v/v Tween) for 2 h at room temperature and then incubated with the antibodies. We used an anti-peptide rabbit IgG antibody raised against maize beta-expansins (BioTrend, Köln, Germany). The blot was incubated in plastic bags containing antisera diluted 1/250 in the same TBS-T (0.1 mL/cm$^2$ PVDF membrane) for 2 h and washed three times with TBS-T (0.1% v/v). Subsequently, the membrane was incubated with horseradish-peroxidase-conjugated goat anti-rabbit IgG (Sigma-Aldrich, Munich, Germany), diluted 1/38 000 in TBS-T, for 1 h at room temperature, as described for the first antibody. Finally, the membrane was washed three times in TBS-T and once in TBS. Signals were detected by using chemiluminescent peroxidase subtrate-3 on Kodak BioMax light film (Sigma, Munich, Germany) with an exposure time of 3 min.

## 3. Data evaluation

The X-ray film was scanned with an image scanner (HP Scan-Jet 4890, UNS; 300 dpi and 16 bits *per* pixel, Böblingen, Germany). WB images were analysed with TINA 2.08 software (Raytest, Straubenhardt, Germany). The F-max test, as outlined by Köhler et al. (1984), was used to test homogeneity of variances between the two methodical procedures by means of the Microsoft Excel program.

## 4. Results and discussion

We tested whether a combined 2D separation of three previously electrofocused protein extracts improved the quality of quantifiable 2D-WB data. For this, three IPG gel strips were embedded side by side onto a single SDS-gel and separated electrophoretically in parallel (modified procedure). The reliability of this procedure was compared with that of a control that was handled according the traditional 2D separation procedure. For this, the three electrofocused protein extracts were each separated on a single SDS-gel. For an adequate comparison of the two procedures, all six IPG gel strips (three for the modified procedure and three for the traditional control procedure) were loaded with identical protein extract and were thus technical replicates. Consequently, the loading controls of the WB shown in Fig. 3 indicate an equivalent protein level, viz.,

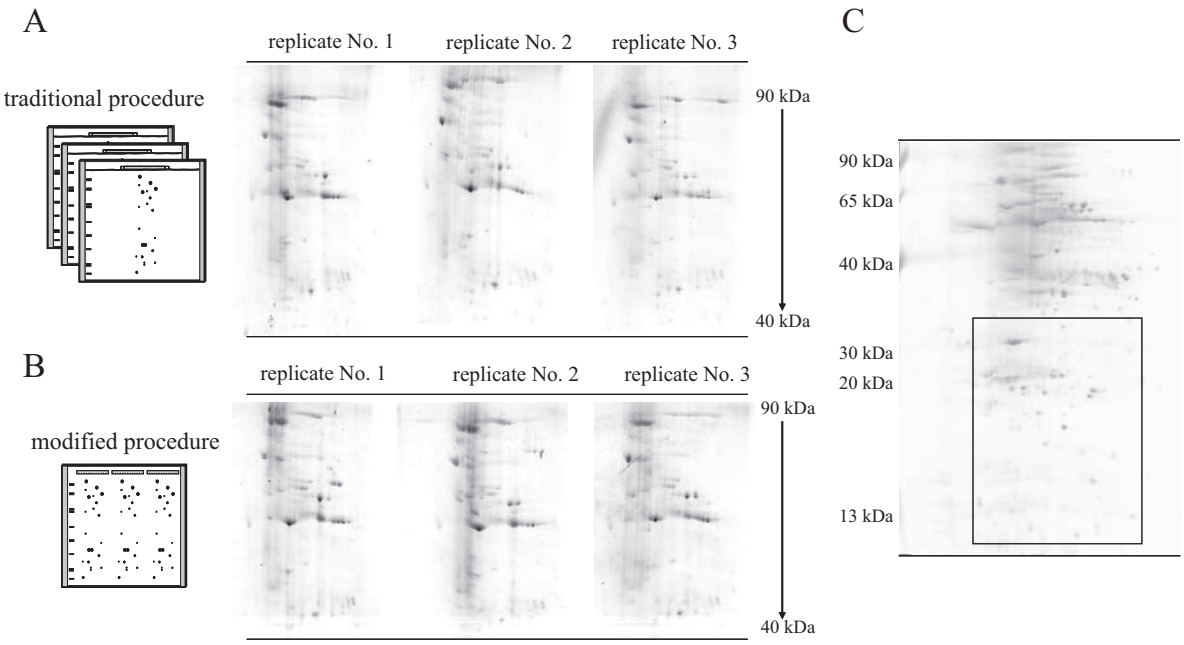


**Fig. 3.** Coomassie-stained loading controls (60 µg protein) corresponding to the Western blot shown in Fig. 4. The gel region smaller than 35 kDa was used for the 2D-blotting procedure, whereas the upper part of the gel was used for indicating equivalent protein level loaded on each gel: (A) traditional procedure and (B) modified procedure. Numbers 1–3 indicate protein extract replicate for each procedure. Right panel (C) represents the complete Coomassie-stained image of the 2D-SDS-gel. The frame corresponds to the gel region that was used for 2D-blotting procedure.

60 µg, loaded onto each IPG gel strip (Fig. 3). Moreover, in this study, all protein extracts were strictly treated equally. IPG gel strips were rehydrated and electrofocused in parallel by using a multiple focusing tray. 2D separation of all SDS-gels was performed in a multi-gel electrophoresis unit simultaneously. Proteins in cropped SDS-gel fragments derived from different gels were electroblotted together onto the same PVDF membrane, followed by immunodetection. This approach allows the elimination of other source of errors that would increases data variability and thus restricts the comparative quantitative analysis of signals that are visualized on different blots (Aksamitiene et al., 2007). Such sources of error arise because each electrophoresis and the following immunoblotting cycles are performed under slightly different conditions because of differences in, for example, the shape of the fibre pads for electroblotting, the time of protein transfer onto the membrane, the strength of contact between the gel and membrane, the quality and dilution of antibodies, the washing of the membrane or the detection of the signal (Aksamitiene et al., 2007).

In the current study, WB analysis revealed the presence of three signals, each indicating a protein isoform henceforth referred to as isoforms I, II and III (Fig. 4). However, isoform I was not detected in the second replication of the traditionally separated protein extract (Fig. 4). As this isoform was detectable in all other protein extracts, and as all six protein extracts were technical replicates, this isoform must have

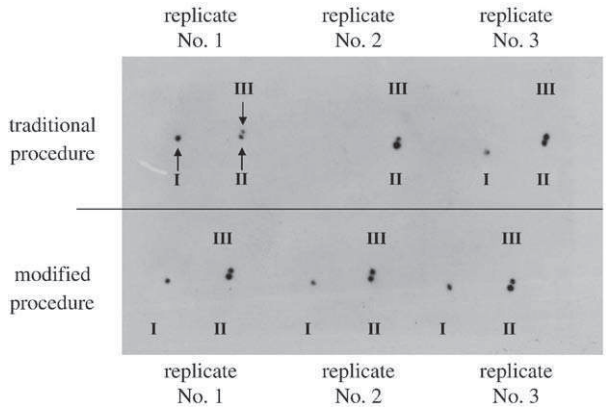


**Fig. 4.** X-ray film showing enhanced chemiluminescence signals on 2D-WB. Roman numbers I–III indicate the three detected protein isoforms. Arabic numbers 1–3 show the replicates for each procedure. Upper half of the X-ray film: traditional control procedure; lower half: modified procedure. Representation indicates position of replicates or cropped SDS-gel fragments.

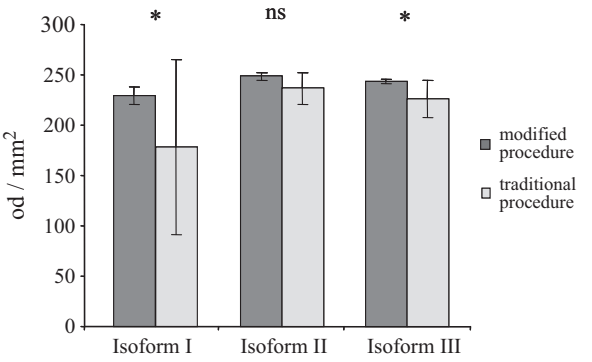


**Fig. 5.** Densiometric analysis of 2D-WB signals. The signals were grouped according to the isoform and plotted as the average of the optical density (od) per $mm^2$. $n = 3 \pm SD$. Asterisks indicate significant heterogeneity of variances calculated between the two procedures. This was carried out for each isoform (F-max test; $p \leq 0.05\%$; ns, not significant). Densiometric analysis was performed with TINA 2.08 software.

existed in the mentioned extract. This indicated that the modified procedure was superior to the traditional procedure in terms of reliability. Moreover, statistical analysis revealed smaller standard deviations for all densiometric WB data that were generated with the modified procedures as compared with the control procedures (Fig. 5). Thus, the modified procedure decreased the variability of the densiometric data not only for isoform I, but also for isoforms II and III. To confirm this, the F-max test was used to test whether any significant differences in the variance homogeneity had occurred. Heterogeneities of variances between both treatments were found for isoforms I and III (F-max test, $p \leq 0.05\%$; Fig. 5). The high coefficients of variation (Table 1) of the control procedure clearly showed that these heterogeneities must have been caused by a higher variability of the data obtained by this conventional procedure.

A combined 2D separation of three IEF strips in parallel on a single SDS-PAGE gel improved the reliability of 2D-WB. The traditional procedure, viz., 2D separation of electrofocused protein extracts each on a single SDS-gel, seems to be prone to systematic or random errors. These findings are remarkable since, in 2D-PAGE studies, replicates (technical and biological) are routinely performed by using different SDS-gels. The inferiority of the traditional procedure might be explained by the use of different SDS-gels for the second dimensional separation of electrofocused protein extracts. In favour of this assumption, Aksamitiene et al. (2007) have reported an augmentation of errors, such as an increased variability of the standard deviation of signal intensities caused by increased gel heterogeneity in terms of one-dimensional proteins separation by using SDS-PAGE.

The suggested multi-strip procedure not only improves the accuracy of immunoblotting, but is also very economical: (i) different or repeated electrofocused protein extracts are separated by using only one SDS-gel, (ii) several SDS-gel strips (each containing multiple protein extracts migrating side by side) are transferred onto a single membrane, and (iii) an analysis of different or repeated protein extracts can occur in one immunoblotting cycle. As a result, this modified procedure saves labour-costs (time), 2D-PAGE and immunoblotting reagents and costly antibodies.

## 5. Conclusion

A combined 2D separation of electrofocused protein extracts side by side on one SDS-PAGE improves the quality of quantifiable 2D-WB data and decreases the costs of labour, immunoblotting and reagents. Moreover, this modified procedure enables multiple protein extracts to be analysed in one immunoblotting cycle, thus increasing throughput. This alternate method can easily be adopted, since no additional equipment or reagents are needed.

## Acknowledgments

Mrs. Stephanie thor Straten is kindly acknowledged for excellent technical assistance. Christoph-Martin Geilfus is in receipt of a grant from the Friedrich-Ebert-Foundation, which is gratefully acknowledged. Mrs. Stephanie thor Straten is kindly acknowledged for excellent technical assistance. This work was supported by a DFG research grant (ZO118/6) which is gratefully acknowledged.

## References

Aksamitiene, E., Hoek, J.B., Kholodenko, B., Kiyatkin, A., 2007. Multistrip Western blotting to increase quantitative data output. Electrophoresis 28 (18), 3163.

Canelle, L., Bousquet, J., Pionneau, C., Deneux, L., Imam-Sghiouar, N., Caron, M., Joubert Caron, R., 2005. An efficient proteomics-based approach for the screening of autoantibodies. J. Immunol. Methods 299, 77.

Köhler, W., Schachtel, G., Voleske, P., 1984. Einführung in die Statistik für Biologen und Agrarwissenschaftler. Springer, Berlin.

Kurien, B.T., Scoflied, R.H., 2006. Western blotting. Methods 38, 283.

Lönnberg, M., Carlsson, J., 2000. Membrane assisted isoform immunoassay: a rapid method for the separation and determination of protein isoforms in an integrated immunoassay. J. Immunol. Methods. 246, 25.

Towbin, H., Staehelin, T., Gordon, J., 1979. Electrophoretic transfer of proteins from polyacrylamide gels to nitrocellulose sheets: procedure and some applications. Proc. Natl. Acad. Sc. USA 76, 4350.

Zellner, M., Babeluk, R., Diestinger, M., Pirchegger, P., Skeledzic, S., Oehler, R., 2008. Fluorescence-based Western blotting for quantitation of protein biomarkers in clinical samples. Electrophoresis 29, 3621.

Zörb, C., Schmitt, S., Neeb, A., Karl, S., Linder, M., Schubert, S., 2004. The biochemical reaction of maize (Zea mays L.) to salt stress is characterized by a mitigation of symptoms and not by a specific adaptation. Plant Sci. 167, 91.

# Chapter 5

# Real-time imaging of leaf apoplastic pH dynamics in response to NaCl stress

Christoph-Martin Geilfus and Karl H. Mühling

Frontiers in Plant Science **2:**13 (2011) doi: 10.3389/fpls.2011.00013

frontiers in
PLANT SCIENCE

METHODS ARTICLE
published: 02 May 2011
doi: 10.3389/fpls.2011.00013

# Real-time imaging of leaf apoplastic pH dynamics in response to NaCl stress

***Christoph-Martin Geilfus and Karl H. Mühling****

*Institute of Plant Nutrition and Soil Science, Christian Albrechts University, Kiel, Germany*

***Edited by:***
*Jan Kofod Schjoerring, University of Copenhagen, Denmark*

***Reviewed by:***
*Doug Van Hoewyk, Coastal Carolina University, USA*
*Alexander Schulz, University of Copenhagen, Denmark*

***Correspondence:**
*Karl H. Mühling, Institute of Plant Nutrition and Soil Science, Christian Albrechts University, Hermann-Rodewald-Str. 2, 24118 Kiel, Germany. e-mail: khmuehling@plantnutrition.uni-kiel.de*

Knowledge concerning apoplastic ion concentrations is important for the understanding of many processes in plant physiology. Ion-sensitive fluorescent probes in combination with quantitative imaging techniques offer opportunities to localize, visualize, and quantify apoplastic ion dynamics *in situ*. The application of this technique to the leaf apoplast is complicated because of problems associated with dye loading. We demonstrate a more sophisticated dye loading procedure that enables the mapping of spatial apoplastic ion gradients over a period of 3 h. The new technique has been used for the real-time monitoring of pH dynamics within the leaf apoplast in response to NaCl stress encountered by the roots.

**Keywords: apoplastic pH, live cell imaging, apoplastic ions, abiotic stress, salinity, pH regulation, fluorescence ratio imaging**

## INTRODUCTION

The apoplast is of major significance for the nutrition of higher plants (Sattelmacher et al., 1998). Knowledge of the apoplastic ion concentrations is necessary for the understanding of many transport processes across the plasma membrane, of membrane potentials, and of cell expansion. The activity of extracellular enzymes, the binding of ligands to receptors, and the wall structure are all likely to be affected by the apoplastic environment, which is known to be a polarized microenvironment for selective ion binding (Grignon and Sentenac, 1991; Canny, 1995; Mühling and Sattelmacher, 1995; Fricker et al., 1999). Because of the quantitative importance of ions and the impact of their apoplastic distribution on metabolic regulation, the localization, and quantification of ions is important for the understanding of the nutritional physiology of higher plants (Grignon et al., 1997).

The combination of ion-sensitive fluorescent probes with quantitative imaging techniques provides opportunities to localize, visualize, and quantify ion dynamics *in situ* via the technique of ratio imaging (Fricker et al., 1997a, 2008). Use of ratiometric analysis allows high temporal and spatial resolution with a minimum of perturbation to be achieved (Fricker et al., 1999). Although ratio imaging has been successfully employed to measure cytoplasmic calcium and pH in plants (as summarized by Fricker et al., 1994), little information is available on the application of this technique to the measurement of apoplastic ion concentrations (Taylor et al., 1996). The method has however been successfully used to measure apoplastic pH (Hoffmann et al., 1992; Hoffmann and Kosegarten, 1995; Mühling et al., 1995; Taylor et al., 1996; Bibikova et al., 1998; Mühling and Läuchli, 2000; Yu et al., 2001; Pitann et al., 2009) and, to a lesser extent, apoplastic potassium (Mühling and Sattelmacher, 1997; Mühling and Läuchli, 2000), calcium (Mühling et al. 1998), and sodium (Mühling and Läuchli, 2002).

**Abbreviations:** CLSM, confocal laser scanning microscopy; ROI, region of interest.

To the authors' knowledge, no ratiometric, non-transgenic *in planta* measurements are available that show leaf apoplastic ion dynamics by using ratio imaging. This is mainly attributable to problems associated with gaining access to the intact leaf apoplast (Fricker et al., 1994). The major difficulty here remains the development of appropriate loading protocols to introduce the fluorescent ion probe into the apoplast of a living plant without destroying the cell membranes, which in consequence would allow the dye to diffuse into the symplast, leading to an erroneous quantification of cytosolic pH signals. However, *in planta* analysis is important because it assures that the apoplast operates in a correct physiological context and hence includes the effects of cell–cell interactions and the mechanical, ionic, and physiological effects of the extracellular matrix of cell–wall interactions (Errington et al., 1997; Fricker et al., 1997b).

Here we present a non-invasive approach for loading a fluorescent ion indicator into the leaf apoplast of an intact plant (*Vicia faba* L.). In combination with camera-based inverse fluorescence microscopy, ratiometric *in planta* mapping of ion dynamics in various apoplastic components was achieved over a period of hours.

## MATERIALS AND METHODS

### CULTIVATION OF PLANT MATERIAL

*Vicia faba* L., minor cv. Scirocco (Saaten-Union GmbH, Isernhagen, Germany) was grown under hydroponic culture conditions in a climate chamber (14/10 h day/night; 20/15°C; 50/60% humidity). Seeds were soaked in an aerated $CaSO_4$ solution (0.5 mM) for 1 day at 25°C and subsequently placed into quartz sand moistened with $CaSO_4$ (1 mM). After 7 days of germination, seedlings were transferred to plastic pots containing one-quarter-strength aerated nutrient solution. Following 2 days of cultivation, the concentration of nutrients was increased to half-strength and, after 4 days of cultivation, to full-strength. The nutrient solution had the following composition: 0.1 mM $KH_2PO_4$, 1.0 mM $K_2SO_4$, 0.2 mM KCl, 2.0 mM

$Ca(NO_3)_2$, 0.5 mM $MgSO_4$, 60 μM Fe–EDTA, 10 μM $H_3BO_4$, 2.0 μM $MnSO_4$, 0.5 μM $ZnSO_4$, 0.2 μM $CuSO_4$, 0.05 μM $(NH_4)_6Mo_7O_{24}$. The solution was changed every third day to avoid nutrient depletion. After 30 days of plant cultivation, intact growing leaves with an average leaf area of 7 $cm^2$ were sampled for *in situ* pH recording.

#### DYE LOADING

For the purpose of ratiometric *in planta* measurements, the fluorescent pH indicator was loaded into the leaf apoplast of an intact plant. For this, the opening of a syringe was carefully pressed onto the abaxial leaf side (no needle was attached on the top of the syringe). By means of gentle pressure, 50 μL of 25 μM Oregon Green 488 dextran (Invitorgen GmbH, Darmstadt, Germany; dissolved in deionized water) were fed into the apoplast, whereby not the complete, but only a small part of the apoplast was loaded. The loading procedure could easily be monitored because the loaded area appeared darker than its surroundings (see **Figure A1** in Appendix). In order to avoid measurement artifacts caused by the possible impact of the loading procedure on leaf physiology, images were collected (1) adjacent to the area that had been loaded and (2) at the adaxial leaf side. This was possible since the dye proved to be mobile within the apoplast (described in detail in section Results and Discussion).

#### INVERSE MICROSCOPY IMAGING

A Leica inverted microscope (DMI6000B; Leica Microsystems, Wetzlar, Germany) connected to a DFC-camera (DFC 360FX; Leica Microsystems, Wetzlar, Germany) via a 20-fold magnification, 0.4 numerical aperture, dry objective (HCX PL FLUOTAR L, Leica Microsystems, Wetzlar, Germany) was used for image collection. An HXP lamp (HXP Short Arc Lamp; Osram, München, Germany) was used for illumination at excitation wavelengths of (ex) 440/20 and 495/10 nm. Exposure time was 25 mS for both channels. Light intensity and camera gain were coupled for both channels, ensuring identical excitation conditions. Excitation filters were switched by means of a filter wheel. The dye fluorescence at both excitation channels was collected by using a 535/25 nm emission bandpass filter (BP 535/25; ET535/25M; Leica Microsystems, Wetzlar, Germany) and a dichromatic mirror (LP518; dichroit T518DCXR BS, Leica Microsystems, Wetzlar, Germany). Time series were collected with a time interval of 2 or 5 min. During the measurements, leaves were not detached from the plant and the plants were supplied with aerated nutrient solution. The use of microscopy-based techniques for mapping ion concentrations in the leaves of living plants over several hours involves the problem that, from time to time, the specimen shifts out of the focal plane. This can be ascribed to the growth of the stem or the leaf; the latter growth can attain 4–6.25 $mm^2$/h (Dennett et al., 1978). In order to avoid any shifting of the specimen, care must be taken that the region of interest is firmly attached to the measuring device.

#### RATIOMETRIC ANALYSIS

Fluorescence ratio analysis corrects quantitative fluorescence imaging with regard to artifacts in signal strength associated with sample path length, dye distribution, leakage, and photobleaching (Bright et al., 1989; Gilroy, 1997). As a measure of pH, the fluorescence ratio $F_{495}/F_{440}$ (Pitann et al., 2009) was obtained by using the pH-sensitive fluophore Oregon Green 488 that is conjugated to 10 kDa dextran. The $F_{440}$ signal was captured because this fluorescence is almost insensitive to protons, whereas the $F_{495}$ signal highly depends on protons. An analysis of a time series was carried out by using Leica Application Suite Advanced Fluorescence, (LAS AF software, version 2.3.5, Leica Microsystems, Wetzlar, Germany). Ratio images were calculated on a pixel-by-pixel basis as $F_{495}/F_{440}$. The background noise values were subtracted at each channel. For pseudo-color display, the ratio was coded by hue on a spectral color scale ranging from purple (no signal), over blue (lowest pH signal; pH 3.9), to pink (highest pH signal; pH 6.3), with the limits being set by an *in situ* calibration. Ratios below 1.1 (corresponds to pH ≤ 3.9) and above 3.6 (corresponds to pH ≥ 6.3) were not considered, because they proved to lie outside the linear range of the *in situ* calibration (**Figure A2** in Appendix). Quantitative measurements were calculated as the ratio of the mean intensity for user-defined regions of interest (ROIs).

#### *IN SITU* APOPLASTIC PH CALIBRATION

For converting fluorescence ratio data taken from living plants into apoplastic pH values, an *in situ* calibration procedure was performed. Hence, 25 μM Oregon Green dye solutions buffered with 100 mM (2-[*N*-morpholino]ethanesulfonic acid, MES) to a pH ranging from 3 to 7 (steps of 0.5 pH units) were loaded into the leaf apoplast. The Boltzmann fit was chosen for fitting sigmoidal curves to calibration data (**Figure A2** in Appendix) as described by Schulte et al. (2006). Fitting was performed by using Origin 7.0 (OriginLab Corp., Northampton, MA, USA).

#### CONFOCAL LASER SCANNING MICROSCOPY

To demonstrate that no Oregon Green 488 dextran had entered the cytosol unintentionally, CLSM-imaging via a Leica TCS SP1 confocal laser scanning system (Leica Microsystems, Wetzlar, Germany) was carried out. For dye excitation, the 488 nm beam line of the Argon laser was chosen. The dye fluorescence was collected by using an emission bandwidth at 514–556 nm (green channel). A planapochromatic objective (HC PL APO CS 10.0 × 0.40; Leica Microsystems, Wetzlar, Germany) was used for image collection. The three-dimensional XYZ-image stack was created on the basis of 30 xy sections. Step size was 2.04 μm.

#### GAS EXCHANGE AND SPAD READINGS

Gas-exchange parameters such as stomatal conductance to $H_2O$ (mol $H_2O$ $m^{-2}$ $s^{-1}$) were measured with an open-flow gas-exchange system (portable photosynthesis system; LI-COR Biosystems GmbH, Bad Homburg, Germany) with an integrated fluorescence chamber head (LI-COR Biosystems GmbH, Bad Homburg, Germany). Leaves were placed across a 2 × 3 cm leaf cuvette. The conditions for the measurements inside the chamber were equal to the outside conditions in the climate chamber. Light was provided by an LED red light source built into the top of the leaf chamber (100 μmol quanta $m^{-2}$ $s^{-1}$) and the $CO_2$ concentration was controlled by a Li-Cor LI-6400 $CO_2$ injection system. Stomatal conductance was calculated by the internal software. The relative chlorophyll concentration of the leaves was measured with a portable chlorophyll meter (SPAD-502, Minolta, Japan). At least fifteen SPAD-502 readings for each leaf were averaged by the internal software of the SPAD-502 meter and were taken as a single data point for each biological replicate.

### LEAF AREA

Leaf area was calculated by means of measuring the length and maximum breadth of the leaflet, whereas lengths and breadths were converted to area by multiplying their product by 0.764 according the formula given by Dennett et al. (1978). Leaf area ($cm^2$) was chosen as a measure for leaf growth.

### DATA EVALUATION

The *t*-test and the paired *t*-test, as outlined by Köhler et al. (1984), were used to test for differences between mean.

## RESULTS AND DISCUSSION

### DYE LOADING PROCEDURE

*In planta* measurements of apoplastic ion dynamics by using microscopy-based ratio analysis require that the ion indicator is inserted into the leaf apoplast of an intact leaf. Traditional dye loading procedures, such as the time-consuming transpiration-driven loading technique via the petiole or the pressure loading technique of cut leaf discs, do not allow the *in situ* monitoring of ion concentrations over an extended period of time. In both cases, such monitoring is not possible because the leaves are detached from the plant. However, by gently feeding the ion indicator into the leaf apoplast with the above-described method (see section Materials and Methods), the dye can be inserted into an intact plant system. A prerequisite for *in situ* studies of the apoplastic microenvironment is that the ion indicator is linked to a dextran molecule that avoids compartmentalization of the indicator into the symplast. Inverse fluorescence microscopy images at ex 495 and ex 440 nm (**Figure 1**) and CLSM images at ex 488 nm (XYZ-image stack; **Movie S1** in Supplementary Material) indicate that the dye does not enter the cells. If the dye had entered the tissue unintentionally, then the dye signals would be emitted from the cells. However, the dye signals solely have their origin in the apoplastic space, whereas the tissue appears dark, indicating that no fluorescence signal is emitted from the cells themselves (**Figures 1A,B**; **Movie S1** in Supplementary Material). Immediately after the dye is loaded, the flooded apoplastic area is filled with water. This represents an artificial surrounding for the plant because, under normal physiological conditions, the apoplastic fluid is only a thin film (Felle, 2001). For this reason, measurements should not be started before the water has disappeared through the stomata of the intact leaves. Evidence that the loaded water can exit the plant apoplast is demonstrated in **Figure 2** and in **Figure A1** in Appendix. The water droplets on the bright-field images in **Figures 2B-i and C-i** strongly suggest that the water has left the apoplast through the stomata. The corresponding fluorescent images in **Figures 2B-ii and C-ii** demonstrate that no dye exits the apoplast together with the water droplets. Otherwise, these droplets would appear in pseudo-green when illuminated with ex 495 nm. The finding that the apoplastic space becomes free of excess water is important for the ratio analysis, because (1) the presence of water within the apoplast causes an acute lack of oxygen to which all the involved cells respond and (2) the water would dilute the apoplastic ion concentration (Felle and Hanstein, 2002). Another point that needs to be considered is the potential mechanical stress to which the leaf is exposed during dye loading. Although only small volumes (max. 50 µL/leaf apoplast) are gently fed into a part of the leaf apoplast, the fluid might interact through adhesive forces with the cell walls and plasma membranes and might thus stretch-activate channels that then release ions and organic acids (Felle and Hanstein, 2002). Hence, images are collected (1) at the earliest at 1.5 h after loading and (2) not at the dye-loaded area itself but adjacent to the loaded area. The latter is possible because the dye is mobile within the leaf apoplast of the living plant and is carried to the faces of the leaf edges (**Figure 3**). The mobility of the dye suggests possible alterations of the initial dye concentration (25 µM) within the apoplast. We have tested whether differences in dye concentration ranging from at least 10–150 µM Oregon Green 488 dextran still produce stable $F_{495}/F_{440}$ ratios. At all concentrations, the ratios are constant at 2.5 (**Table 1**). Moreover, changes in dye concentration do not represent a major problem, because differences in local indicator concentrations are corrected by mean of the ratio analysis (Gilroy, 1997).

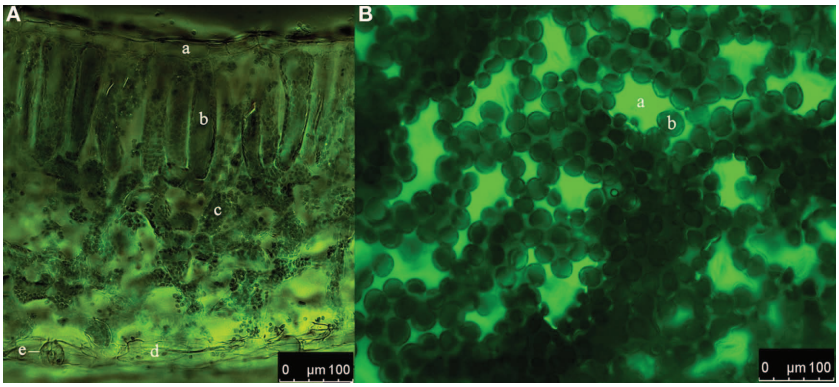


**FIGURE 1 | Distribution of the dextran-conjugated dye Oregon Green 488 within the leaf apoplast of *Vicia faba* L. directly after loading.**
**(A)** Cross-section. Overlay of ex 495 nm pseudo-green fluorescence image and ex 440 nm pseudo-red fluorescence image. a, adaxial epidermis cell; b, palisade cell; c, spongy cell; d, abaxial epidermis cell; e, stomatal apparatus. **(B)** Adaxial leaf face. Pseudo-green fluorescence image at ex 495 nm. a, stomatal cavity; b, palisade cell. Tissue in **(A)** and **(B)** appears dark indicating that no fluorescence signals are emitted. This demonstrates that no dye has entered the cells. In contrast, the apoplastic space appears in pseudo-color because of the dye emission.

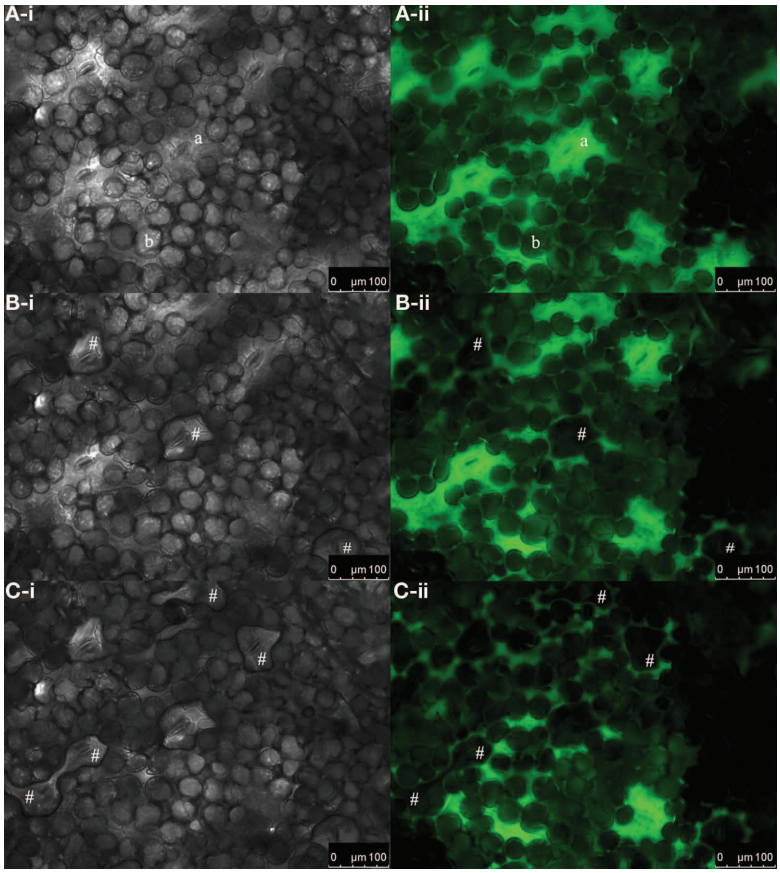


**FIGURE 2 | Excessive water exits the apoplast through the stomata.** Bright-field images of the adaxial leaf face (gray-scaled; **A-i**, **B-i**, and **C-i**) and corresponding pseudo-green fluorescence images at ex 495 nm (**A-ii, B-ii**, and **C-ii**). Images were collected **(A)** immediately after dye loading and at **(B)** 2 min and **(C)** 10 min after loading. **(A-i, -ii)** Immediately after loading, no water droplets are found to be located onto the stomata. **(B-i)** Water droplets that had left the apoplast through the stomata 2 min after dye insertion are indicated by #. **(B-ii)** The corresponding fluorescence image at ex 495 nm reveals that these droplets did not contain any dye, as otherwise fluorescence signals would be emitted at ex 495 nm and appear in pseudo-green. **(C-i** and **C-ii)** After 10 min, more water had left the apoplastic space as indicated by #. a, stomatal cavity; b, palisade cell.

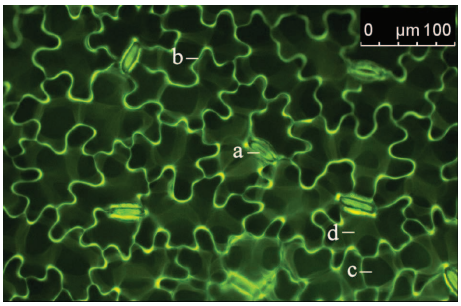


**FIGURE 3 | Distribution of the dextran-conjugated dye Oregon Green 488 at 1.5 h after the loading event.** Adaxial leaf face. Overlay of pseudo-green fluorescence image at ex 495 nm and pseudo-red fluorescence image at ex 440 nm. Images were collected at the leaf edges adjacent to the area that was loaded with the dye. The detection of dye emission signals at an area that was not loaded with the dye itself indicates that the dye is mobile within the leaf apoplast. This allows apoplastic pH to be measured in areas of the leaf apoplast not affected by the dye loading. a, stomatal apparatus; b, epidermal apoplast; c, palisade cell (dark structure; no dye signal); d, apoplast surrounding palisade mesophyll.

**Table 1 | Effects of various Oregon Green 488 concentrations on the $F_{495}/F_{440}$ ratio.**

| Oregon Green 488 dextran (µM) | *In situ* ratio $F_{495}/F_{440}$ | |
|---|---|---|
| | **Mean** | **SE** |
| 0 | / | / |
| 10 | 2.54 | 0.037 |
| 20 | 2.52 | 0.039 |
| 30 | 2.58 | 0.040 |
| 40 | 2.50 | 0.019 |
| 150 | 2.55 | 0.028 |

*Testing the effect of dye concentration on the $F_{495}/F_{440}$ ratio was performed by using the same dye loading procedure and the same optical set-up as for in situ measurements. At all concentrations, ratios were constant at ≈2.5. At a concentration of 0 µm Oregon Green 488, no signal was obtained as indicated by /. Values represent the mean ± SE (n = 4 biological replicates). t-test revealed no significant mean differences at $p \leq 0.05$.*

### *IN PLANTA* REAL-TIME IMAGING OF LEAF APOPLASTIC PH DYNAMICS

To demonstrate that the improved dye loading procedure enabled *in planta* monitoring and the quantification of apoplastic pH dynamics in real-time, an intact *Vicia faba* leaf was prepared with the pH indicator. Subsequently, the intact leaf was placed on the measuring device. Throughout the experiment, the plant itself was well supplied with aerated nutrient solution. An effect of the leaf apoplastic pH was induced by adding 50 µL of a 10 mM NaCl solution onto the surface of a *Vica faba* leaf. Within 5 min, leaf pH within the stomatal cavity, the epidermal apoplast, and the apoplast surrounding the palisade tissue transiently increased, whereas the pH within the palisade apoplast became the most alkaline (**Figure 4**). After 25 min, the pH began to normalize and finally reached the range at which the alkalinzation had started before the leaves were treated with NaCl stress. This time course demonstrated the suitability of this dye loading approach for quantitatively monitoring leaf apoplastic pH dynamics. In general, such monitoring is also possible with ion-sensitive micro-electrodes. However, micro-electrodes take measurements at a single point, i.e., the stomatal cavity, whereas microscopy-based techniques enable quantitative data to be averaged over a larger area of the leaf apoplast. Furthermore, the high resolution of these microscopy-based imaging analyses allows spatial ion gradients to be discriminated in various apoplastic components (**Figure 4**). Therefore, the informative value of a single measurement now increases since the data provide more information about the spatial concentration and the temporal course of the ion of interest. For this reason, a single measurement enables for a more detailed and accurate detection of the stress responses, which in consequence, facilitates the physiological interpretation of the data.

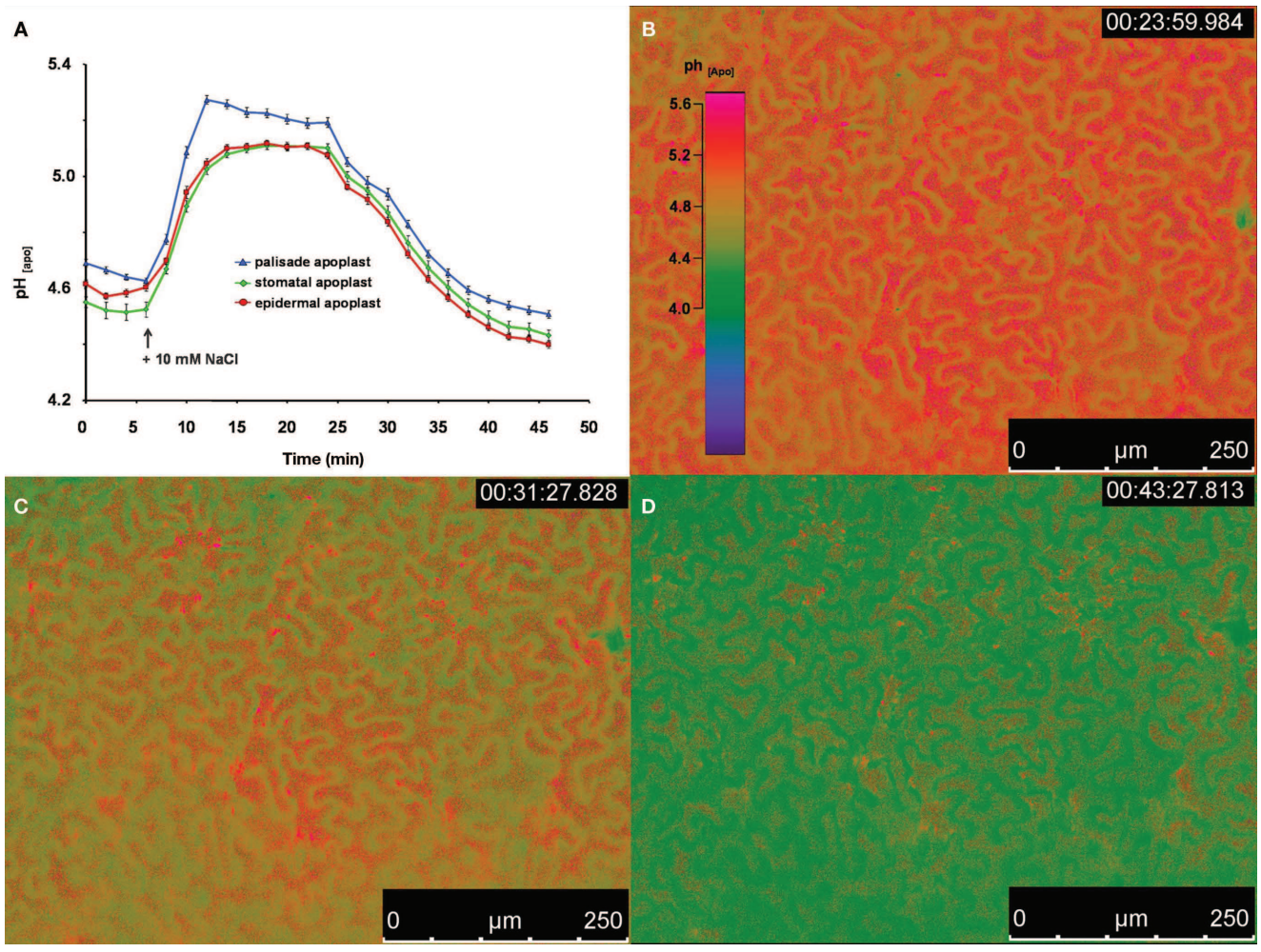


**FIGURE 4 | Ratiometric real-time quantitation of leaf apoplastic pH in response to the addition of 50 µL of a 10 mM NaCl solution onto the leaf.** **(A)** pH as recorded at the adaxial face of *Vicia faba* leaves is plotted over time. Black arrow indicates the time of the addition of the 10 mM NaCl stress stimulus onto the surface of the leaf. Leaf apoplastic pH was discriminated within three apoplastic components, viz. in the stomatal cavity ($n$ = 10 ROI; green kinetic; mean ± SE of ROIs), in the epidermal apoplast ($n$ = 20 ROI; red kinetic; mean ± SE of ROIs) and in the apoplast surrounding the palisade mesophyll ($n$ = 20 ROI; blue kinetic; mean ± SE of ROIs). Ratiometric images **(B–D)** show the time series of apoplastic leaf pH at **(B)** 23, **(C)** 31, and **(D)** 43 min after measurement had started (time of image acquisition is presented in the upper right corner of the ratio images). Ratios were color-coded on a spectral color scale (see lookup-table as inset in **B**). Representative kinetics of five equivalent recordings of plants gained from independent experiments.

In a second experiment, we demonstrated that the new dye loading procedure also enabled *in planta* monitoring of leaf apoplastic pH dynamics in response to a NaCl stress treatment applied to the roots. NaCl was added to the nutrient solution yielding a concentration of 20 mM (**Figure 5**). The pH transiently increased over a period ranging from 60 to 70 min, with an alkalinization occurring in the three apoplastic compartments, viz. the stomatal cavity, the epidermal apoplast, and the palisade apoplast, starting circa 20 min after NaCl was added to the roots. Similar to the transient alkalinization described in **Figure 4A**, the pH was the most alkaline within the apoplast built by the palisade tissue. To the authors' knowledge, this is the first time that a physiological

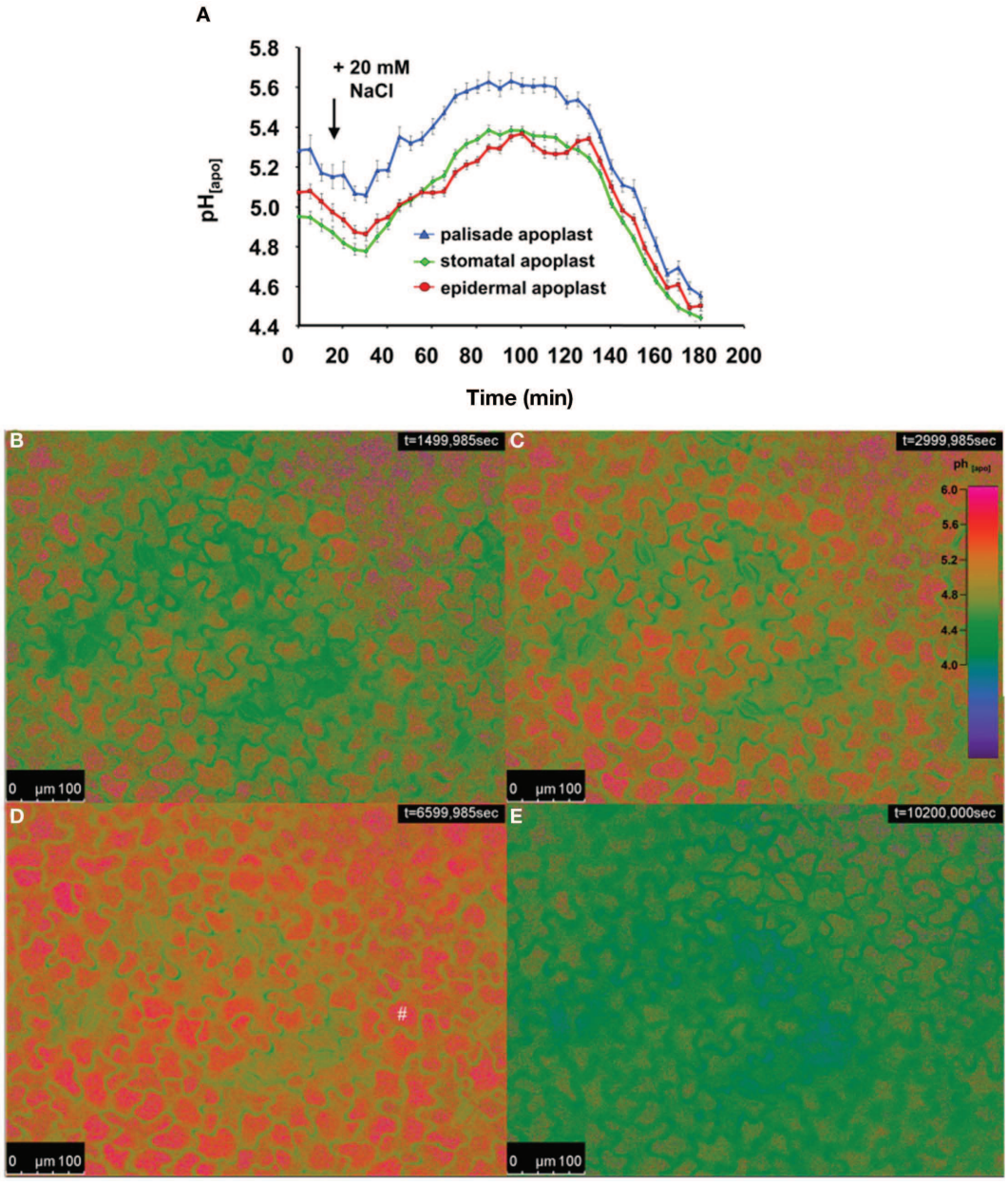


**FIGURE 5 | Ratiometric real-time quantitation of spatial leaf apoplastic pH gradients in response to 20 mM NaCl stress added to the roots. (A)** Leaf apoplastic pH response was discriminated within three apoplastic components, viz. in the stomatal cavitiy ($n$ = 9 ROI; green kinetic; mean ± SE of ROIs), in the epidermal apoplast ($n$ = 20 ROI; red kinetic; mean ± SE of ROIs) and in the apoplast surrounding the palisade mesophyll ($n$ = 20 ROI; blue kinetic; mean ± SE of ROIs). Black arrow indicates the time of the addition of the 20 mM NaCl stress stimulus into the nutrient solution. Ratiometric images **(B–E)** show the time series of apoplastic leaf pH at **(B)** 25, **(C)** 50, **(D)** 110 min, and **(E)** 170 min after measurement had started (time of image acquisition is presented in the upper right corner). Ratios were color-coded on a spectral color scale (see lookup-table as inset in **B**). The ratio images under the most alkaline conditions suggest that fluorescent signals come directly from the palisade cells as indicated by the # in **(D)**. This phenomenon is explained in section "Discussion." Representative kinetics of four equivalent recordings of plants gained from independent experiments.

stress response that was induced by adding NaCl to the roots has been ratiometrically monitored within the intact leaf apoplast in a resolution that allows spatial ion gradients to be discriminated in various apoplastic components over a period of 3 h *in planta*.

The pseudo-color ratios presented in **Figures 4 and 5** require additional comment. The ratio images at the most alkaline conditions suggest that fluorescent signals come directly from within the palisade cells (indicated by # in **Figure 5D**). This implies that, in addition to the apoplastic pH signals, cytosolic pH signals have been quantified erroneously. Such an idea can however be rejected for several reasons. (1) A XYZ-image stack showing the leaf apoplastic space that was labeled with Oregon Green 488 dextran was created using CLSM. Dye excitation with an Argon laser line at 488 nm (**Movie S1** in Supplementary Material) clearly demonstrated that the dye signals were solely emitted from the apoplast. The mesophyll cells appeared dark, providing evidence that no dye had unintentionally entered the cells. Thus the appearance of cytosolic or cellular pH signals can be rebutted. (2) The pH probe is covalently linked to a 10 kDa dextran, which would require pressure microinjection for loading into the cytoplasm (Fricker et al., 1999). (3) The cytosolic pH is known to be around 7.2 (Schwarzländer et al., 2008; D'Onofrio and Lindberg, 2009), whereas the quantified pH-values shown in **Figures 4A and 5A** do not exceed a value of pH 5.4 and 5.6, respectively. (4) Even supposing the dye had entered the cytosol unintentionally, the apoplastic pH response shown in **Figures 4 and 5** could not drop back to its initial level at pH 4.2, because the cytosol never reaches such an acid milieu. Nevertheless, why do the ratio images at the most alkaline conditions suggest that fluorescent signals come directly from within the palisade cells (indicated by # in **Figure 5D**)? Immediately after dye was loaded into the apoplast, the inserted water exits the leaf through the stomata (shown in **Figure 2**). However, the dye has been demonstrated to remain within the apoplast (**Figures 2A-ii, B-ii**, and **C-ii**). We presume that the dye is dissolved within the apoplastic fluid, which is a thin film that is attached to the surface of the cells (Felle and Hanstein, 2002). Consequently, the fluorescent dye is closely attached around the palisade cells, thus, light that is emitted by the dye mimics the shape of the cells. However, in response to a physiological alkalinization of the apoplastic fluid that surrounds the palisade cells, the intensity of the emitted light raises, because the emission triggered by the $F_{495}$ channel increases with decreasing $[H^+]$. This strong $F_{495}$ fluorescence erroneously conveys (see above) the impression that these signals arise within the cell (indicated by # in **Figure 5D**).

## POTENTIAL ARTIFACTS

Several potential artifacts might occur during ratio imaging experiments and, if not considered, might introduce errors in quantitation. A point that needs to be considered during imaging is the level of background signals, viz. autofluorescence coming from the measuring devices (i.e., lens elements), the specimen (i.e., cell wall or chloroplasts), the shot noise associated with sampling of the signal (Fricker et al., 1997b, 2001), and the noise arising from residual light in the laboratory (i.e., computer LEDs, monitor screens). For the testing of the level of autofluorescence, the specimen without the dye is illuminated (background signal intensity) and compared with the specimen plus dye (total signal intensity). Only negligible noise has been detected (0.1% of the weakest fluorescence signals and 0.03‰ of the strongest; **Figure 6**). The background noise values are subtracted at each channel. In addition to the occurrence of background fluorescence, confirmation is required that the NaCl molecules themselves do not influence the $F_{495}/F_{440}$ ratio and thus the quantification. Such an effect might occur because the NaCl that is added to the nutrient solution might be transported through the xylem into the leaf apoplast where it might interact with the fluorophore. In order to exclude such an effect, we have demonstrated that NaCl concentrations ranging from 0 to 125 mM do not affect the Oregon Green 488 ratio (**Figure 7**). Moreover, we have tested

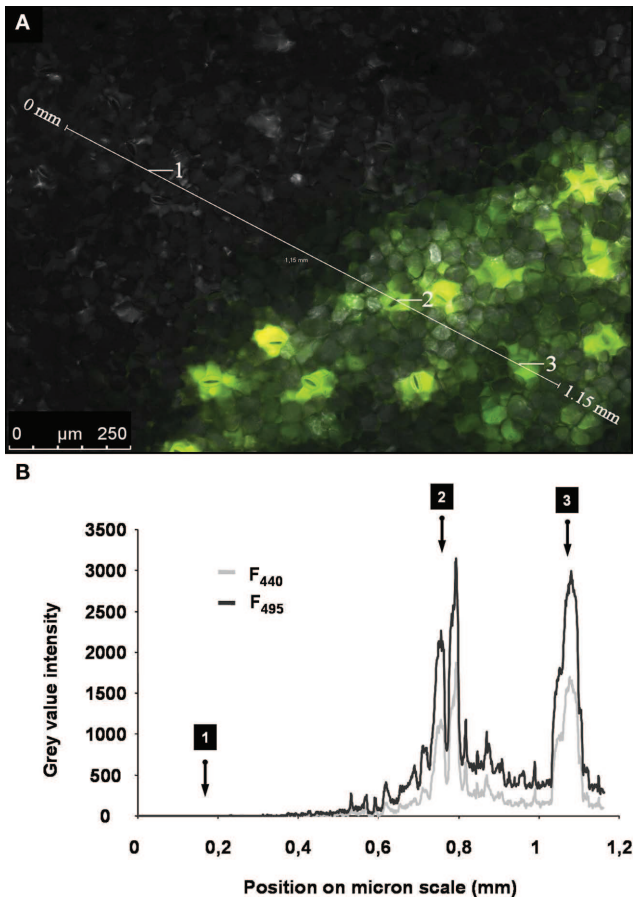


**FIGURE 6 | Specific dye signals versus unspecific noise signals.** **(A)** Adaxial leaf face. Overlay of ex 495 nm pseudo-green fluorescence image, ex 440 nm pseudo-red fluorescence image, and the corresponding bright-field image (gray-scaled). The apoplast was partially loaded with the dye (lower right part of the image). Dye-loaded areas appear light green when illuminated, because pseudo-red and pseudo-green are mixed within the overlay. The gray area was not loaded with the dye (upper left part of the image). Such a specimen represents a suitable object to compare the amount of unspecific signals (noise) to specific signals being emitted from the dye. The intensity of gray values was chosen as a measure for signal intensity. A profile of the gray-value intensity was taken from the area tagged with the scale bar (1.15 mm length; white line in **A**) and is presented in **(B)**. This profile is displayed for both fluorescence excitation channels (ex 495 and ex 440 nm). Negligible signals were emitted from the area of the leaf without dye (i.e., detail 1). The signals were much higher in the dye-loaded areas (i.e., detail 2 and 3; in both cases, signal intensity at stomatal cavity).

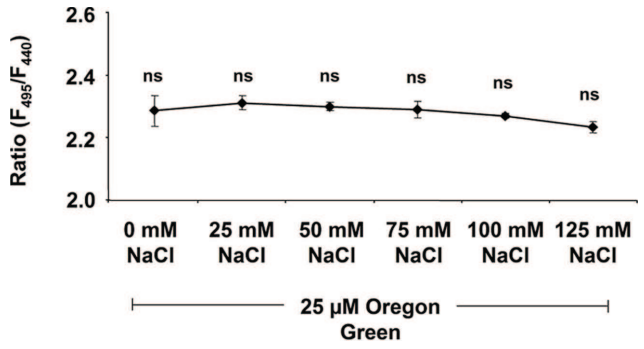


**FIGURE 7 | Dependency of the Oregon Green 488 $F_{495}/F_{440}$ ratio on NaCl.** Ratios are displayed against NaCl concentration. NaCl ranging from 0 to 125 mM was mixed into the dye solution (25 µM Oregon Green). Ratios were stable and thus not affected by NaCl. Values represent the mean ± SE ($n = 4$ biological replicates). *t*-Test revealed no significant mean differences at $p \leq 0.05$.

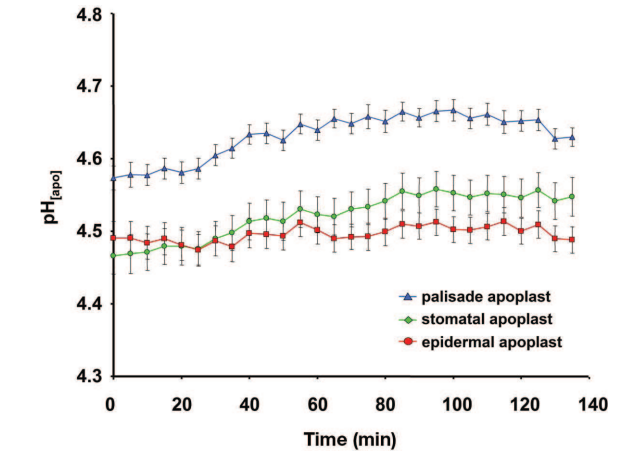


**FIGURE 8 | Ratiometric real-time quantitation of leaf apoplastic pH in response to the given illumination regime used for inverse microscopy image acquisition.** pH as recorded at the adaxial face of *Vicia faba* leaves is plotted over time. Leaf apoplastic pH was discriminated within three apoplastic components, viz. in the stomatal cavity ($n = 6$ ROI; green kinetic; mean ± SE of ROIs), in the epidermal apoplast ($n = 20$ ROI; red kinetic; mean ± SE of ROIs) and in the apoplast surrounding the palisade mesophyll ($n = 20$ ROI; blue kinetic; mean ± SE of ROIs). No effects on apoplastic pH were detected that were attributable to the illumination of the specimen with the excitation or emission wavelengths used for imaging. Representative kinetics of four equivalent recordings of plants gained from independent experiments.

whether the presence of NaCl within the leaf apoplast increases background noise signal intensity when illuminated with ex 495 and ex 440 nm. After the loading of NaCl solution directly into the leaf apoplast, no additional unspecific noise signals have been detected (**Figure A3** in Appendix). Another problem relates to the physiological response that the excitation or emission wavelengths used for imaging might trigger in the specimen (Fricker et al., 1994). To check whether the illumination regime itself influences the apoplastic pH, a time series of ex 495 and ex 440 nm images has been collected. No effects on apoplastic pH have been detected (**Figure 8**) supporting the proposal that the transient pH increases demonstrated in **Figures 4 and 5** are solely attributable to the salt treatment. Furthermore, the dye loading procedure represents a potential event of (local) mechanical stress and the presence of the dye itself within the apoplast might have an impact on the apoplastic space. Hence, leaf growth, stomatal conductance, and chlorophyll concentrations have been compared in loaded leaves and in leaves not loaded with ion indicator (control leaves). None of the tested parameters is influenced (**Figure 9**). The monitoring of the physiological ion dynamics as demonstrated in **Figure 5**

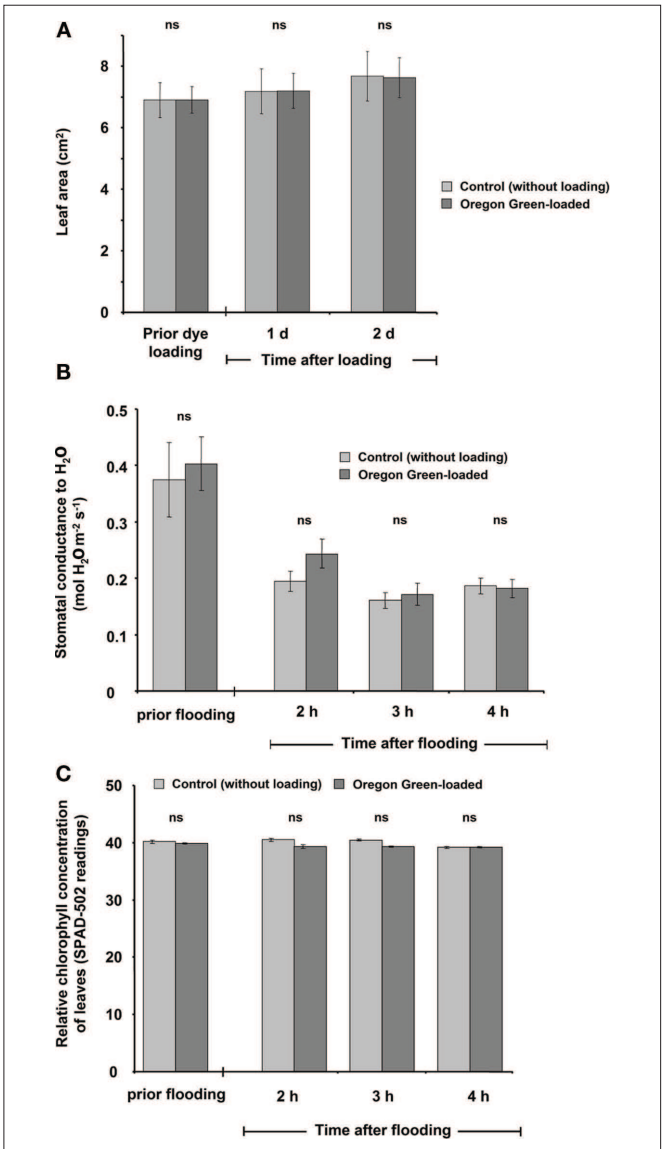


**FIGURE 9 | Leaf growth (A), stomatal conductance (B), and relative chlorophyll concentration (C) as influenced by the dye and the loading procedure.** To test whether these parameters were affected, a paripinnate leaf was used. One leaflet was loaded with the dye, whereas the second was not loaded with the dye and was used as control. Leaves were tested **(A)** prior to loading and at 1 and 2 days after loading or **(B,C)** prior to loading and 2, 3, and 4 h after loading. The parameters were not influenced by the presence of the dye or the loading procedure. The data are mean of four biological replicates gained from independent experiments ± SE. Paired *t*-test revealed no significant (ns) mean differences at $p \leq 0.05$.

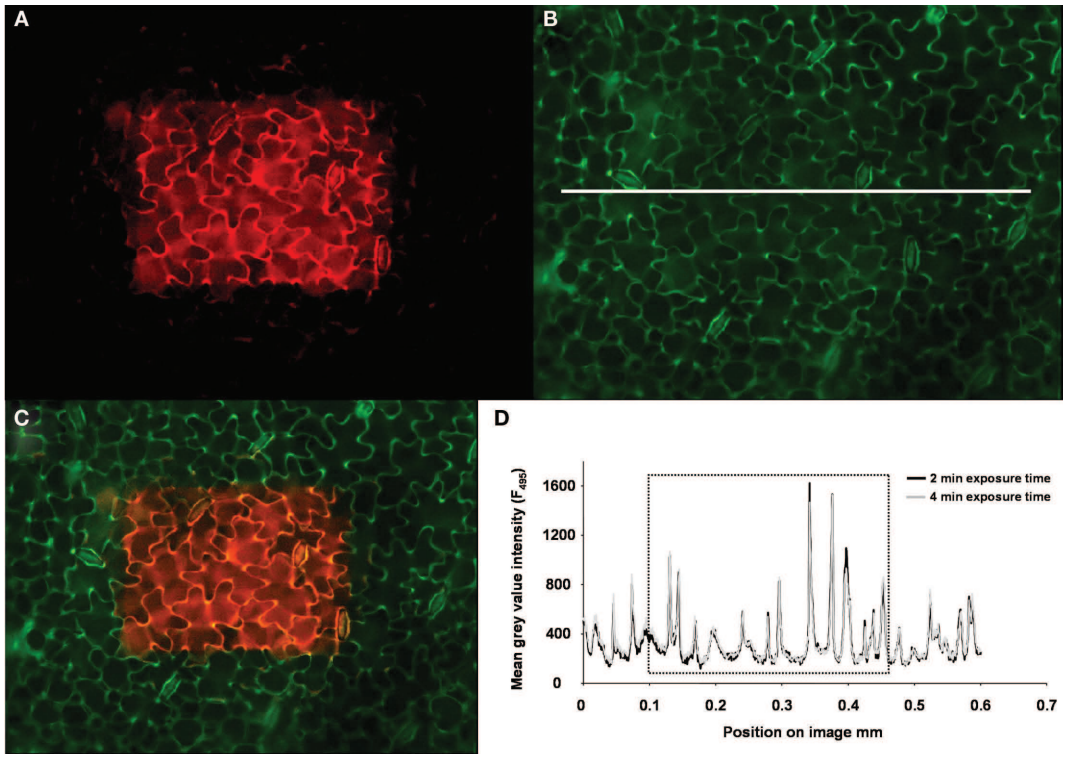


**FIGURE 10 | Photostability of the fluorescent ion indicator. (A)** To test whether the dye was prone to bleaching, a selected area in the middle of the specimen (presented in pseudo-red) was continuously excited by 495 nm illumination over a period of 2 min. The outer edges of the specimen were not illuminated because the field diaphragm foreclosed the illumination of this area, thus representing the control area of the leaf (control area = dark area within the image). **(B)** After 2 min continuous excitation, the field diaphragm was opened for collecting an image at ex 495 nm (exposure time was 25 mS). The image is presented in pseudo-green and contains the part of the specimen that was continuously illuminated plus the adjacent edges of the specimen that were not exposed to the continuous illumination at ex 495 (control). Image **(C)** presents the merged overlay of **(A, B)**. The pseudo-orange area (mixing pseudo-red and pseudo-green yields orange) represents the part of the leaf with the possibly bleached dye, whereas the pseudo-green area represents the control part of the leaf. Image **(B)** was used to create a profile of the gray-value intensity from the area tagged by the white line as a measure for the dye signal intensity after 2 min of continuous excitation at 495 nm (dark-gray profile) and after 4 min of continuous excitation (light-gray profile). The gray-value intensity profiles are presented in **(D)**. The dotted rectangle in **(D)** flags the gray-value intensity from the region that was exposed to continuous illumination. The gray-value intensity outside of the rectangle represents the control values. A comparison of the signal intensities between the possibly bleached part of the specimen and the control reveals that no dye-bleaching had actually occurred after 2 min of continuous illumination. This was also confirmed after 4 min.

requires 3 h. Altogether, 36 fluorescence images at each channel have been captured at an exposure time of 25 mS/image, yielding in an accumulated exposure time of 1800 mS. Obviously, a probe is required that is not prone to (photo-)bleaching. Fortunately, dextran-linked Oregon Green 488 is extremely photostable under circumstances of up to $2.4 \times 10^5$ mS of continuous $F_{495}$-light exposure (**Figure 10**).

## CONCLUSION

Our new dye loading procedure has been demonstrated to be suitable for ratiometric *in planta* mapping and the quantification of apoplastic pH dynamics. The spatial resolution of the microscopy-based imaging allows the discrimination of spatial gradients within the leaf apoplastic ion milieu. The more sophisticated dye loading procedure in combination with camera-assisted ratio imaging enables the real-time mapping of spatial apoplastic ion gradients over a period of 3 h *in situ*. Moreover, we have used this technique to monitor leaf apoplastic pH dynamics in response to NaCl stress events.

## ACKNOWLEDGMENTS

Christoph-Martin Geilfus is the grateful recipient of a grant from the Friedrich-Ebert-Foundation. We thank Dr. Christoph Plieth (Center of Biochemistry and Molecular Biology, University of Kiel) for giving advice with regard to fitting calibration data to a sigmoidal Boltzmann fit and for providing help with CLSM-imaging. Many thanks are also due to Christina Neuhaus for giving critical comments on the manuscript.

## SUPPLEMENTARY MATERIAL

The Movies S1 for this article can be found online at http://www.frontiersin.org/plant_nutrition/10.3389/fpls.2011.00013/abstract/

**VIDEO S1 | Confocal XYZ-image stack showing abaxial leaf apoplast of *Vicia faba* as labeled with Oregon Green 488 dextran.** Excitation with an Argon laser line at 488 nm; emission at 514–556 nm (green channel); Leica TCS SP confocal laser scanning system; HC PL APO CS 10.0 × 0.40 planapochromatic objective. Dye signals are emitted from the apoplast (green color), whereas the mesophyll cells appear dark. This establishes that no Oregon Green 488 dextran had entered the cytosol unintentionally, as otherwise signals would be detectable from the cells.

## REFERENCES


Bibikova, T. N., Jacob, T., Dahse, I., and Gilroy, S. (1998). Localized changes in apoplastic and cytoplasmic pH are associated with root hair development in *Arabidopsis thaliana*. *Development* 125, 2925–2934.

Bright, G. R., Fisher, G. W., Rogowska, J., and Taylor, L. D. (1989). Fluorescence ratio imaging microscopy. *Meth. Cell Biol.* 30, 157–192.

Canny, M. J. (1995). Apoplastic water and solute movement: new roles for an old space. *Annu. Rev. Plant Physiol. Plant Mol. Biol.* 46, 215–236.

Dennett, M. D., Auld, B. A., and Elston, J. (1978). A description of leaf growth in *Vicia faba* L. *Ann. Bot.* 42, 223–232.

D'Onofrio, C., and Lindberg, S. (2009). Sodium induces simultaneous changes in cytosolic calcium and pH in salt-tolerant quince protoplasts. *J. Plant Physiol.* 166, 1755–1763.

Errington, R. J., Fricker, M. D., Wood, J. L., Hall, A. C., and White, N. S. (1997). Four-dimensional imaging of living chondrocytes in cartilage using confocal microscopy: a pragmatic approach. *Am. J. Physiol. Cell Physiol.* 272, C1040–C1051.

Felle, H. H. (2001). pH: signal and messenger in plant cells. *Plant Biol.* 3, 577–591.

Felle, H. H., and Hanstein, S. (2002). The apoplastic pH of the substomatal cavity of *Vicia faba* leaves and its regulation responding to different stress factors. *J. Exp. Bot.* 53, 73–82.

Fricker, M. D., Chow, C. M., Errington, R. J., May, M., Mellor, J., Meyer, A. J., Tlalka, M., Vaux, D. J., Wood, J., and White, N. S. (1997a). Quantitative imaging of intact cells and tissues by multi-dimensional confocal fluorescence microscopy. *Exp. Biol.* 2, 1–23.

Fricker, M. D., Errington, R. J., Wood, J. L., Tlalka, M., May, M., and White, N. S. (1997b). "Quantitative confocal fluorescence measurements in living tissues," in *Signal Transduction - Single Cell Research*, eds B. Van Duijn and A. Wiltnik (Heidelberg: Springer-Verlag), 569–596.

Fricker, M. D., Lee, J. A., Bebber, D. P., Tlalka, M., Hynes, J., Darrah, P. R., Watkinson, S. C., and Boddy, L. (2008). Imaging complex nutrient dynamics in mycelial networks. *J. Microsc.* 231, 317–331.

Fricker, M. D., Parsons, A., Tlalka, M., Blancaflor, E., Gilroy, S., Meyer, A., and Plieth, C. (2001). "Fluorescent probes for living plant cells," in *Plant Cell Biology: A Practical Approach*, 2nd Edn, eds C. Hawes and B. Satiat-Jeunemaitre (Oxford: University Press), 35–84.

Fricker, M. D., Plieth, C., Knight, H., Blancaflor, E., Knight, M. R., White, N. S., and Gilroy, S. (1999). "Fluorescent and luminescent techniques to probe ion activities in living plant cells," in Fluorescent and luminescent probes, ed. W. T. Mason (London: Academic Press), 569–596.

Fricker, M. D., Tlalka, M., Ermantraut, J., Obermeyer, G., Dewey, M., Gurr, S., Patrick, J., and White, N. S. (1994). Confocal fluorescence ratio imaging of ion activities in plant cells. *Scanning Microsc.* 8, 391–405.

Gilroy, S. (1997). Fluorescence microscopy of living plant cells. *Annu. Rev. Plant Physiol. Plant Mol. Biol.* 48, 165–190.

Grignon, C., and Sentenac, H. (1991). pH and ionic conditions in the apoplast. *Annu. Rev. Plant Physiol. Plant Mol. Biol.* 42, 103–128.

Grignon, N., Halpern S., Jeusset, J., Briançon, C., and Fragu, P. (1997). Localization of chemical elements and isotopes in the leaf of soybean (*Glycine max*) by secondary ion mass spectrometry microscopy: critical choice of sample preparation procedure. *J. Microsc.* 186, 51–66.

Hoffmann, B., and Kosegarten, H. (1995). FITC-dextran for measuring apoplast pH and apoplastic pH gradients between various cell types in sunflower leaves. *Physiol. Plant* 3, 327–335.

Hoffmann, B., Plänker, R., and Mengel, K. (1992). Measurements of pH in the apoplast of sunflower leaves by means of fluorescence. *Physiol. Plant* 84, 146–153.

Köhler, W., Schachtel, G., and Voleske, P. (1984). *Einführung in die Statistik für Biologen und Agrarwissenschaftler*. Berlin: Springer.

Mühling, K. H., and Läuchli, A. (2000). Light-induced pH and $K^+$ changes in the apoplast of intact leaves. *Planta* 212, 9–15.

Mühling, K. H., and Läuchli, A. (2002). Determination of apoplastic $Na^+$ in intact leaves of cotton by *in vivo* fluorescence ratio imaging. *Funct. Plant Biol.* 29, 1491–1499.

Mühling, K. H., Plieth, C., Hansen, U. P., and Sattelmacher, B. (1995). Apoplastic pH of intact leaves of *Vicia faba* as influenced by light. *J. Exp. Bot.* 46, 377–382.

Mühling, K. H., and Sattelmacher, B. (1995). Apoplastic ion concentration of intact leaves of field bean (*Vicia faba*) as influenced by ammonium and nitrate nutrition. *J. Plant Physiol.* 147, 81–86.

Mühling, K. H., and Sattelmacher, B. (1997). Determination of apoplastic $K^+$ in intact leaves by ratio imaging of PBFI fluorescence. *J. Exp. Bot.* 48, 1609–1614.

Mühling, K. H., Wimmer, M., and Goldbach, H. E. (1998). Apoplastic and membrane-associated $Ca^{2+}$ in leaves and roots as affected by boron deficiency. *Physiol. Plant* 102, 179–184.

Pitann, B., Kranz, T., and Mühling, K. H. (2009). The apoplastic pH and its significance in adaptation to salinity in maize (*Zea mays* L.): comparison of fluorescence microscopy and pH-sensitive microelectrodes. *Plant Sci.* 176, 497–504.

Sattelmacher, B., Mühling, K. H., and Pennewiß, K. (1998). The apoplast – its significance for the nutrition of higher plants. *J. Plant Nutr. Soil Sci.* 161, 485–498.

Schulte, A., Lorenzen, I., Böttcher, M., and Plieth, C. (2006). A novel fluorescent pH probe for expression in plants. *Plant Methods* 2, 7.

Schwarzländer, M., Fricker, M. D., Müller, C., Marty, L., Brach, T., Novak, J., Sweetlove, L. J., Hell, R., and Meyer, A. J. (2008). Confocal imaging of glutathione redox potential in living plant cells. *J. Microsc.* 231, 299–316.

Taylor, D. P., Slattery, J., and Leopold, A. C. (1996). Apoplastic pH in corn root gravitropism: a laser scanning confocal microscopy measurement. *Physiol. Plant* 97, 35–38.

Yu, Q., Kuo, L., and Tang, C. (2001). Using confocal laser scanning microscopy to measure apoplastic pH change in roots of *Lupinus angustifolius* L. in response to high pH. *Ann. Bot.* 87, 47–52.


**Conflict of Interest Statement:** The authors declare that the research was conducted in the absence of any commercial or financial relationships that could be construed as a potential conflict of interest.

*Received: 02 March 2011; accepted: 16 April 2011; published online: 02 May 2011.*
*Citation: Geilfus CM and Mühling KH (2011) Real-time imaging of leaf apoplastic pH dynamics in response to NaCl stress. Front. Plant Sci. 2:13. doi: 10.3389/fpls.2011.00013*
*This article was submitted to Frontiers in Plant Nutrition, a specialty of Frontiers in Plant Science.*

## APPENDIX


**FIGURE A1 | Dye-loaded leaf apoplast of *Vica faba* L.** To prepare a leaf for measurement, dye is partially loaded into the leaf apoplast. The loading procedure can be monitored by the darker appearance of the leaf apoplast. This dark shade disappears after the water has left the leaf through the stomata (compare with **Figure 2**). Images were taken immediately after the dye was loaded **(A)**, 2 min after loading **(B)** and **(C)** 15 min after loading. This time series demonstrates that the water exits the leaf through the stomata after at least 15 min.

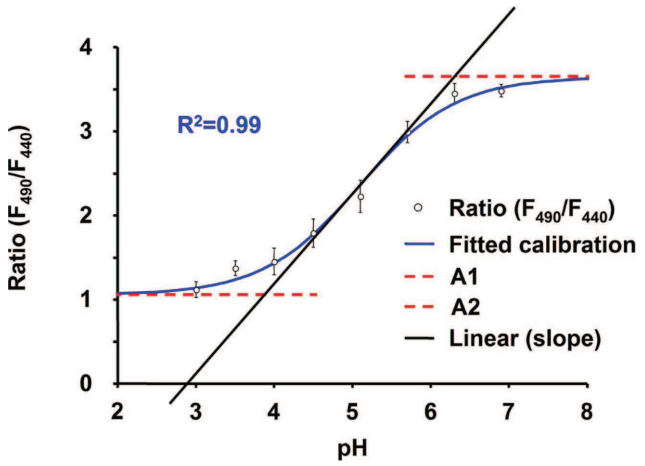


**FIGURE A2 | Calibration curve for Oregon Green 488 dextran fluorescence excitation ratio R (495ex/440ex; 525em).** The Boltzmann fit was chosen for fitting sigmoidal curves to *in situ* calibration ratio data. Fitting resulted in an optimal dynamic range for pH measurements between 3.9 and 6.3 (corresponds to the ratios 1.1 and 3.6). *In situ* calibration was conducted on six different plants ($n = 6$ biological replicates), each biological replicate was technically replicated a further five times ($n = 5$ technical replicates), whereas at least five regions of interest were averaged to yield one technical replicate ($n \geq 5$ ROI). Data are mean of the six biological replicates ± SE.

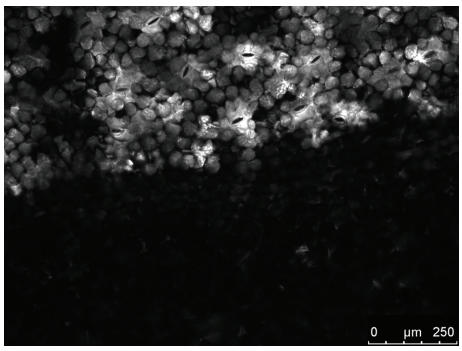


**FIGURE A3 | NaCl does not increase noise signal intensity.** Adaxial leaf face. Overlay of a pseudo-green fluorescence image at ex 495 nm, a pseudo-red fluorescence image ex at 440 nm and the corresponding bright-field image (gray-scaled). The upper light-gray area was loaded with 50 mM NaCl (not with Oregon Green). After the NaCl solution had been loaded directly into the leaf apoplast, no additional unspecific noise signals were detected after illumination with ex 495 and ex 440 nm. Noise signals, if present, would have appeared in pseudo-green or pseudo-red within the light-gray area of the image.

# Chapter 6

# Transient alkalinization in the leaf apoplast of *Vicia faba* L. depends on NaCl stress intensity: an *in situ* ratio imaging study

Christoph-Martin Geilfus and Karl Hermann Mühling

*Submitted*

# Transient alkalinization in the leaf apoplast of *Vicia faba* L. depends on NaCl stress intensity: an *in situ* ratio imaging study

Christoph-Martin Geilfus and Karl Hermann Mühling*

Institute of Plant Nutrition and Soil Science, Christian Albrechts University, Hermann-Rodewald-Str. 2, 24118 Kiel, Germany

*Correspondence: Prof. Dr. Karl H. Mühling, Institute of Plant Nutrition and Soil Science, Christian Albrechts University, Hermann-Rodewald-Str. 2, 24118 Kiel, Germany. Phone (+49) 0431-8803189, FAX (+49) 0431-8801625, E-mail: khmuehling@plantnutrition.uni-kiel.de

Key words: apoplastic pH, live cell imaging, environmental stress, salinity, pH signalling, fluorescence ratio imaging.

Running title: NaCl-induced apoplastic alkalinizations

## Abstract

The apoplast is suggested to be involved not only in the response, but also in the perception and transduction of various environmental signals. In this context, apoplastic alkalinization has previously been discussed as a general stress factor caused by abiotic and biotic stress events. In this study, an ion-sensitive fluorescence probe in combination with inverted fluorescence microscopy has been used for *in planta* monitoring of apoplastic shoot pH during challenging of *Vicia faba* L. plants by NaCl stress encountered at the roots. We demonstrate that transient increases in leaf apoplastic pH are dependent on the NaCl stress intensity. Moreover, we have visualized spatial pH gradients within the leaf apoplast. Our results indicate that these pH responses are propagated from root to leaf and that this occurs along the apoplast.

## Introduction

Terrestrial plants cannot choose the site in which they grow and thus have to endure a variety of environmental challenges, e.g. salinity, drought or low temperatures (Shinozaki & Yamaguchi-Shinozaki 1997; Felle 2001). The apoplast is the first plant compartment that encounters abiotic or biotic stress signals (Gao et al. 2004; Felle et al. 2009) and is suggested to be involved not only in the response, but also in the perception and transduction of various environmental signals, as summarized by Hoson (1998). Information regarding an (ongoing) stress event at the roots might have to be rapidly transferred to the leaves. Such information has to be carried systematically and might be transformed into another signal to reach more distant plant organs such as the leaves (Felle et al. 2005). In this context, apoplastic alkalinization has been discussed as a general stress factor caused by abiotic and biotic stress events (Wilkinson & Davies 1997; Wilkinson 1999; Felle 2001 & 2005; Felle & Hanstein 2002; Felle et al. 2005). Nevertheless, whether apoplastic pH is involved in signalling either

directly or in cross talk with plant hormones or calcium is unclear (Hartung et al. 1989; Gilroy & Trewavas 1994; Roos 2000; Felle 2001; Gao et al. 2004; Monshausen et al. 2011).

*In vivo* measurements of the apoplastic pH are not straightforward, because of the problem of gaining access to the apoplastic fluid, which has been characterized by Felle & Hanstein (2002) as being an extremely thin film. Apoplastic pH can be measured by using diverse techniques, such as proton-selective electrodes (e.g. Felle 1998), fluorescence dyes (e.g. Hoffmann et al. 1992; Mühling et al. 1995), or by collecting apoplastic fluid (e.g. Husted & Schjoerring, 1995). The limited number of *in vivo* measurements of apoplastic pH changes available from intact plants under abiotic stress persuaded Gao et al. (2004) to produce transgenic *Arabidopsis* plants expressing pH indicators in the apoplast. To study extracellular pH dynamics, they targeted pHfluorins as fusion proteins to the apoplast by means of an *Arabidopsis* chitinase signal sequence (summarized in Minorsky 2004). In addition, Geilfus and Mühling (2011) have recently developed a technique for inserting ion-sensitive fluorescence dyes into the apoplast of intact plants. In combination with microscopy-based imaging, this dye loading approach enables the high spatial-resolution quantitation of apoplastic pH dynamics over a period of several hours *in situ*. In the present study, this novel technique has been used for the ratiometric real-time monitoring of apoplastic pH in *Vicia faba* L. plants challenged by NaCl stress encountered at the roots. Our aim has been to investigate (1) whether the magnitude of a stress-induced pH response depends on the dose of the stress treatment and (2) whether this pH response occurs equally within the different regions of the leaf apoplast.

## Materials and methods

### Cultivation of plant material

*Vicia faba* L., minor cv. Scirocco (Saaten-Union GmbH, Isernhagen, Germany) was grown under hydroponic culture conditions in a climate chamber (14/10 h day/night; 20/15°C;

50/60% humidity). Seeds were soaked in an aerated $CaSO_4$ solution (0.5 mM) for 1 day at 25°C and subsequently placed into quartz sand moistened with $CaSO_4$ (1 mM). After 7 days of germination, seedlings were transferred to plastic pots containing one-quarter-strength aerated nutrient solution. After 2 days of cultivation, the concentration of nutrients was increased to half-strength and, after 4 days of cultivation, to full-strength. The nutrient solution had the following composition: 0.1 mM $KH_2PO_4$, 1.0 mM $K_2SO_4$, 0.2 mM KCl, 2.0 mM $Ca(NO_3)_2$, 0.5 mM $MgSO_4$, 60 µM Fe-EDTA, 10 µM $H_3BO_4$, 2.0 µM $MnSO_4$, 0.5 µM $ZnSO_4$, 0.2 µM $CuSO_4$, 0.05 µM $(NH_4)_6Mo_7O_{24}$. The solution was changed every 3$^{rd}$ day to avoid nutrient depletion. After 30 days of plant cultivation, growing *Vicia faba* L. plants were taken for *in vivo* pH-recording.

**Dye loading**

For the purpose of the ratiometric *in planta* measurement of apoplastic pH, the fluorescent indicator was loaded into the apoplast as described elsewhere (Geilfus & Mühling, 2011). Briefly, 25 µM Oregon Green 488-dextran (Invitorgen GmbH, Darmstadt, Germany) was directly inserted into the leaf or internodial apoplast by using a syringe (without needle). For this, the opening of the syringe was carefully attached onto the surface of the relevant plant organ. By means of gentle pressure, the dye was loaded into the apoplast of the living plant. According to Geilfus and Mühling (2011), the dye is distributed within the apoplast, whereas any excess of loaded water originating from the dye solution leaves the apoplast through the stomata. Following this, measurements were conducted in a water-free apoplast. After 2 h, the measurement was started.

**Fluorescence microscopy imaging**

Fluorescence images were collected as time series with a Leica inverted microscope (DMI6000B; Leica Microsystems, Wetzlar, Germany) connected to a DFC-camera (DFC

360FX; Leica Microsystems, Wetzlar, Germany) via a 20-fold magnification, 0.4 numerical aperture, dry objective (HCX PL FLUOTAR L, Leica Microsystems, Wetzlar, Germany). An HXP lamp (HXP Short Arc Lamp; Osram, München, Germany) was used for illumination at excitation wavelengths of 440/20 nm and 495/10 nm. The exposure time was 25 mS for both channels. The dye fluorescence at both excitation channels was collected by using a 535/25 nm-emission band-pass filter (BP 535/25; ET535/25M; Leica Microsystems, Wetzlar, Germany) and a dichromatic mirror (LP518; dichroit T518DCXR BS, Leica Microsystems, Wetzlar, Germany). During measurements, intact plants were supplied with aerated nutrient solution.

**Ratiometric analysis**

As a measure of pH, the fluorescence ratio $F_{495}/F_{440}$ was obtained by using the pH-sensitive fluophore Oregon Green 488 conjugated to 10 kDa dextran. In combination with the dextran, the dye molecule is not membrane permeable and thus does not enter the symplast. The $F_{440}$ signal was captured because this fluorescence is almost insensitive to protons, whereas the $F_{495}$ signal highly depends on protons. Image analysis was carried out by using LAS AF software (version 2.3.5, Leica Microsystems, Wetzlar, Germany). Ratio images were calculated on a pixel-by-pixel basis as $F_{495}/F_{440}$. The background noise values were subtracted at each channel. For pseudo-colour display, the ratio was coded by hue on a spectral colour scale ranging from purple (no signal), over blue (lowest pH signal; pH 3.9), to pink (highest pH signal; pH 6.3), with the limits being set by an *in situ* calibration. Ratios below 1.1 (corresponds to pH $\leq$ 3.9) and above 3.6 (corresponds to pH $\geq$ 6.3) were not considered because they proved to lie outside the linear range of the *in situ* calibration. Quantitative measurements were calculated as the ratio of the mean intensity for user-defined regions of interest (ROIs).

### *In situ* and *ex situ* apoplastic pH calibration

Two different calibration procedures for the conversion of fluorescence ratio data taken from living plants into apoplastic pH values were tested comparatively. For this, 25 µM Oregon Green dye solutions were pH-buffered with 100 mM MES (2-[*N*-morpholino]ethanesulfonic acid) in order to obtain pH values ranging from 2.5 to 7.5 (in steps of 0.5 pH units). *In situ* calibration was carried out by loading the pH-buffered solutions into the leaf apoplast as described above (see Dye loading section). Images were collected 2 h after the loading of the dye. For *ex situ* calibration, the pH-buffered solutions of Oregon Green 488 dextran were measured by using the same optical settings as described for the *in situ* calibration but without loading the solutions into a plant. The Boltzmann fit was chosen for fitting sigmoidal curves to the calibration data as described by Schulte et al. (2006). Fitting was performed by using Origin 7.0 (data not shown; OriginLab Corp., Northhampton, MA, USA).

### Gas exchange

Gas exchange parameters such as photosynthesis (µmol $CO_2$ $m^{-2}s^{-1}$) and intercellular $CO_2$ concentration (µmol $CO_2$ $mol^{-1}$) were measured with an open-flow gas-exchange system (LI-COR Biosystems GmbH, Bad Homburg, Germany). Leaves were placed across a 2x3 cm leaf cuvette. The conditions for the measurements inside the chamber were equal to the outside conditions in the greenhouse: Light was provided by an LED red light source built into the top of the leaf chamber (100 µmol quanta $m^{-2}s^{-1}$) and the $CO_2$ concentration was controlled by a Li Cor LI-6400 $CO_2$ injection system (380 µmol $CO_2$ $mol^{-1}$).

## Results and discussion

### pH calibration and dye loading into the apoplast of intact plants

By using microscopy-based ratio analysis combined with a novel dye-loading protocol allowing the insertion of a proton-sensitive fluorescent dye into the apoplast of intact plants

(procedure described by Geilfus & Mühling, 2011), we studied apoplastic shoot pH when *Vicia faba* L. plants were challenged by NaCl stress encountered at the roots. For converting fluorescence ratio data taken from living plants into apoplastic pH values, two different calibration procedures were tested comparatively. With regards to *in situ* calibration, the pH-buffered calibration dye solutions were loaded into the apoplast of living plants by using the dye loading procedure described in the Materials and methods section. In contrast, calibration dye solutions were not loaded into the plant for *ex situ* calibration. Each of the calibration procedures gave different results, viz. the ratios for the identical pH values that were set by the pH-buffered calibration solution were different (Figure 1). Since the *in situ* calibration procedure accounts for optical effects of the specimen on the fluorescent dye signal intensity, such as leaf thickness, the *in situ* calibration seemed to be more suitable for converting ratio data in pH values and thus was chosen for calculation.

The insertion of the ion indicator into the plant's apoplast represents a potential event of mechanical stress and/or the presence of the dye within the apoplast might have an impact on the apoplastic space of the living plant. To exclude the occurrence of such negative effects, we have previously tested whether parameters such as leaf growth, stomatal conductance and the chlorophyll concentrations within leaves that have been dye-loaded change compared with leaves that have not been loaded with the ion indicator; neither of these parameters is influenced by the dye or the dye loading event (Geilfus & Mühling, 2011). In addition, an effect of the dye loading procedure on photosynthesis and on the intercellular $CO_2$ concentration has been tested; neither of these parameters is influenced (Figure 2). Since photosynthesis as a part of the primary metabolism of the plant is not affected (Figure 2A), we have concluded that the pH measurements do not perturb the plants. The finding that apoplastic $CO_2$ concentrations are identical in dye-loaded leaves and in leaves that have not been loaded (Figure 2B) demonstrates that no water (originating from the loading step) remains in the apoplast and thus displaces the apoplastic air. This is attributable to the fact

that the inserted water is leaving the apoplast over the stomata within a period of 2 to 10 minutes after dye loading (demonstrated by Geilfus & Mühling, 2011). Unaffected apoplastic $CO_2$ concentrations are of major significance for the measurement of apoplastic pH, since apoplastic $CO_2$ fluctuations are known to affect the apoplastic pH immediately and quantitatively (Savchenko et al. 2000).

**Leaf apoplastic pH transiently alkalizes in response to NaCl stress encountered by the root system**

NaCl stress imposed on roots causes a systematic apoplastic alkalinization that is detectable in the leaves and is thought to be involved in the transmission of information from the site of the trigger (e.g. root) to distant plant tissues (e.g. shoot; Felle et al. 2005; Wilkinson & Davies 1997). In accordance with these findings, our ratiometric *in planta* quantitation of the leaf apoplastic pH established the occurrence of such an alkalinization when 20 mM NaCl was added to the nutrient solution of faba beans (*Vica faba* L.; Figure 3). In response to the initiation of NaCl stress at the root site, leaf pH within the stomatal cavity, the epidermal apoplast and the apoplast surrounding the palisade tissue increased, whereas the pH within the palisade apoplast became the most alkaline. At 60 minutes after the stress was encountered, the nutrient solution was changed in order to remove the added NaCl. The removal of the stress stimulus out of the nutrient solution was followed by a decrease of the apoplastic pH. However, this pH decrease also occurred when NaCl was not removed as demonstrated in response to the second 20 mM NaCl application (see second transient pH increase within time-course shown in Figure 3A). To determine that this transient pH increase was induced by the stress treatment and not by the illumination of the specimen by the dye-specific excitation or emission wavelengths (as discussed by Fricker et al. 1994), a time series of excitation at 495 nm and 440 nm was performed. No effects of the illumination regime on the apoplastic pH were detectable (Figure 4). This represents evidence that the transient pH increases as

demonstrated in Figure 3 are solely attributable to the salt treatment. Such an impact on the apoplastic pH is generally possible because the buffering capacity of the apoplast is, at 5 mM $H^+$/pH units, relatively low compared with the 10 times higher buffering capacity of the cytoplasm (Hanstein & Felle 1999, Felle et al. 2008).

A comparable stress-induced apoplastic alkalinization was previously described by Felle and Hanstein (2002) who measured pH dynamics in *Vicia faba* L. leaves in response to a 20 mM NaCl treatment by using proton-sensitive microelectrodes. They demonstrated that the alkalinization dropped down to its initial level after the sodium chloride was removed. However, in the present study (Figure 3), we demonstrated that the alkalinization was transient, although the stress stimulus was still present. This transient nature of the pH increase and the finding that the pH response is triggered at the root site and is detectable in distant leaves is indicative for a role in systemic signalling. Such an interpretation of the function of the above-described pH dynamics agrees with that of Felle et al. (2008) who describe transient apoplastic alkalinizations that are similar in shape and magnitude and are thought to be a pH signal. In detail, the authors demonstrate a transient leaf apoplastic alkalinization in response to the inoculation of *Hordeum vulgare* with conidia of the powdery mildew fungus *Blumeris graminis* f. sp. *hordei* (Felle et al. 2008; first pH peak presented in figure 2 therein). This pH dynamic is interpreted to be a root-to-shoot signal, since it accompanies a simultaneous decrease in apoplastic $Ca^{2+}$ (Felle et al. 2004), transient cytoplasmic acidifications and a likewise rapid increase in cytoplasmic $Ca^{2+}$ activity (Felle et al. 2008). The aim of the apoplastic alkalinizations may be to signal the occurrence of stress events to distant plant organs (Wilkinson 1999). However, the explanation for the drop in pH to its initial level after stress-induced alkalinization fails at this point, as the mechanisms responsible for the pervious stress-induced alkalinization are not fully understood (Bacon et al. 1998). Felle and Hanstein (2002) propose that the idea of a NaCl-induced apoplastic alkalinization attributable to the stimulated uptake of the $Cl^-$ via a $2H^+/Cl^-$ plasma membrane

symport is not valid, because salt-induced alkalinization also occurs in the presence of the membrane-impermeable gluconate$^-$ used instead of $Cl^-$ as the $Na^+$-accompanying anion. As a more likely explanation for apoplastic pH increases in response to increased salt concentration, the authors report a reduction in $H^+$-ATPase activity, as discussed by Hartung & Radin (1989) and Yang et al. (2004), or changes in strong ion concentrations that result in pH changes without reducing proton concentration, according to the concept of strong ions as derived for plants by Gerendás & Schurr (1995).

**Magnitude of transient alkalinization depends on doses of NaCl stress treatment**

Since the application of abiotic stress in terms of 20 mM NaCl to the roots was shown to induce a transient pH response in distant plant organs such as the leaves, we tested whether the magnitude of this response changed with increasing dosages of NaCl. For this, 50 mM NaCl (Figure 5 and corresponding Video Clip 1) or 75 mM NaCl (Figure 6 and corresponding Video Clip 2) were added to the nutrient solution. As in the response to the 20 mM NaCl treatment, the pH was transiently alkalized over a period ranging from 40 to 60 minutes in the three apoplastic compartments, viz., the stomatal cavity, the epidermal apoplast and the palisade apoplast, starting circa 15 to 20 minutes after stress was initialized. Again, pH was the most alkaline within the apoplast built by the palisade tissue. The pseudo-colour ratios presented in the Video Clips 1 and 2 require additional comment. The ratio images under the most alkaline conditions suggest that fluorescent signals come directly from within the cells. This implies that, in addition to apoplastic pH signals, cytosolic pH signals have been quantified erroneously. This can be rejected as demonstrated elsewhere in detail (Geilfus & Mühling, 2011). Briefly, the fluorescent pH probe used in this study is covalently linked to 10 kD dextran and thus cannot migrate through the membrane of the cell. Even supposing the dye had entered the cytosol unintentionally, the apoplastic pH response shown in Figure 3, Figure 5 and corresponding Video Clip 1 and in Figure 6 and corresponding Video Clip 2

cannot drop back to its initial level at pH 4.5/4.6, because the cytosol never reaches such an acid milieu.

Figures 3A, 5 and 6 clearly demonstrate a relationship between the NaCl concentration of the stress treatment and the pH dynamics: the more NaCl is added to nutrient solution, the stronger the apoplastic alkalization. This is true for all three stress treatments, viz. 20 mM, 50 mM and 75 mM NaCl, and for all three apoplastic compartments: in response to the 20 mM NaCl treatment, a maximal pH of 4.5 within the stomatal cavity and the epidermal apoplast and a maximal pH of 4.8 within the palisade apoplast has been recorded (Figure 3A). The magnitude of the alkalinization increases to 5.0/5.1 and 5.2 when 50 mM NaCl is added (Figure 5) and to 5.4/5.5 and 5.7 when 75 mM NaCl is added (Figure 6. These varying NaCl stress treatments demonstrate (1) that a dependency exists between the magnitude of the apoplastic alkalinization and the severity of the NaCl stress treatments (dose dependency) and (2) that the leaf apoplast does not alkalizes equally over the leaf area but shows spatial differences.

**What does the plant gain from a transient leaf apoplastic alkalinization?**

Generally, the above-shown treatments demonstrate that the pH is more alkaline within the apoplast that is formed by the palisade cells compared with the stomatal cavity and the epidermal apoplast (Figures 3A, 5, and 6). Hence the question raises as to the nature of the gain to the plant of an pH increase within the (palisade) apoplast. In this context, the significance of the apoplastic pH for the distribution of abscisic acid (ABA) and, thus, in consequence for the closure of the stomata needs to be considered. High pH and ABA are known to act in concert as reviewed by Wilkinson (1999): under normal (non-stressed) physiological conditions, ABA sourced from roots, stems or leaves is transported along the transpirational stream and is translocated to the leaves. Within the acid apoplastic milieu, the weak acid ABA is present in its undissociated form (ABAH). The lipophilic ABAH diffuses

across the lipid plasma membrane of the cells. When ABAH enters the alkaline cytoplasm, it dissociates to $ABA^-$ + $H^+$ and becomes trapped inside the cells because of its lipophobic character. The trapped $ABA^-$ can rapidly be catabolized, helping to maintain the concentration gradient for further ABA uptake (Kaiser & Hartung 1981; Gowing et al. 1993; Daeter & Hartung 1995; Hartung et al. 1998; Wilkinson 1999). However, in stressed plants, we have demonstrated that the apoplastic pH increases (Figures 3, 5, and 6; see also other authors: Wilkinson & Davies 1997; Gao et al. 2004). This may in turn reduce the pH gradient across the plasma membrane for mesophyll and epidermal cells as explained by Wilkinson (1999). Moreover, the increased apoplastic pH causes undissociated weak acids to dissociate to the anionic form, which is then trapped within the alkalized apoplast (Heilmann et al. 1980). In consequence, $ABA^-$ accumulates in the apoplast and finally reaches the guard cells and causes stomatal closure (Wilkinson & Davies 1997; Jiang & Hartung 2008; Schmidt et al. 1995). In other words, a drought, salt or cold stress-induced apoplastic alkalinization indirectly causes the guard cell ABA receptors to become activated and thus the stomata to be closed, enabling the plant to retain water (Wilkinson 1999). In the current study, no ABA concentrations were measured, and thus an effect of the apoplastic alkalinization on the ABA concentration within the apoplast could not be demonstrated. However, taking into account (1) that ABA is synthesized in response to stress and is translocated within the apoplast, (2) that ABA mediates the responsiveness of plants to environmental stresses such as drought, cold or salt and (3) that an alkalinization has been discussed as a signal in situations in which the plant must communicate the occurrence of a root-sourced stress event to the shoot (Felle 2001; Felle & Hanstein 2002; Becker et al. 2003; Wilkinson & Davies 2008), we consider it likely that the above-described alkalinization (Figures 3, 5 and 6) acts on the ABA distribution within the plant. Moreover, since the mesophyll tissue is thought to be a major sink for cytosolic-trapped ABA (Wilkinson 1999), strong alkalinization around the palisade cells, as

recorded in the Figures 3, 5 and 6, might have a physiological meaning with respect to avoiding cytosolic ABA-trapping.

In the current work, we have studied apoplastic pH dynamics in responses to NaCl stress encountered at the roots of the faba beans. Since the stress treatment is initiated by the addition of NaCl into the nutrient solution, we need to preclude that the application of the NaCl changes the pH of the nutrient solution itself. This is important because changes in the pH of the hydroponic growth media are known to be rapidly sensed by a so-called pH response system that can speedily alter the global patterns of gene expression accompanying $Ca^{2+}$ signalling (Lager et al. 2010). Thus, changes in the pH of the external growth media are also likely to affect the pH in the plant apoplast. To exclude such an effect, we have demonstrated that the addition of NaCl to the nutrient solution does not alter the pH of the nutrient solution (Figure 5, $2^{nd}$ ordinate). Thus, we can conclude that the pH kinetics described above are solely attributable to NaCl stress and not to changes in the pH of the nutrient solution.

**Propagation of the pH response throughout the plant**

Although apoplastic pH is broadly described to act as a stress signal, little is known about the signal translocation from root to shoot. Wilkinson and Davies (2008) assume that pH changes that are generated by the roots in response to drought stress are propagated along the xylem vessels and penetrate to the leaf apoplast where they can function as a chemical messenger. Thus, pH changes might function as a chemical signal to leaves in response to stress (Wilkinson 1999). In the current study, the recording of pH dynamics within the internodial stem apoplast has revealed the occurrence of a transient alkalinization in response to 50 mM NaCl stress application (Figure 7). Interestingly, this alkalinization occurs as early as 10 minutes after stress application to the roots, whereas the pH response occurs no earlier than at 20 minutes in more elevated leaves (compare with Figures 3, 5, and 6). The finding that the

transient stress-induced pH response is detectable within the internodial apoplast and that it arrives 10 minutes earlier than in leaves located above these internodes is indicative of the ideas that (1) the pH response is propagated from root to shoot and (2) this occurs via the apoplast. The more distant the plant organs are from the site of the stress stimulus, the more time the alkalinization needs to occur.

## Resume of the main conclusions

Here, we demonstrate systemic effects of NaCl stress treatments encountered by the roots of *Vica faba* L. on leaf apoplastic pH. The transient nature of the increase in leaf apoplastic pH is indicative of its role in stress signalling. The data presented here suggest a dependency between the magnitude of the transient leaf apoplastic alkalinization and the NaCl stress treatment (dose dependency). In addition, we have demonstrated that the leaf apoplast does not alkalize equally over the leaf area but shows spatial differences as visualized by fluorescence ratio imaging.

## Acknowledgment

Christoph-Martin Geilfus is the grateful recipient of a grant from the Friedrich-Ebert-Stiftung. We thank Dr. Christoph Plieth (Center of Biochemistry and Molecular Biology, University of Kiel) for advice on fitting calibration data with a sigmoidal Boltzmann fit.

## Supplementary Material

The Video clips 1 and 2 of this manuscript can be found on the attached compact disc

## Figure legends

**Figure 1.** Calibration curves for Oregon Green 488 dextran fluorescence excitation ratio R(490ex/440ex; 525em). Blue curve: *in situ* calibration; means ± SE. The Boltzmann fit was chosen for fitting sigmoidal curves to *in situ* calibration data. Fitting (data not shown) resulted in an optimal dynamic range for pH measurements between 3.9 and 6.3 (corresponds to the ratios 1.1 and 3.6). *In situ* calibration was conducted on 6 different plants (n =6 biological replicates), each replicated 5 times (n = 5 technical replicates) with at least 5 regions of interest (ROI) being quantified for each image ($n \geq 5$). Red curve: *ex situ* calibration; means ±SE; (n = 10).

**Figure 2.** Photosynthetic rate (A) and intercellular $CO_2$ concentration (B) as influenced by the dye and the loading procedure. To test whether these parameters were affected, a paripinnate leaf was used. One leaflet was loaded with the dye (green bar), whereas the second was used as control (blue bar). Leaves were tested prior loading and at 2 h, 3h and 4 h after loading. Neither parameter was influenced by the presence of the dye or the loading procedure. Data are means of four biological replicates ± SE. ns = no statistical significance at $p \leq 0.05$.

**Figure 3.** Ratiometric real-time quantitation of leaf apoplastic pH when plants challenged by the addition of 20 mM NaCl to the root system. (A) pH as recorded at the adaxial face of *Vicia faba* L. leaves is plotted over time. Black arrows indicate time of addition/removal of 20 mM NaCl stress stimulus in/out of the nutrient solution. Leaf apoplastic pH was discriminated within three apoplastic components, viz. in the stomatal cavity (n = 10 regions of interest; green kinetic), in the epidermal apoplast (n = 20 ROI; red kinetic) and in the apoplast surrounding the palisade mesophyll (n = 20 ROI; blue kinetic). Ratiometric images (B-D) show time series of apoplastic leaf pH at (B) 20 minutes, (C) 50 minutes and (D) 100 minutes

after measurement had started (time of image acquisition is presented in the upper right corner of the ratio images). Ratios were colour-coded on a spectral colour scale (see inset in B). Representative kinetics of three equivalent recordings of plants gained from independent experiments.

**Figure 4.** Ratiometric real-time quantitation of leaf apoplastic pH when plants challenged by the given illumination regime during inverse microscopy image acquisition. pH as recorded at the adaxial face of *Vicia faba* L. leaves is plotted over time. Leaf apoplastic pH was discriminated within three apoplastic components, viz. in the stomatal cavity (n = 10 ROI; green kinetic), in the epidermal apoplast (n = 20 ROI; red kinetic) and in the apoplast surrounding the palisade mesophyll (n = 20 ROI; blue kinetic). No effects on apoplastic pH are detected attributable to the illumination of specimen with the excitation or emission wavelengths used for imaging. Representative kinetics of three equivalent recordings of plants gained from independent experiments.

**Figure 5.** Ratiometric real-time quantitation of leaf apoplastic pH when plants challenged by the addition of 50 mM NaCl to the root system. Left ordinate: leaf apoplastic pH as recorded at the adaxial face of *Vicia faba* L. leaves is plotted over time. Black arrow indicates time of addition of 50 mM NaCl stress stimulus in the nutrient solution. Leaf apoplastic pH was discriminated within three apoplastic components, viz. in the stomatal cavity (n = 10 ROI; green kinetic), in the epidermal apoplast (n = 20 ROI; red kinetic) and in the apoplast surrounding the palisade mesophyll (n = 20 ROI; blue kinetic). Representative kinetics of three equivalent recordings of plants gained from independent experiments. The corresponding ratiometric images of this pH kinetic are also presented as a video clip (see Video Clip 1). Right ordinate: pH in nutrient solution as challenged by the addition of NaCl

into the nutrient solution (black kinetic): pH in the nutrient solution was not affected by the addition of NaCl.

**Figure 6.** Ratiometric real-time quantitation of leaf apoplastic pH when plants challenged by the addition of 75 mM NaCl to the root system. pH as recorded at the adaxial face of *Vicia faba* L. leaves is plotted over time. Black arrow indicates time of addition of 75 mM NaCl stress stimulus in the nutrient solution. Leaf apoplastic pH was discriminated within three apoplastic components, viz. in the stomatal cavity (n = 10 ROI; green kinetic), in the epidermal apoplast (n = 20 ROI; red kinetic) and in the apoplast surrounding the palisade mesophyll (n = 20 ROI; blue kinetic). Representative kinetics of three equivalent recordings of plants gained from independent experiments. The corresponding ratiometric images of this pH kinetic are also presented as a video clip (see Video Clip 2).

**Figure 7.** Ratiometric real-time quantitation of apoplastic pH within the internodes when plants challenged by the addition of 50 mM NaCl to the root system. pH was plotted over time. Black arrow indicates time of addition of 50 mM NaCl stress stimulus in the nutrient solution. pH was averaged over the complete focused area (630 µm x 475 µm) of the specimen. Representative kinetics of three equivalent recordings of plants gained from independent experiments.

## Video clip legends

**Video clip 1.** Time-series demonstrating development of the leaf apoplastic pH when plants challenged by the addition of 50 mM NaCl to the root system. Adaxial face of *Vicia faba* L.. Ratiometric images were collected every 5 minutes over a period of 160 minutes (compare with time course in Figure 5). NaCl was added 20 minutes after the measurement was started (images no. 4 after 1200 s). The time of image acquisition (in seconds) is presented in the upper right corner of the ratio images. Ratios were colour-coded on a spectral colour scale (see table). Representative kinetic of three equivalent recordings of plants gained from independent experiments. Movie duration = 5 seconds. The pseudo-colour ratios require additional comment. The ratio images at the most alkaline conditions suggest that fluorescent signals come directly from within the cells. This implies that, in addition to apoplastic pH signals, cytosolic pH signals have been quantified erroneously. This can be rejected as demonstrated elsewhere (Geilfus & Mühling, 2011). Briefly, the fluorescent pH probe used in this study is covalently linked to 10 kD dextran and thus cannot migrate through the membrane in the cell.

**Video clip 2.** Time-series demonstrating development of the leaf apoplastic pH when plants as challenged by the addition of 75 mM NaCl to the root system. Adaxial face of *Vicia faba* L.. Ratiometric images were collected every 5 minutes over a period of 180 minutes (compare with time course in Figure 6). NaCl was added 10 minutes after the measurement was started (images no. 2 after 600 s). The time of image acquisition (in seconds) is presented in the upper right corner of the ratio images. Ratios were colour-coded on a spectral colour scale (see table). Representative kinetic of three equivalent recordings of plants gained from independent experiments. Movie duration = 8 seconds.

## Literature

Bacon M.A., Wilkinson S. & Davies W.J. (1998) pH-regulated leaf cell expansion in droughted plants is abscisic acid dependent. *Plant Physiol* 118, 1507-1511.

Becker D., Hoth S., Ache P., Wenkel S., Roelfsema M.R.G., Meyerhoff O., Hartung W. & Hedrich R. (2003) Regulation of the ABA-sensitive potassium channel gene GORK in response to water stress. *FEBS Letters* 554, 119-126.

Daeter W. & Hartung W. (1995) Stress-dependent redistribution of abscisic acid (ABA) in *Hordeum vulgare* L leaves: the role of epidermal ABA metabolism, tonoplastic transport and the cuticle. *Plant, Cell Environ* 18, 1367-1376.

Felle H.H. (1998) The apoplastic pH of the *Zea mays* root cortex as measured with pH-sensitive microelectrodes: aspects of regulation. *J Exp Bot* 49, 987-995.

Felle H.H. (2001) pH: signal and messenger in plant cells. *Plant Biol* 3, 577-591.

Felle H.H. & Hanstein S. (2002) The apoplastic pH of the substomatal cavity of *Vicia faba* leaves and its regulation responding to different stress factors. *J Exp Bot* 53, 73-82.

Felle H.H., Herrmann A., Hanstein S., Hückelhoven R. & Kogel K.H. (2004) Apoplastic pH signalling in barley leaves attacked by the powdery mildew fungus *Blumeria graminis f.sp. hordei*. *Mol Plant Microbe In* 17, 118-123.

Felle H.H. (2005) pH regulation in anoxic plants. *Ann Bot* 96, 519-532.

Felle H.H., Hermann A., Hückelhoven R. & Kogel K.H. (2005) Root-to-shoot signalling: apoplastic alkalinization, a general stress response and defence factor in barley (*Hordeum vulgare*). *Protoplasma* 227, 17-24.

Felle H.H, Herrmann S., Schäfer P., Hückelhoven R. & Kogel K.H. (2008) Interactive signal transfer between host and pathogen during successful infection of barley leaves by *Blumeria graminis* and *Bipolaris sorokiniana*. *J Plant Physiol* 165, 52-59.

Felle H.H., Waller F., Molitor A. & Kogel K.H. (2009) The mycorrhiza fungus *Piriformospora indica* induces fast root surface pH signaling and primes systemic alkalinization of the leaf apoplast upon powdery mildew infection. *Mol Plant Microbe In* 22, 1179-1185.

Fricker M.D., Tlalka M., Ermantraut J., Obermeyer G., Dewey M., Gurr S., Patrick J. & White N.S. (1994) Confocal fluorescence ratio imaging of ion activities in plant cells. *Scanning Microscopy* 8, 391-405.

Gao D., Trewavas A.J., Knight M.R., Sattelmacher B. & Plieth C. (2004) Self-reporting *Arabidopsis thaliana* expressing pH- and $[Ca^{2+}]$- indicators unveil ion dynamics in the cytoplasm and in the apoplast under abiotic stress. *Plant Physiol* 134, 898-908.

Geilfus C.M. & Mühling K.H. (2011). Real-time imaging of leaf apoplastic ion dynamics in response to abiotic stress. *Front Plant Sci* **2(**13). doi: 10.3389/fpls.2011.00013.

Gerendás J. & Schurr U. (1995) Physicochemical aspects of ion relations and pH regulation in plants - a quantitative approach. *J Exp Bot* 50, 1101-1114.

Gilroy S. & Trewavas T. (1994) A decade of plant signals. *BioEssays* 16, 677-682.

Gowing D.J.G., Jones H.G. & Davies W.J. (1993) Xylem transported abscisic acid: the relative importance of its mass and its concentration in the control of stomatal aperture. *Plant, Cell Environ* 16, 453-459.

Hanstein S. & Felle H.H. (1999) The influence of atmospheric $NH_3$ on the apoplastic pH of green leaves: a non-invasive approach with pH-sensitive microelectrodes. *New Phytol* 143, 333-338.

Hartung W. & Radin J.W. (1989) Abscisic acid in the mesophyll apoplast and in the root xylem sap of water stressed plants. The significance of pH gradients. *Curr Top Plant Biochem Physiol* 8, 120-134.

Hartung W., Radin J.W. & Hendrix D.L. (1998) Abscisic acid movement into the apoplastic solution of water-stressed cotton leaves. Role of apoplastic pH. *Plant Physiol* 86, 908-913.

Heilmann B., Hartung W. & Gimmler H. (1980) The distribution of abscisic acid between chloroplasts and cytoplasm of leaf cells and the permeability of the chloroplast envelope for abscisic acid. *Z Pflanzenphysiol* 97, 67-78.

Hoffmann B., Plänker R. & Mengel K. (1992) Measurements of pH in the apoplast of sunflower leaves by means of fluorescence. *Physiol Plant* 84, 146-153.

Hoson T. (1998) Apoplast as the site of response to environmental signals. *J Plant Res* 111, 167-177.

Husted S. & Schjoerring J.K. (1995) Apoplastic pH and ammonium concentration in leaves of *Brassica napus* L. *Plant Physiol* 109, 1453-1460.

Jiang F. & Hartung W. (2008) Long-distance signalling of abscisic acid (ABA): the factors regulating the intensity of the ABA signal. *J Exp Bot* 59, 37-43.

Kaiser W.M. & Hartung W. (1981) Uptake and release of abscisic acid by isolated photoautotrophic mesophyll cells, depending on pH gradients. *Plant Physiol* 68, 202-206.

Lager I., Andréasson O., Dunbar T.L., Andreasson E., Escobar M.A. & Rasmusson, A.G. (2010) Changes in external pH rapidly alter plant gene expression and modulate auxin and elicitor responses. *Plant, Cell Environ* 33, 1513-1528.

Minorsky P.V. (2004) On the inside. *Plant Physiol* 134, 881-882.

Monshausen G. B., Miller N. D., Murphy A. S. & Gilroy S. (2011) Dynamics of auxin-dependent $Ca^{2+}$ and pH signalling in root growth revealed by integrating high-resolution imaging with automated computer vision-based analysis. *Plant J* 65, 309-318.

Mühling K.H, Plieth C., Hansen U.P. & Sattelmacher, B. (1995) Apoplastic pH of intact leaves of *Vicia faba* as influenced by light. *J Exp Bot* 46, 377-382.

Roos W. (2000) Ion mapping in plant cells: methods and applications in signal transduction research. *Planta* 210, 347-370.

Savchenko G., Wiese C., Neimanis S., Hedrich R. & Heber U. (2000) pH regulation in apoplastic and cytoplasmic cell compartments of leaves. *Plant*a 211, 246-255.

Schmidt C., Schelle I., Liao Y.J. & Schroeder J.I. (1995) Strong regulation of slow anion channels and abscisic acid signalling in guard cells by phosphorylation and dephosphorylation events. *PNAS* 92, 9535-9539.

Schulte A., Lorenzen I., Boetcher M. & Plieth C. (2006) A novel fluorescent pH probe for expression in plants. *Plant Methods* 2, 7.

Shinozaki K. & Yamaguchi-Shinozaki K. (1997) Gene expression and signal transduction in water-stress response. *Plant Physiol* 115, 327-334.

Wilkinson S. & Davies W.J. (1997) Xylem sap pH increase: a drought signal received at the apoplastic face of the guard cell that involves the suppression of saturable abscisic acid uptake by the epidermal symplast. *Plant Physiol* 113, 559,573.

Wilkinson S. (1999) pH as a stress signal. *Plant Growth Regul* 29, 89-99.

Wilkinson S. & Davies W.J. (2008) Manipulation of the apoplastic pH of intact plants mimics stomatal and growth responses to water availability and microclimatic variation. *J Exp Bot* 59, 619-631.

Yang Y.L., Guo J.K., Zhang F., Zhao L.Q. & Zhang L.X. (2004) NaCl induced changes of the $H^+$-ATPase in root plasma membrane of two wheat cultivars. *Plant Sci* 166, 913-918.

# Figure files

## Figure 1

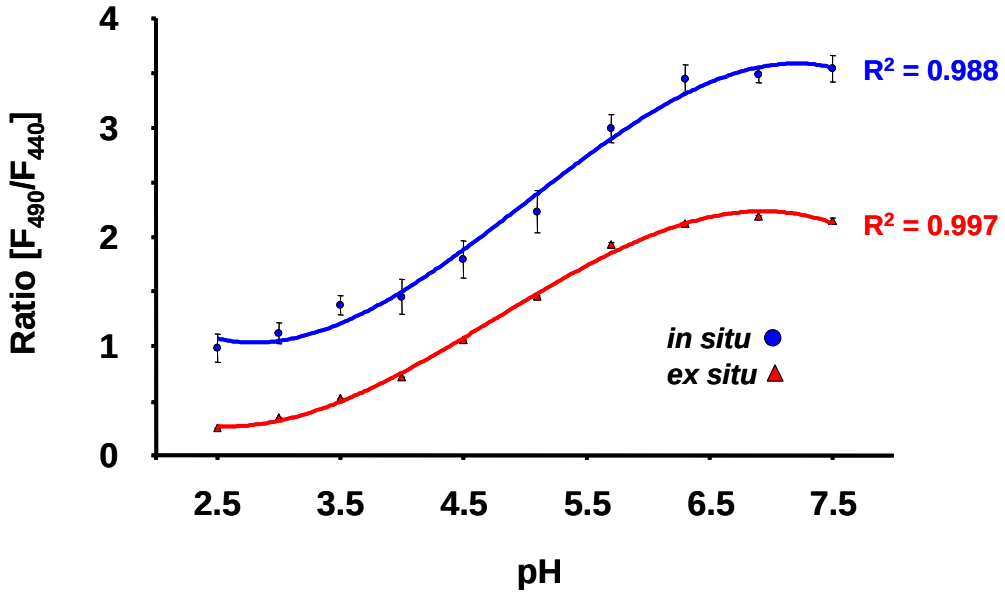


## Figure 2

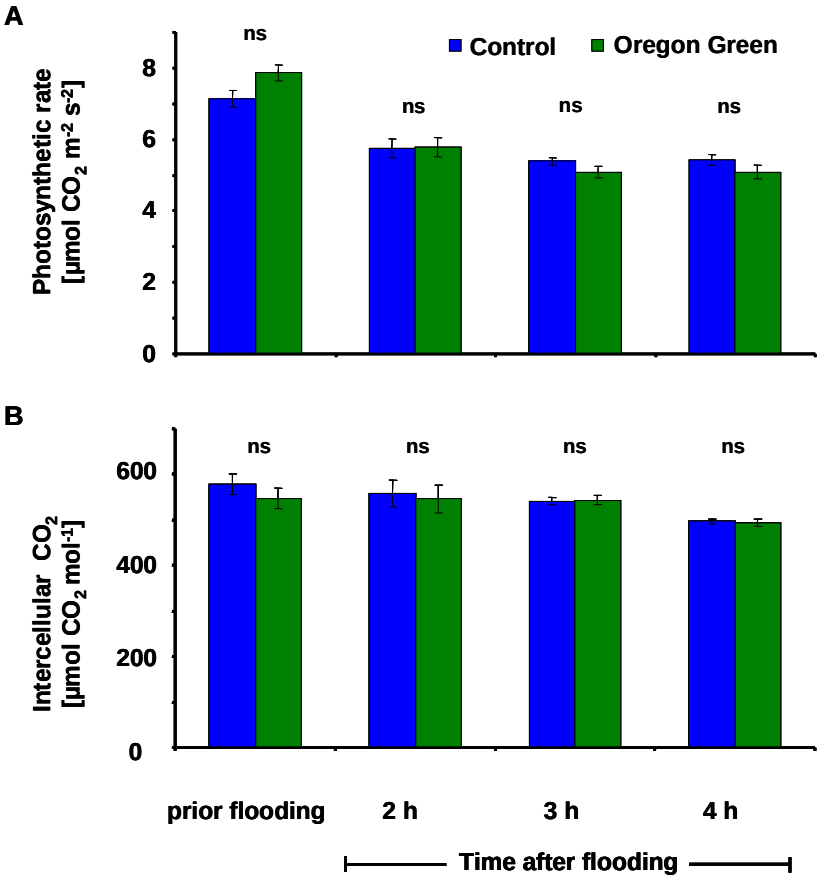

**Figure 3**

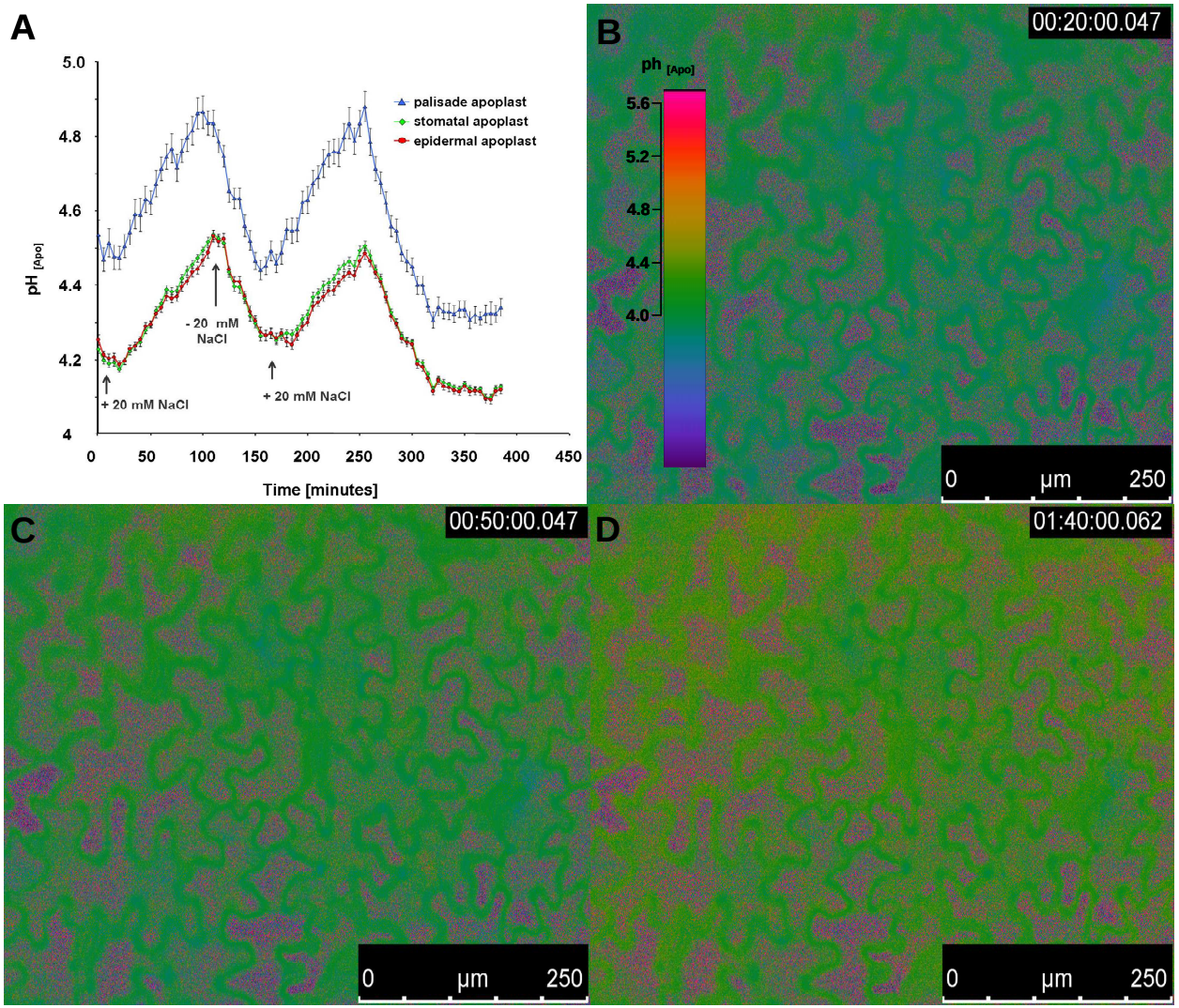
A
5.0
4.8
4.6
4.4
4.2
4
pH [Apo]
palisade apoplast
stomatal apoplast
epidermal apoplast
- 20 mM NaCl
+ 20 mM NaCl
+ 20 mM NaCl
0
50
100
150
200
250
300
350
400
450
Time [minutes]
B
00:20:00.047
ph [Apo]
5.6
5.2
4.8
4.4
4.0
0
µm
250
C
00:50:00.047
0
µm
250
D
01:40:00.062
0
µm
250

**Figure 4**

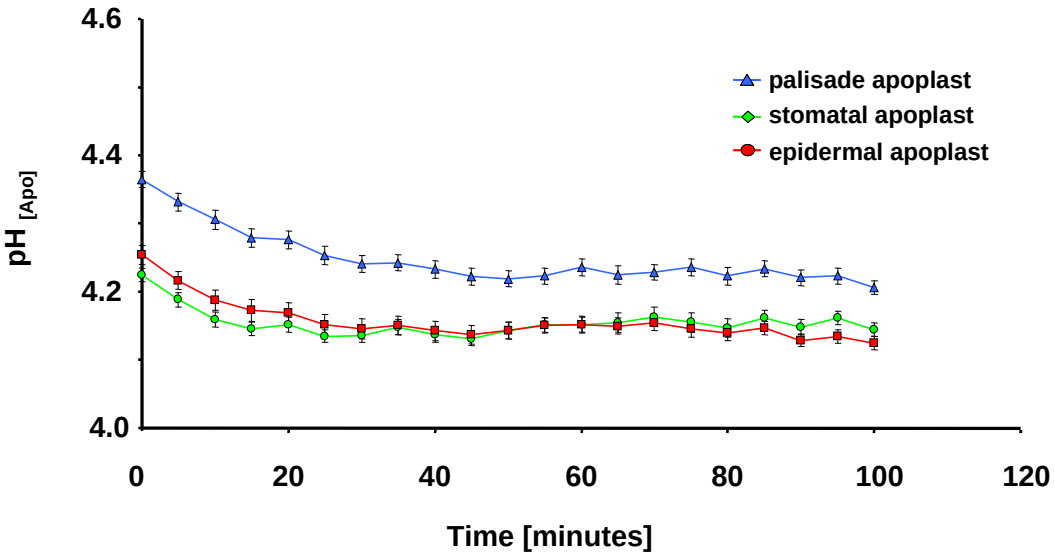


**Figure 5**

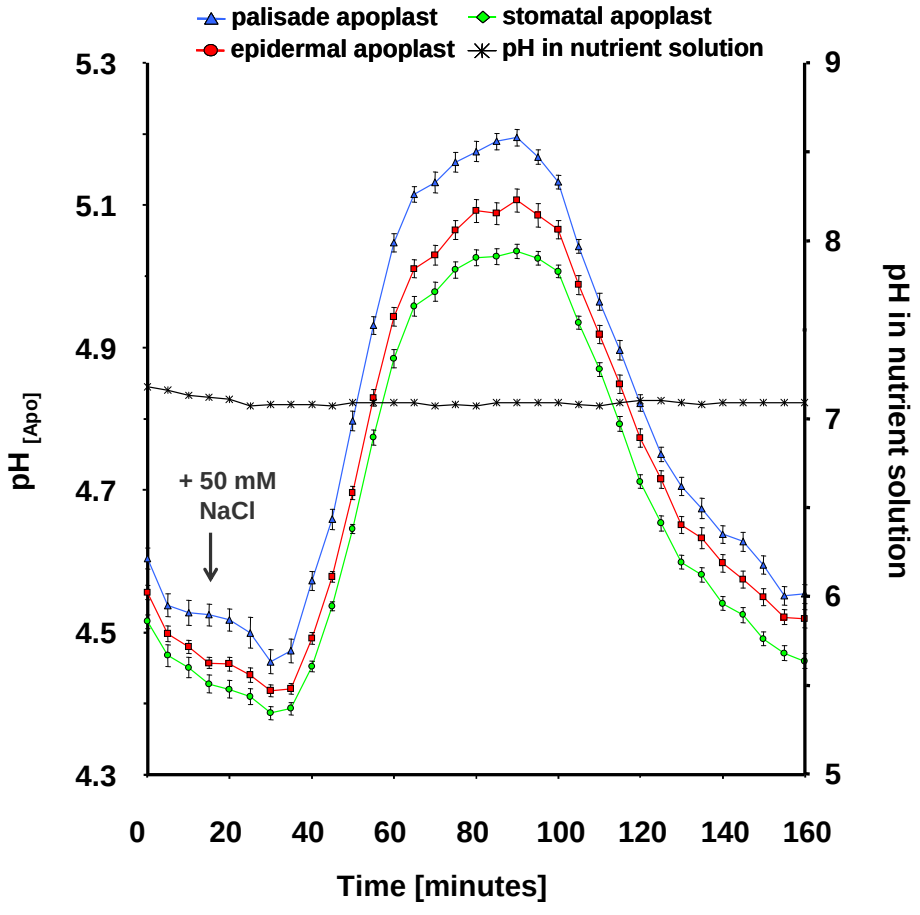

**Figure 6**

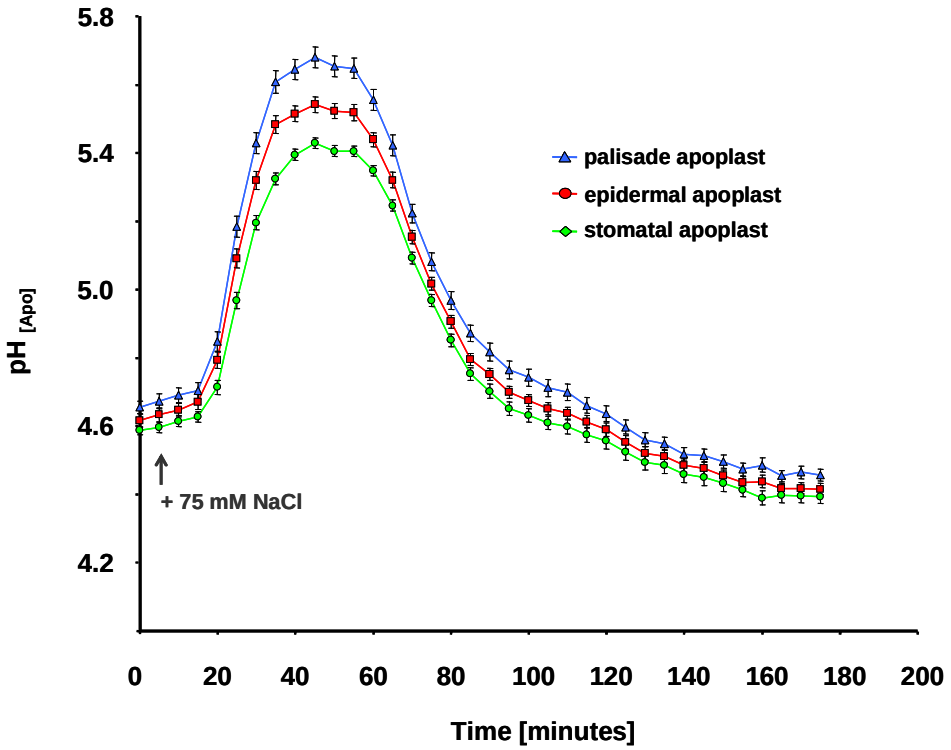


**Figure 7**

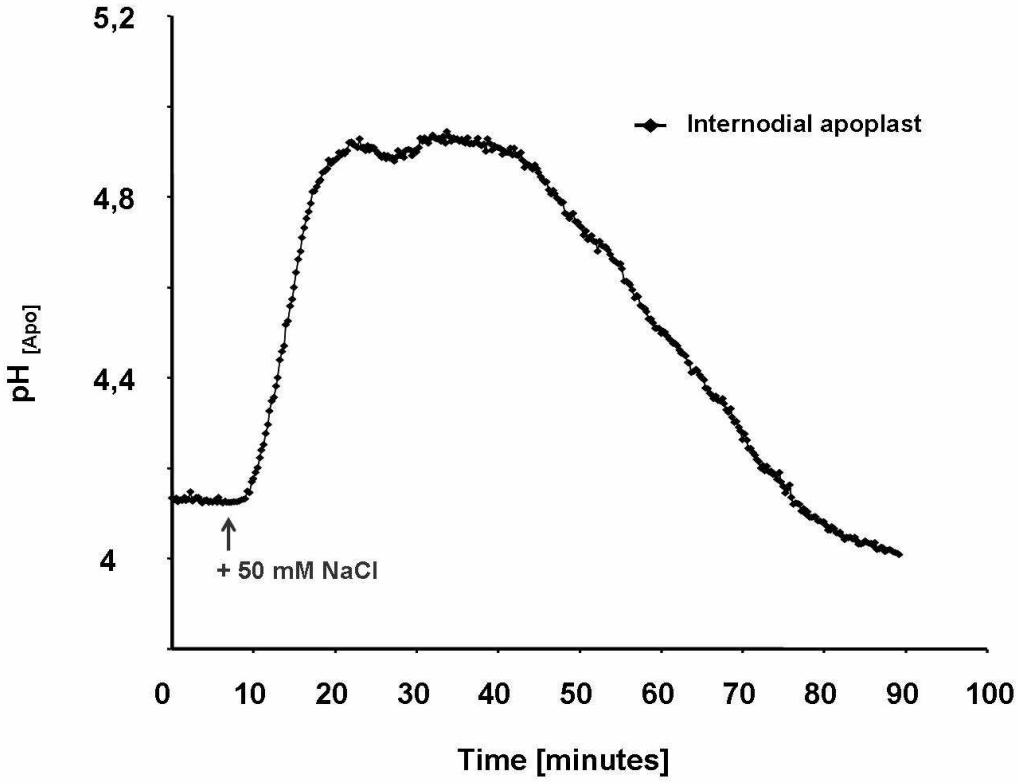

# Chapter 7

## Differences in β-expansin abundance and apoplastic pH in expanding leaves of salt resistant and sensitive maize hybrids

Christoph-Martin Geilfus, Dietrich Ober, Karl Hermann Mühling and Christian Zörb

*Submitted*

# Differences in β-expansin abundance and apoplastic pH in expanding leaves of salt resistant and sensitive maize hybrids

Christoph-Martin Geilfus [1], Dietrich Ober[2], Karl Hermann Mühling[1]and Christian Zörb[1]

[1]Institute of Plant Nutrition and Soil Science, Christian Albrechts University, Hermann-Rodewald-Str. 2, 24118 Kiel, Germany.

[2]Botanical Institute, Biochemical Ecology and Molecular Evolution, Christian-Albrechts, Am Botanischen Garten 1-9, 24098 Kiel, Germany.

Abbreviations:

real-time qRT-PCR, real-time quantitative Reverse Transcriptase-Polymeras Chain Reaction; 2D WB, two-dimensional Western blotting; 1D WB, one-dimensional Western blotting; MES, 2-[*N*-morpholino]ethanesulfonic acid; PVDF, polyvinylidene difluoride;

## Abstract

Salt-sensitive crop plants such as maize (*Zea mays* L.) show a strong and rapid growth reduction in response to NaCl-induced stress that is attributable to a decline of cell division and elongation. Wall-loosening agents such as apoplastic expansins are of major impact for cell wall extensibility and growth. Expansins are thought to be the primary mediators of acid-induced growth. Our study was designed in order to identify and to characterize genotype-specific growth responses of the leaves under salinity. For this purpose, a comparison of the salt-sensitive maize hybrid Lector and the highly salt-resistant hybrid SR03 under saline condition was conducted. Different expansin protein isoforms were monitored using gel-based two-dimensional proteomics and a subsequently two-dimensional Western blotting approach. In result, the abundance of one β-expansin protein isoform decreased in leaves of the salt-sensitive hybrid, possibly contributing to salinity-induced leaf growth reduction. Expansins were formerly reported to be pH depending proteins, being activated by an increased acidity. Camera-based *in planta* ratio imaging of the pH revealed a leaf apoplastic acidification in the salt-resistant hybrid under NaCl stress. Interestingly, this salt resistant maize hybrid maintained leaf growth. Therefore, it is concluded that the acidification of the leaf apoplast might be a part of the mechanism of highly salt-resistant maize to counteract to growth reduction under salinity. A confirmation of this assumption is that the salt-sensitive hybrid shows a significant growth reduction but did not acidify the leaf apoplast under saline growth conditions.

Key words: salinity, growth, β-expansins, apoplastic pH, *Zea mays* L., fluorescence ratio imaging, two-dimensional Western blotting, real-time quantitative RT-PCR.

## Introduction

Salinity has a global impact on agricultural production because as fertile soils become salinized, the yield of conventional crops decreases (Munns, 2005, Rozema and Flowers, 2008). Salt stress reduces the leaf growth rate by shortening the length of the leaf elongating zone and decreasing the growth intensity in its central and distal portions (Bernstein et al., 1993). However, the mechanism that down-regulates the growth of young leaves under salt stress is not jet precisely known (Munns and Tester, 2008).

According to the acid growth theory, an auxin-mediated acidification of the leaf apoplast is the major requirement for increasing wall extensibility (Hager et al., 1971). Auxin is assumed to activate the plasma membrane proton pump to pump protons from the cytosol into the apoplast, resulting in wall-loosening and cell expansion (Moriau et al., 1999). In accordance to this, it was found for maize (*Zea mays* L.) leaves, that higher growth rates are associated with increasing acidification of the apoplast (Van Volkenburgh and Boyer, 1985). The pH of the apoplast of growing cells typically spans from 4.7 to 6 (Mühling et al., 1995), which is the range in which acidification activates expansin activity (Cosgrove, 2005). Expansins are cell wall-loosening agents implicated in plant growth (Cosgrove et al., 1997). As summarized by Sella Kapu and Cosgrove (2010), expansins are involved in plant cell enlargement and they have the ability to mediate acid-induced extension of isolated cell walls (McQueen-Mason et al., 1992). Recently, it was demonstrated that differences in protein abundance of β-expansin occur in leaves of salt-stressed maize cultivars that differ in terms of salt resistance (Geilfus et al., 2010a and 2011). Reduced β-expansin protein abundance was found to correlate positively with a reduced leaf growth in salt-sensitive maize hybrid Lector. In contrast, the salt-resistant SR03 hybrid maintained shoot growth under salinity and exhibited an unaffected abundance of growth-mediating β-expansin proteins in the leaves.

The aim of this study was to clarify which β-expansin protein isoforms were down-regulated in salt-affected leaves of salt-sensitive Lector in response to an 8-d treatment with 100-mM NaCl. Moreover, genotypic differences within the apoplastic leaf pH between the sensitive and the resistant hybrid were compared in order to provide insights regarding the possible role of the apoplastic pH within the leaf growth inhibition under salt stress.

## Results

### Leaf growth

All measurements were based on expanding leaves that had started to develop one day after the full 100 mM NaCl treatment was applied. Thus, only leaves that exclusively grew under stress were taken into account. As demonstrated for the salt-sensitive cultivar Lector, the daily growth increase of leaf length was significantly reduced after an 8 d treatment of 100 mM NaCl (Figure 1A). In contrast, the reduction of the daily length growth proved to be minor for the salt-resistant hybrid SR03 (Figure 1A). In accordance, the corresponding leaf area proved to be significantly reduced in the salt-sensitive hybrid, but was only minor reduced in the salt-resistant SR03 (Figure 1B). The leaf fresh weight (Figure 1C), and the relative leaf thickness (Figure 2) reacted in the same manner.

### Relative chlorophyll concentration

Under condition of NaCl stress, the relative chlorophyll concentration in the leaves as measured with a portable chlorophyll meter (SPAD-502) was not affected in the leaves of both genotypes, viz., in Lector or SR03, (Figure 3).

### Relative *ZmXTH1* transcript abundance

The effect of the salt treatment on the relative abundance of *Zea mays* xyloglucan endotranshydrolases 1 (*ZmXTH1*) transcripts was studied on the basis of purified poly $(A)^+$

RNA using real-time qRT-PCR technique. In response to 8-d salt stress, *ZmXTH1* transcripts were down-regulated in the salt-sensitive hybrid Lector by 88% but in contrast were up-regulated by 135% in the salt-resistant hybrid SR03 (Figure 4).

**Detection of β-expansin isoforms in leaves of salt-sensitive Lector**

It was possible to isolate different β-expansin isoforms from expanding leaves which developed under salt treatment. The β-expansin isoforms were immunochemically labelled using a polyclonal antibody (anti-ZmExpB) raised against a conserved 15 amino acid region shared by seven different, vegetatively expressed, β-expansin isoforms (see material section). Under control treatment (no salt), two dimensional Western blot analysis (2D WB) revealed the presence of four signals, viz., spots, with a molecular weight varying from 20 to 30 kDa and an isoelectric point ranging from pI 4 to pI 10 (Figure 5A). This corresponds to the range of the *in-silico* predicted pI of the ß-expansins (Table 1). One particular β-expansin spot signal that appeared under control conditions was not detectable at salt stress condition (labelled by the arrow in Figure 5A). The loading controls of the 2D-PAGE gels indicated equivalent amounts of protein in all replicates (Figure 5B). A negative control with preimmune serum did not detect any bands (data not shown).

**Epidermal cell size**

After 8-d of salt treatment, the relative length of the adaxial epidermal leaf cells (Figure 6A) was significantly reduced in the salt-sensitive Lector, whereas no size reduction was measured for the salt-resistant hybrid SR03 (Figure 6A). This was also found for the corresponding relative cell width (Figure 6B), and for the relative area of the epidermal cells (Figure 6, C - G).

**1D Western blotting-detection of β-expansins in the epidermal surface of maize leaves**

To test whether β-expansins are located within the outermost epidermal surface of leaves, a 1D WB-procedure was performed. This was implemented on the basis of the leaf epidermal surface proteome that was extracted according to Yeats et al (2010) in combination with an anti-peptide antibody (anti-ZmExpB) that labels the vegetatively expressed β-expansin isoforms. Western blotting revealed the presence of a strong signal band between 25 kDa and 35 kDa within the epidermal surface proteome derived from the salt-sensitive hybrid Lector (Figure 6). This is the molecular weight range in which *in-silico* analysis predicted the ß-expansins to occur (Table 1). To confirm the specificity of the labelling, various control experiments were performed. Wheatear to check that no false-positive signal was present, incubation with pre-immune serum was conducted and yielded in no signal (data not shown). To test whether unspecific signals were detected erroneously, the labelling experiment was repeated with the addition of a synthetic 15-amino-acid peptide which corresponds to the ß-expansin antibody epitope. (This particular peptide has been used for immunization of a rabbit for the purpose of antibody production). In case of a specific labelling of β-expansins, the label decreases by pre-incubation of the antibody with the added peptide (method according to Moll et al., 2002). Two different peptide concentrations were used, resulting in a molar ratio of antibody to added peptide of 2:1 and 5:1. Figure 7, B-D, shows that an addition of the synthetic peptide reduces (5:1 ratio, Figure 7C) or almost completely blocks (2:1 ratio; Figure 7B) the specific labelling, whereas under normal condition (1:0 ratio; Figure 7D) the signal was proved to be the most intensive. Altogether, these tests verified the specificity of the β-expansin antibodies used in the Western blots.

**Ratiometric *in planta* measurements of leaf apoplastic pH**

Microscopy-based ratio imaging was used for *in planta* quantification of the pH in three leaf apoplastic compartments, viz., the stomatal cavity, the epidermal apoplast and the apoplast

built by the palisade cells. In the expanding leaves of salt-sensitive Lector, the apoplastic pH was not affected in none of the three apoplastic compartments under conditions of an 8-d, 100-mM NaCl treatment (Figure 8A). On the contrary, pH was significantly reduced in all three apoplastic compartments in the salt-resistant SR03 after salt treatment (Figure 8B). The pH was also visualized by means of ratio images as represented in Figure 8, C-F.

## Discussion

### Leaf growth

Growth-related differences between salt-sensitive and salt-resistant hybrids were studied in order to achieve a more comprehensive understanding of growth-related responses of maize leafs under salt stress. The salt-sensitive maize hybrid Lector was compared with the salt-resistant SR03. The hybrid SR03 was developed in a salt resistance breeding programme and characterized as being highly salt-resistant (Schubert et al., 2009). The SR03 hybrid shows nearly no harvest deficits under soil salinity of 10 dS $m^{-1}$, whereas a conductivity of 6 dS $m^{-1}$ usually leads to a 50% reduced harvest of almost all recent maize hybrids (Doorenbos and Kassam, 1976). Thus, the salt-resistant SR03 hybrid provides an excellent tool for analysing physiological traits possibly related to salt resistance.

The decrease in leaf growth and biomass production, especially the reduced growth of expanding leaves of the salt-sensitive hybrid Lector (Figures 1 and 2), indicates a sodium-induced shoot growth inhibition. Such an inhibition is generally known to occur in the first phase of salt stress which is dominated by osmotic stress rather than sodium toxicity (Sümer et al., 2004; Munns and Tester, 2008). The cross-sections of the maize leaves (Fig. 2, B–E) indicate that these plants have grown in the first phase of salt stress, otherwise tissue would partially be chlorotic. The relative chlorophyll concentration of the relevant leaves was not affected in response to salinity (Figure 3), underlining that the leaves do not sustain chlorotic

lesions that are indicative for ion toxicity symptoms. Furthermore, there was no visible damage on the leaf surface after final 8 d of salt treatment underlining that sodium toxicity symptoms that are characteristic for the second stress phase did not occur (Munns, 1993). The salt-sensitive hybrid SR03 is characterized as highly salt-resistant and, thus, nearly maintained growth under stress condition (Figures 1 and 2). This is remarkable because salinity usually inhibits growth of young leaves *via* inhibition of cell division and cell elongation (Mühling and Läuchli, 2002). In accordance to the above described results, it was demonstrated (Geilfus et al., 2011) that the wall extensibility in expanding leaves that grew under saline conditions was less reduced in the salt-resistant maize hybrid SR03 as compared with the salt-sensitive hybrid Lector. Therefore, the authors suggested altered rheological properties of the cell wall that possibly contribute to the salt resistance of the SR03 hybrids.

**Genotype-specific *XTH1* transcript abundances**

To test whether genotypic differences in terms of leaf growth might be attributable to the expression of the xyloglucan endotranshydrolases (XTH), an enzyme known to be a wall-loosening factor (Vissenberg et al., 2005), the transcript expression rate of *ZmXTH1* was tested under salt stress. Genovesi et al. (2008) demonstrated that (*i*) *ZmXTH1* is expressed in growing tissues and (*ii*) that it is weakly bound to the cell wall where it possibly alters the architecture of the cell wall by modifying polymer cross-links. A decrease of *ZmXTH1* transcript abundance as detected in the leaves of the salt-sensitive Lector (Figure 4) probably contributes to the lower abundance of this enzyme in the cell wall of salinity-affected leaves. On the contrary, an increase of *ZmXTH1* transcripts in the leaves of salt-resistant SR03 (Figure 4) is indicative for a higher abundance of this protein under salinity. This higher abundance might contribute to counteract the decrease in plant growth, possibly explaining why SR03 does not show a salinity-induced reduction in biomass. In favour of this

hypothesis, Hernández-Nistal et al. (2010) suggested that XTH1 proteins significantly participate to the elongation growth in the cell wall of *Cicer arietinum.*

**NaCl-stress decreases β-expansin protein abundance in salt-sensitive Lector**

Besides *ZmXTH1*, transcript abundance of other cell wall-loosening agents proved to be adversely regulated within both genotypes, viz., down-regulated in salt-sensitive Lector but up-regulated in salt-resistant SR03 under NaCl stress. This was demonstrated, *inter alia*, for the α-expansins *ZmEXPA1* (Geilfus et al., 2011), and for the β-expansin *ZmEXPB2*, *ZmEXPB6*, and *ZmEXPB8* (Geilfus et al., 2010a). Expansins are one of the best characterized cell wall-loosening agents (Sella Kapu and Cosgrove, 2010) and are though to be the primary mediators of acid-induced growth (Cosgrove, 2005). Experimental evidence supports the idea that expansins intercalate within carbohydrate matrices in the cell wall, leading to a transient loosening of non-covalent interactions, and thus enhance the ability of these matrices to move relative to each other (Cosgrove, 2000; Cosgrove, 2005). It was formerly suggested Geilfus et al. (2010a) that a down-regulation of the β-expansin transcripts *ZmEXPB2*, *ZmEXPB6*, and *ZmEXPB8* in salinity-affected, expanding leaves of the salt-sensitive hybrid Lector might causally explain the reduction in the composite β-expansin protein abundance. The reduced β-expansin protein abundance was found to positively correlate with a reduced shoot growth under stress (Geilfus et al., 2010a). Since expansins regulate cell wall enlargement in growing cells (McQueen-Mason, 1995), we suggest that the decrease of expansin proteins in leaves of the salt-sensitive hybrid Lector possibly accounts for the inhibition of shoot growth in salt-stressed plants. In favour of this assumption, the β-expansin protein abundance was not reduced in leaves of the salt-resistant SR03 plants that maintained growth under salinity (Geilfus et al., 2010a). Following this, the β-expansin proteins might remain acting as a wall-softening factor in salt-affected leaves of SR03 and thus, possibly explain the maintenance of shoot growth of salt-resistant maize under salt stress.

However, to test which particular isoform(s) may account for the salinity-induced decrease of the composite β-expansin protein abundance in salt-sensitive Lector, a two-dimensional Western blot was performed (Figure 5). The absence of one particular β-expansin isoform possibly explains the decrease in the composite protein abundance described previously for the salt-sensitive Lector (Geilfus et al., 2010a; figure 2 therein). The isoform that has disappeared in the salt-sensitive cultivar Lector under condition of salt stress has an apparent molecular weight of ~30 kDa and an isoelectric point within the alkaline range. *In-silico* analysis limits the identity of this vegetatively expressed isoform to three possible candidates. Only the β-expansin isoforms ZmEXPB4, ZmEXPB6, and ZmEXPB8 have a theoretical molecular mass of ~30 kDa and an isoelectric point in an alkaline range (Table 1). Moreover, target site-prediction suggests that ZmEXPB4, ZmEXPB6, and ZmEXPB8 are designated to the secretory pathway, which is indicative for the isoforms to be located and to function at the cell wall (Table 1). This target site-prediction provides additional hint for a possible role of these particular isoforms in growth and consequentially in a salt-induced growth-reduction. However, this is not an unambiguous assignment of the identity of the isoform of interest. Nonetheless, the *in silico* analysis suggest one of the above mentioned β-expansin isoforms to be the particular isoform that decreased in the salt-sensitive hybrid under salinity. Moreover, it was shown in previous work that the transcript abundance of the isoforms ZmEXPB6 and ZmEXPB8 were down-regulated in salt-sensitive Lector under salinity (Geilfus et al., 2010a). These findings strengthen the idea that one of ZmEXPB6 or ZmEXPB8 is the isoform responsible for maintenance of growth under salinity.

**Genotype-specific growth reduction of the epidermal cell**

A clear correlation between a salinity-induced growth reduction and the expression pattern of expansins was demonstrated for non-salt-resistant maize (Veselov et al., 2007; Geilfus et al., 2010a and 2011; this study Figure 5). However, these studies do not provide information

about the tissue-specific localisation of the expansin proteins. Interestingly, Yeats et al (2010) found cell wall-modifying and structural proteins, such as expansin, xyloglucan endotransglucosylase-hydrolase, and extensin, to be located within the outermost epidermal surface of tomatoes. This so called "outermost epidermal surface" consists of a hydrophobic cuticle that is continuous with the outer polysaccharide cell wall of the epidermis and is known to be involved in growth processes of plants (Kurdyukov et al., 2006; Yeats et al., 2010). For this reason we have tested whether vegetatively expressed β-expansins are located within this outermost epidermal surface of expanding maize leaves. Western blotting revealed the occurrence of a clear signal band (Figrue 6A) that appears in the range in which *in-silico* analysis predict the ß-expansins to occur (Table 1). In accordance to these findings, target side prediction suggested that some β-expansin isoforms, viz., ZmEXPB4, ZmEXPB6, ZmEXPB7, and ZmEXPB8, are designated to the secretory pathway (Table 1). Moreover, Cosgrove et al. (2002) reported expansins to be located within growing regions of epidermis cells of cucumber hypocotyls. However, the occurrence of growth-mediating vegetatively expressed expansin proteins within the epidermal surface of expanding leaves is indicative for their role in outermost epidermal surface growth. Interestingly, in the recent study we detected genotypic difference between salt-sensitive and salt-resistant hybrids in terms of the size of the epidermal cells. In response to an 8-d salt treatment, epidermal cell size, including length, width and area, was significantly reduced within the salt-sensitive maize hybrid Lector, whereas epidermal cell size of the salt-resistant SR03 hybrid was not affected (Figure 7). The reduced size of the leaf epidermal cells may explain the reduced size of the leaves; because there is evidence that the epidermis both drives and restricts plant shoot growth (Savaldi-Goldstein et al., 2007). In accordance, the epidermal cell size was not affected by salinity in the leaves of SR03 (Figure 7) that is known to maintain cell wall extensibility (Geilfus et al., 2011) and growth (Figures 1-2).

Taking together, (*i*) epidermal cells are known to drive and restrict plant shoot growth (Savaldi-Goldstein et al., 2007), and (*ii*) the epidermal cells of the salt-sensitive Lector were significantly reduced in size under salinity (Figure 7), and (*iii*) growth-mediating β-expansin proteins are located in the epidermal cell walls of expanding maize leafs (Figrue 6). These findings altogether support the idea that salinity effects leaf growth via reduction of the size of epidermal cells in salt-sensitive plants.

**Apoplastic pH appears to be involved in genotype-specific growth reduction**

According to the acid growth theory, an auxin-mediated acidification of the leaf apoplast is the major requirement for increasing wall extensibility (Hager, 2003). We used non-invasive microscopy-based ratio imaging for the *in planta* quantification of leaf apoplastic pH in the stomatal cavity, the epidermal apoplast, and the apoplast built by the palisade tissue. As measured for the salt-resistant maize hybrid SR03, the pH within the expanding leaves proved to acidify within all three apoplastic compartments under salinity (Figure 8B): Control-treated SR03 plants exhibited a leaf apoplastic pH of 4.5, whereas the pH was decreasing in response to an 8-day 100 mM NaCl treatment to pH 3.5. A pH of 3.5 is more acidic than the lowest reported apoplastic values that are just above pH 4 (Grignon and Sentenac, 1991). This low pH might be attributable to the fact that the transcript abundance of the plasma membrane proton pump (PM-$H^+$-ATPase) increased in response to salinity (Geilfus et al., 2011). This is indicative for a higher abundance of the PM-$H^+$-ATPase. Under saline conditions, the $H^+$-pump possibly acidifies the leaf apoplast of the salt resistant hybrid SR03 by pumping protons from the cytosol into the apoplast.

Taking into account that (*i*) a decreased cell wall pH is generally thought to promote wall-loosening events necessary for growing cell enlargement (Rayle and Cleland, 1992) and (*ii*) expansins exhibit reduced activity at the more alkaline pH (McQueen-Mason, 1995), the apoplastic acidification under stress might provide one mechanism to counteract a growth reduction. Following this assumption, this salt-induced apoplastic acidification possibly contributes to the maintenance of leaf

growth as demonstrated in Figures 1, 2 and 7. In favour of this assumption, the leaf apoplast of the salt-sensitive Lector did not acidify but exhibited a significant growth reduction.

## Conclusion

The abundance of one growth-mediating β-expansin protein isoform decreased in salt-affected leaves of the salt-sensitive hybrid Lector, possibly contributing to the salinity-induced growth reduction. *In silico* analysis limited the identity of this particular β-expansin isoform to one of the isoforms ZmEXPB4, ZmEXPB6 or ZmEXPB8. Genotype-specific responses of the salt treatment on the apoplastic pH were compared via camera-based *in planta* ratio analysis. A leaf apoplastic acidification was found to occur in the salt-resistant SR03 under salinity. Since a decreased cell wall pH is generally thought to promote wall-loosening events, this apoplastic acidification possibly counteracts a salt-induced growth reduction. In favour of this hypothesis, the leaf apoplast of the salt-sensitive Lector did not acidify but exhibited a significant growth reduction.

## Material and methods

### Plant cultivation

The salt-sensitive maize hybrid Lector and the highly salt-resistant maize hybrid SR03 (*Zea mays* L.; Schubert et al. (2009) were grown in hydroponic culture in a greenhouse The seeds were embedded in 1 mM $CaSO_4$ in an aerated solution at 25°C for 1 d and placed between filter papers moistened with 1 mM $CaSO_4$ for a period of 3 d until germination. Subsequently, the seedlings were transferred to 4.5-L plastic pots (3 plants per pot) containing one-quarter-strength nutrient solution. After 2 d of cultivation, the concentration of nutrients was increased to half-strength and, after 4 d of cultivation, to full-strength. The nutrient solution had the following composition: 2.5 mM $Ca(NO_3)_2$, 1.0 mM $K_2SO_4$, 0.2 mM $KH_2PO_4$, 0.6 mM $MgSO_4$, 5.0 mM $CaCl_2$, 1 mM NaCl, 1.0 µM $H_3BO_4$, 2.0 µM $MnSO_4$, 0.5 µM $ZnSO_4$, 0.3 µM $CuSO_4$, 0.005 µM $(NH_4)_6Mo_7O_{24}$, 200 µM Fe-EDTA. The

solution was changed every 2nd d to avoid nutrient depletion. NaCl treatment was started 2 d after the full-nutrient concentration had been reached and was increased stepwise by 25-mM increments every 2nd d to a final concentration of 100 mM (controls without NaCl). Temperature was kept constant at 26°C for light period and at 18°C for dark period; relative humidity was set to about 70%. Expanding leaves that had started to develop one d after the full 100 mM NaCl stress-treatment was applied were taken for all measurements. Leaves used for RNA and protein analysis were ground in liquid nitrogen and stored at -80° C. The experimental set-up consisted of at least four independent replicates of the salt-treated plants (100 mM NaCl) and the corresponding control plants.(without additional salt)

**Leaf growth analysis**

Leaf area was measured with a leaf area meter (Li-3100; Li-Cor, Inc., Lincoln, Nebraska). Leaf length was measured non-destructively using a ruler on a daily basis starting one d after NaCl was applied for the first time.

**Microscopy-based measurement of relative leaf thickness and relative epidermal cell size**

Leaf thickness and epidermal cell size (including length, width and area) were measurement after embedding leaves in a histological sectioning-medium suitable for light microscopy. These parameters are referred as to "relative" since measurements were obtained with the inherent spatial inaccuracy resulting from the embedding procedure (Pyke et al., 1991).

*Tissue embedding.* Leaves were cut into small segments and immediately fixed as described elsewhere (Moll et al., 2002). Afterwards, the leaf segments were dehydrated in a graded ethanol series and embedded in Technovit 7100 (Heraeus-Kulzer, Hanau, Germany). Subsequently, epidermal cell size was measured. For measuring leaf thickness, cross-sections (10 µm) were cut with a microtome.

*Leaf thickness and epidermal cell size.* An inverted microscope (DMI6000B; Leica Microsystems, Wetzlar, Germany) with a 20-fold/10-fold magnification was used for image collection. Measurements were carried out on the basis of the corresponding images using the calibrated scale bar provided by the LAS AF software (Leica Microsystems, Wetzlar, Germany). Cell area was calculated as a function of the pixel-per-area.

**SPAD readings**

The relative chlorophyll concentration of the leaves was measured with a portable chlorophyll meter (SPAD-502, Minolta, Japan). At least fifteen SPAD-502 readings for each leaf were averaged by the internal software and were taken as a single data point for each replicate.

**Real-time qRT-PCR**

*Primer design.* Primer for amplifying *Zea mays* xyloglucan endotranshydrolases 1 (*ZmXTH1*, Supplemental material 1) were designed by means of Primer3Plus and Primer-BLAST software (http://bioinformatics.nl/cgi-bin/primer3plus/primer3plus.cgi; http://www.ncbi.nlm.nih.gov/). To demonstrate the specificity of the primer, the real-time qRT-PCR products were sequenced (MWG Eurifons, Munich, Germany). Sequencing revealed that no undesired PCR products were generated (Supplemental material 2). Furthermore, after qRT-PCR measurements agarose gels (1.5 %) were run to ensure that only PCR products of correct length were amplified (Supplemental material 3).

*RNA extraction and cDNA synthesis.* RNA extraction and cDNA synthesis was carried out as described previously (Geilfus et al. 2011). Briefly, RNA was isolated out of 100 mg ground leaf material. RNA purification was conducted with oligo$(dT)_{25}$-coupled paramagnetic particles (Dynabeads® mRNA Purification Kit, Invitrogen GmbH, Karlsruhe, Germany), purified maize poly $(A)^+$ RNA was reverse-transcribed with a first-strand cDNA synthesis system following the manufacturer's instructions (SuperScript® VILO cDNA synthesis kit, Invitrogen, Karlsruhe, Germany).

*Real-time qRT-PCR.* SYBR-Green-based qRT-PCR was performed as described in detail (Geilfus et al. 2011) on an Applied Biosystems 7300 real-time PCR system using single-stranded cDNA for each reaction. After an initial denaturation step (92°C, 2 min), real-time quantitative RT-PCR was carried out over 40 cycles (denaturation: 92°C, 30 s; annealing: 60°C, 40 s; elongation: 72°C, 20 s). To check the specificity of the amplification, dissociation kinetics were performed at the end of the experiment (60–95°C, continuous fluorescence measurement). By using the comparative Ct (threshold cycles) method, the Ct values were normalized by comparison with the endogenous reference gene (ubiquitin-conjugating enzyme; Hong et al., 2008). The normalized Ct values were then used to compare NaCl-treated plants and corresponding controls. Data were expressed as the relative change in transcript expression (+100 relative expression = 2-fold up-regulation; -100 relative expression = 2-fold down-regulation). Threshold cycles as calculated by the internal software were the means of three biological replicates of each run being replicated in triplicate.

**2D Western blotting-detection of β-expansin isoforms**

*Protein extraction.* Proteins for isoelectric focusing were extracted out of 100 mg ground leaf material (cultivar Lector) by using a dithiothreitole (DTT)-trichloroacetic acid (TCA)-acetone precipitation method adopted from Zörb et al. (2004). Precipitated proteins were resuspended in 1 mL protein sample buffer (8 M urea; 2 M thiourea; 0.5% v/v pharmalyte buffer, pH 3–10; 4% w/v CHAPS; 30 mM DTT; 20 mM TRIS, pH 8.8; 5 mM Pefablock) and were solubilized by incubation for 2 h at 33 °C, followed by a 10-min incubation in an ultrasonic bath. Samples were centrifuged (18 000 x *g;* 30 min, 4°C) and the supernatant was subjected to IEF.

*First-dimension isoelectric focusing (IEF).* IEF was carried out on a Protean IEF Cell system (Biorad, Munich, Germany). Proteins (100 µg; 2D QUANT protein determination kit, GE-Healthcare, München, Germany) were diluted in a total volume of 200 µL IPG sample buffer and were loaded on pre-cast IPG strips (110×3.0×0.5 mm, pH 3–11, linear, GE-Healthcare, Munich, Germany). Gels were rehydrated at 20°C for 12 h at 50 V. IEF was performed for 37400 Vh with

the initial voltage set to 250 V for 30 min, then a gradient up to 500 V for 30 min, followed by a gradient up to 3000 V for 30 min, and finally separation at 3000 V for 4 h. For the 2nd dimension, strips were equilibration as described elsewhere Geilfus et al. (2010b)

*2D PAGE.* For achieving high reproducibility within the 2D WB detection, an improved 2D Western blotting-procedure according to Geilfus et al. (2010b) was used. Briefly, all three biological replicates of each treatment, viz., 100 mM NaCl or the corresponding controls, were simultaneously extracted side by side on one SDS-PAGE. Two-dimensional separation was carried out with a Multi-Gel Electrophoresis unit that enabled all gels to be run in parallel (Protean 2 Multi Cell, Biorad, Munich, Germany): The equilibrated IPG gel were run at 30 mA/gel for 6.5 h (120 W) at 15 °C. The apparent molecular mass of proteins was determined using a pre-stained molecular weight marker.

*2D-blotting procedures.* Gel fragments ≥ 40 kDa were not used for the blotting procedure because β-expansin proteins are known to range from 20 to 30 kDa (Table 1). Instead, this part of the SDS-gel was used as loading control for indicating equivalent amount of proteins in all replicates. The lower part of the SDS-gel that contains proteins < 40 kDa was used for β-expansin detection. Proteins were electroblotted to a PVDF membrane (BioTrace, PALL Life Sciences, Pensacola, USA) by using a semi-dry transfer system (SemiPhor, Hoefer Pharmacia Biotech, San Francisco, USA) as described previously (Geilfus et al. 2010b). Briefly, SDS-gel fragments and the PVDF membrane were equilibrated 15 min in Towbin buffer (25 mM TRIS-base; 192 mM glycine; 20% v/v methanol; 0.01% w/v SDS; pH 8.3) and subsequently placed between soaked sheets of filter paper (Whatman gelblot paper; 1.2 mm, Sigma, Munich, Germany). Transfer was conducted for 75 min at 40 V, 0.8 mA/cm$^2$. Transfer efficiency was checked with the pre-stained protein marker.

*Immunodetection.* For immunostaining, the membrane was saturated in a solution of milk powder in TRIS-buffered saline (TBS) with Tween (TBS-T; 2.5% w/v bovine skimmed milk; 0.1% v/v Tween) for 2 h at room temperature and then incubated with the antibodies. For the labelling of the β-expansin isoforms, a polyclonal anti-peptide rabbit IgG antibody (anti-ZmExpB) was used. The

antibody was raised against a conserved 15 amino acid region shared by seven different, vegetatively expressed, β-expansin isoforms (Geilfus et al., 2010b) and was purchased from BioTrend (Cologne, Germany). The blot was incubated with the antisera diluted 1/250 in the same TBS-T (0.1 mL/cm$^2$ PVDF membrane) for 2 h and washed three times with TBS-T (0.1% v/v). Subsequently, the membrane was incubated with horseradish-peroxidase-conjugated goat anti-rabbit IgG (Sigma-Aldrich, Munich, Germany), diluted 1/38000 in TBS-T, for 1 h at room temperature. Finally, membrane was washed three times in TBS-T and one-time in TBS. Signals were detected by using chemiluminescent peroxidase subtrate-3 on Kodak BioMax light film (Sigma, Munich, Germany) with an exposure time of 4 minutes.

**1D Western blotting-detection of β-expansins in epidermal surface proteome**

*Extraction of the epidermal surface proteome.* Proteins of the outermost epidermal surface of expanding maize leaves of the cultivar Lector were extracted as previously described (Pyee et al., 1994). Briefly, leaves were dipped for 10 s in chloroform:methanol (2:1) that was gently stirred by a magnetic stir bar. The extract was then evaporated to dryness by rotary evaporation at 50°C with reduced pressure (Yeats et al., 2010). Proteins were suspended in protein sample buffer (5% v/v glycerol, 1,15% SDS, 2.5% β-mercaptoethanol, 0.125% bromephenol blue, 31.5 mM Tris-HCl, at pH 6.8) and sebsequently protein concentration within the sample buffer was increased using a chloroform:methanol-precipitation (Wessel and Flüge, 1984). Afterwards, proteins were resuspended in sample buffer.

*1D PAGE, blotting procedure and immunodetection.* For Western blotting, 15 µg protein were separated by 15% SDS-PAGE and transferred to a PVDF membrane as described above for the 2D-WB. For immunostaining, the membrane was saturated in a solution of milk powder in TBST (2.5% w/v bovine skimmed milk; 0.1% v/v Tween) and was incubated for 2 h with the antibody (anti-ZmExpB, 1/250) in the same buffer with additionally added 1% (w/v) BSA and 0.1% (w/v) fish skin gelatine. The membrane was washed three times with TBST (0.1% v/v) and afterwards

incubated for 1 h with the goat anti-rabbit IgG conjugated to horseradish peroxidase (1:38000; Sigma-Aldrich, St. Louis, USA). The membrane was washed in TBST and TBS buffer, and signals were detected using enhanced chemiluminescence on BioMax film (Kodak, Sigma, Munich, Germany).

**Ratiometric *in planta* measurements of leaf apoplastic pH**

Non-invasive apoplastic pH measurements were carried out on expanding leaves using camera-based ratio analysis in combination with a pH-sensitive fluorophore.

*Dye loading.* For the purpose of *in planta* measurement, the fluorescent pH indicator was loaded into the apoplast as described elsewhere (Geilfus & Mühling, 2011). Briefly, 25 µM Oregon Green 488-dextran conjugated to 10 kDa dextran (Invitorgen GmbH, Darmstadt, Germany) was directly inserted into the leaf apoplast by using a syringe.

*Inverse microscopy imaging.* A inverted microscope (DMI6000B; Leica Microsystems, Wetzlar, Germany) connected to a DFC-camera (DFC 360FX; Leica Microsystems, Wetzlar, Germany) via a 20-fold magnification, 0.4 numerical aperture, dry objective (HCX PL FLUOTAR L, Leica Microsystems) was used for image collection. An HXP lamp (HXP Short Arc Lamp; Osram, München, Germany) was used for illumination at excitation wavelengths of (ex) 440/20 nm and 495/10 nm. Excitation filters were switched by means of a filter wheel and exposure time was 150 mS for both channels. The dye fluorescence at both excitation channels was collected by using a 535/25 nm emission band-pass filter (BP 535/25; ET535/25M; Leica Microsystems) and a dichromatic mirror (LP518; dichroit T518DCXR BS, Leica Microsystems, Wetzlar, Germany).

*Ratiometric analysis.* As a measure of pH, the fluorescence ratio $F_{495}/F_{440}$ was calculated on a pixel-by-pixel basis using the LAS AF software. Background noise values were subtracted at each channel. For pseudo-colour display, the ratio was coded by hue on a spectral colour scale ranging from purple (no signal), over blue (lowest pH signal; pH 3.2), to pink (highest pH signal; pH 6.6), with the limits being set by an *in situ* calibration (see below). Quantitative measurements were

calculated as the ratio of the mean intensity for user-defined regions of interest (ROIs). The high spatial resolution allowed for quantifying pH within three apoplastic compartments, viz., the stomatal cavity, the epidermal apoplast and the palisade apoplast (Supplemental material 4).

*In situ apoplastic pH calibration.* For converting fluorescence ratio data taken from living plants into apoplastic pH values, an *in situ* calibration procedure was performed. Hence, 25 µM Oregon Green buffered with 100 mM MES to a pH ranging from 3 to 7 were loaded into the leaf apoplast. The Boltzmann fit was chosen for fitting sigmoidal curves to calibration data (Supplemental material 5) as described by Schulte et al. (2006). Fitting was performed by using Origin 7.0 (OriginLab Corp., Northhampton, MA, USA). Ratios below 0.95 (corresponds to pH $\leq$ 3.2) and above 2.15 (corresponds to pH $\geq$ 6.6) proved to lie outside the linear range of the *in situ* calibration and were therefore not considered.

**Data evaluation**

The t-Test, as outlined by Köhler et al. (1984), was used to test for differences between means. For pH data, the t-Test was calculated based on delogarithmized pH values. Biological replicates as indicated in the respective figure legend.

## Acknowledgments

Christoph-Martin Geilfus is the grateful recipient of a grant from the Friedrich-Ebert-Stiftung. We wish to thank Prof. Dr. Sven Schubert for the kind provision of the SR03 hybrids and Prof. Dr. Henning Kage for providing the leaf area meter. We also thank Stephanie thor Straten, Brigitte Schemmerling and Martina Bach for excellent technical assistance. This work was supported by a research grant of the Deutsche Forschungsgemeinschaft (ZO118/6).

## Literature

Bernstein, N., Silk, W.K. and Läuchli, A. (1993) Growth and development of sorghum leaves under conditions of NaCl stress: spatial and temporal aspects of leaf growth inhibition. *Planta.* 191: 433-439.

Cosgrove, D.J., Bedinger, P. and Durachko, D.M. (1997) Group I allergens of grass pollen as cell wall-loosening agents. *PNAS.* 94: 6559-6564.

Cosgrove, D.J. (2000) Loosening of plant cell walls by expansins. *Nature.* 407: 321-326.

Cosgrove, D.J., Li, L.C., Cho, H.T., Hoffmann-Benning, S., Moore, R.C. and Blecker D. (2002) The growing world of expansins. *Plant Cell Physiol.* 43: 1436-1444.

Cosgrove, D.J. (2005) Growth of the plant cell wall. *Nat Rev Mol Cell Biol.* 6: 850-861.

Doorenbos, J. and Kassam, A.H. (1976) Yield response to water. In: *FAO irrigation and drainage paper.* Edited by FAO. p. 160. FAO, Rome.

Geilfus, C.M., Zörb, C. and Mühling, K.H. (2010a) Salt stress differentially affects growth-mediating β–expansin in resistant and sensitive maize (*Zea mays* L.) cultivars. *Plant Physiol Biochem.* 48: 993-998.

Geilfus, C.M., Mühling, K.H. and Zörb, C. (2010b) A methodical approach for improving the reliability of quantifiable two-dimensional Western blots. *J Immunol Methods.* 362: 59-94.

Geilfus, C.M., Zörb, C., Neuhaus, C., Hansen, T., Lüthen, H. and Mühling, K.H. (2011) Differential transcript expression of wall-loosening candidates in leaves of maize cultivars differing in salt resistance**.** *J Plant Growth Regul*. DOI: 10.1007/s00344-011-9201-4.

Geilfus, C.M. and Mühling, K.H. (2011). Real-time imaging of leaf apoplastic pH dynamics in response to NaCl stress. *Front Plant Sci*. 2:13. doi: 10.3389/fpls.2011.00013

Genovesi, V., Fornalé, S., Fry, S.C., Ruel, K., Ferrer, P., Encina, A., Sonbol, F.M., Bosch, J., Puigdomènech, P., Rigau, J. and Caparrós-Ruiz, D. (2008) ZmXTH1, a new xyloglucan endotransglucosylase/hydrolase in maize, affects cell wall structure and composition in

*Arabidopsis thaliana*. *J Exp Bot*. 59: 875-889.

Grignon, C. and Sentenac, H. (1991) pH and ionic conditions in the apoplast. *Annu Rev Plant Physiol Plant Mol Bio*. 142: 103-28.

Hager, A., Menzel, H. and Krauss, A. (1971) Versuche und Hypothese zur Primärwirkung des Auxins beim Streckungswachstum. *Planta*. 100: 47-75.

Hager, A. (2003) Role of the plasma membrane $H^+$-ATPase in auxin-induced elongation growth: historical and new aspects. *J Plant Res.* 116: 483-505.

Hernández-Nistal, J., Martin, I., Labrador, E. and Dopico, D. (2010) The immunolocation of XTH1 in embryonic axes during chickpea germination and seedling growth confirms its function in cell elongation and vascular differentiation. *J Exp Bot*. 61: 4231-4238.

Hong, S.Y., Seo, P.J., Yang, M.S., Xiang, F. and Park, C.M. (2008) Exploring valid reference genes for gene expression studies in *Brachypodium distachyon* by real-time PCR. *BMC Plant Biol.* 8: 112-122.

Köhler, W., Schachtel, G. and Voleske, P. (1984) Einführung in die Statistik für Biologen und Agrarwissenschaftler. p. 101. Springer, Berlin.

Kurdyukov, S., Faust, A., Nawrath, C., Bar, S., Voisin, D., Efremova, N., Franke R., Schreiber, L., Saedler, H., Metraux, J.P. and Yephremov, A. (2006) The epidermis-specific extracellular BODYGUARD controls cuticle development and morphogenesis in Arabidopsis. *Plant Cell.* 18: 312-339.

McQueen-Mason, S., Durachko, D.M. and Cosgrove, D.J. (1992) Two endogenous proteins that induce cell wall extension in plants. *Plant Cell*. 4: 1425-1433.

McQueen-Mason, S. (1995) Expansins and cell wall expansion. *J Exp Bot*. 46: 1639-1650.

Moll, S., Anke, S., Kahmann, U., Hänsch, R., Hartmann, T. and Ober, D. (2002) Cell-specific expression of homospermidine synthase, the entry enzyme of the pyrrolizidine alkaloid pathway in *Senecio vernalis*, in comparison with its ancestor, deoxyhypusine synthase1. *Plant Physiol*. 130: 47-57.

Moriau, L., Michelet, B., Bogaerts, P., Lambert, L., Oufattole, M. and Boutry, M. (1999) Expression analysis of two gene subfamilies encoding the plasma membrane $H^+$-ATPase in *Nicotiana plumbaginifolia* reveals the major transport functions of this enzyme. *Plant J*. 19: 31-41.

Mühling, K.H., Plieth, C., Hansen, U.P. and Sattelmacher, B. (1995) Apoplastic pH of intact leaves of *Vicia faba* as influenced by light. *J Exp Bot*. 46: 377-382.

Mühling, K.H., Läuchli, A. (2002) Effect of salt stress on growth and cation compartmentation in leaves of two plant species differing in salt tolerance. *J Plant Physiol.* 159: 137-146.

Munns, R. (1993) Physiological processes limiting plant growth in saline soils: some dogmas and hypotheses. *Plant Cell Environ*. 16: 15-24.

Munns, R. (2005) Genes and salt tolerance: bringing them together. *New Phytol*. 167: 645-663.

Munns, R. and Tester, M. (2008) Mechanism of salinity tolerance. *Annu Rev Plant Biol*. 59: 651-681.

Pyee, J., Yu, H. and Kolattukudy, P.E. (1994) Identification of a lipid transfer protein as the major protein in the surface wax of broccoli (*Brassica oleracea*) leaves. *Arch Biochem Biophys*. 311: 460-468.

Pyke, K.A., Marrison, J.L. and Leech, R.M. (1991) Temporal and spatial development of the cells of the expanding first leaf of *Arabidopsis thaliana* (L.) Heynh. *J Exp Bot*. 42: 1407-1416.

Rayle, D.L. and Cleland, R.E. (1992) The acid growth theory of auxin-induced cell elongation is alive and well. *Plant Physiol.* 99: 1271-1274.

Rozema, J. and Flowers, T. (2008) Crops for a salinized world. *Science.* 322: 1478-1480.

Savaldi-Goldstein, S., Peto, C. and Chory, J. (2007) The epidermis both drives and restricts plant shoot growth. *Natur*. 446: 199-202.

Schubert, S., Neubert, A., Schierholt, A., Sümer, A. and Zörb, C. (2009) Development of salt resistant maize hybrids: the combination of physiological strategies using conventional breeding methods. *Plant Sci*. 177: 196-202.

Schulte, A., Lorenzen, I., Böttcher, M. and Plieth, C. (2006) A novel fluorescent pH probe for expression in plants. *Plant Methods.* 2: 7.

Sella Kapu, N.U. and Cosgrove, D.J. (2010) Changes in growth and cell wall extensibility of maize silks following pollination. *J Exp Bot.* 61: 4097-4107.

Sümer A., Zörb C., Yan, F., Schubert S. (2004) Evidence of $Na^+$ toxicity for the vegetative growth of maize (*Zea mays* L.) during the first phase of salt stress. *J Appl Bot Food Qual*. 78, 135-139.

Van Volkenburgh, E. and Boyer, J.S. (1985) Inhibitory effects of water deficit on maize leaf elongation. *Plant Physiol*. 77: 190-194.

Veselov, D.S., Sabirzhanova, I.B. and Chemeris, A.V. (2007) Changes in expansin gene expression, IAA content, and extension growth of leaf cells in maize plants subjected to salinity. *Russ J Plant Physiol.* 55: 101-106.

Vissenberg, K., Fry, S.C., Pauly, M., Hofte, H. and Verbelen, J.P. (2005) XTH acts at the microfibril-matrix interface during cell elongation. *J Exp Bot*. 56, 673-683.

Wessel, D. and Flüge, U.I. (1984) A method for the quantitative recovery of protein in dilute solution in the presence of detergents and lipids. *Anal Biochem.* 138: 141-143.

Yeats, T.H., Howe, K.J., Matas, A.J., Buda, G.J., Thannhauser, T.W. and Rose, J.K.C. (2010) Mining the surface proteome of tomato (*Solanum lycopersicum*) fruit for proteins associated with cuticle biogenesis. *J Exp Bot.* 61: 3759-3771.

Zörb, C., Schmitt, S., Neeb, A., Karl, S., Linder, M. and Schubert, S. (2004) The biochemical reaction of maize (*Zea mays* L.) to salt stress is characterized by a mitigation of symptoms and not by a specific adaptation. *Plant Sci*. 167: 91-100.

## Table

Table 1

*In silico* prediction of the isoelectric point (pI), the molecular weight (Mw), and the target site of the vegetatively expressed β-expansin isoforms. Theoretical pI and Mw were calculated using the *Compute pI/Mw* tool (http://www.expasy.org/tools/pi_tool.html) and target site was predicted with the *TargetP 1.1* tool (http://www.cbs.dtu.dk/services/TargetP/). Column 1, abreviation of β-expansin isoforms; column 2, corresponding Genbank accsssion number; column 3, description of the isoforms; column 4 and 5, computed pI and Mw; column 6, predicted localization of the isoforms, (unknown = winning network output score was below the requested cutoff). Column 7, Reliability score (RC) with information about the quality of the analysis (the lower the value of RC the safer the prediction; maximum is RC = 5, minimum RC = is 1). All predictions were based on predefined set of cut-offs >0.95.

| **β-expansin isoform** | **Accession number** | **Description** (NCBI's Genbank) | **Prediction pI/Mw** | | **Target prediction** | |
|---|---|---|---|---|---|---|
| | | | **pI** | **kDa** | **localization** | **RC** |
| ZmExpB2 | AF332175 | wall loosening protein | 8.80 | 20.07 | unknown | 4 |
| ZmExpB3 | AF332176 | wall loosening protein | 4.84 | 23.70 | unknown | 3 |
| ZmExpB4 | AF332177 | wall loosening protein; with predicted N-linked glycosylation sites | 9.54 | 32.66 | secretory pathway | 4 |
| ZmExpB5 | AF332178 | wall loosening protein | 7.11 | 19.86 | unknown | 4 |
| ZmExpB6 | AF332179 | wall loosening protein; contains predicted N-linked glycosylation sites | 8.80 | 30.26 | secretory pathway | 1 |
| ZmExpB7 | AF332180 | wall loosening protein; contains predicted N-linked glycosylation sites | 5.17 | 28.95 | secretory pathway | 1 |
| ZmExpB8 | AF332181 | wall loosening protein; contains predicted N-linked glycosylation sites | 8.07 | 31.62 | secretory pathway | 1 |

## Figure legends

**Figure 1 Genotype-specific leaf growth under NaCl-stress**

Leaf growth and biomass production in response to an 8-d, 100-mM NaCl treatment. All measurements were based on expanding leaves that had started to develop one d after the full 100 mM NaCl treatment was applied (corresponding control plants without additional NaCl). (A) Daily increases of leaf length as averaged over the 8-d, 100-mM NaCl treatment, (B) leaf area, and (C) leaf fresh weight. Light-grey, control; dark-grey, 100 mM NaCl. Sensitive maize hybrid, Lector; resistant hybrid, SR03. All measurements were means of four biological replicates, each run being replicated in triplicate ± SE. Asterisks indicate significant differences between means of salt treatment and control (*$p \leq 0.05$ and ** $p \leq 0.01$; ns = not significant; t-Test).

**Figure 2 Effect of 100 mM NaCl treatment on the relative leaf thickness**

Leaf thickness was measured using cross-sections that were embedded in a histological sectioning-medium. This is why leaf thickness is referred as to “relative” since measurements were obtained with the inherent spatial inaccuracy resulting from the embedding procedure. Leaf thickness was quantified on basis of bright-field images with the scale bar provided by the imaging software.(A) relative leaf thickness (light-grey, control; dark-grey, 100 mM NaCl), (B-E) representative bright-field images showing the leaf thickness of NaCl-treated (100 mM) and controls of maize hybrids. Sensitive hybrid, Lector; resistant hybrid, SR03. All measurements were means of four biological replicates, each run being replicated in triplicate ± SE. Asterisks indicate significant mean differences between salt treatment and control (*$p \leq 0.05$; ns = not significant; t-Test).

**Figure 3 Relative chlorophyll concentrations of leaves grown under saline conditions**

The 8-d, 100 mM NaCl treatment did not affect the relative chlorophyll concentration of the leaves as measured with a SPAD-502-chlorophyll meter. Light-grey, control; dark-grey, 100 mM NaCl. Sensitive hybrid, Lector; resistant hybrid, SR03. All measurements were based on four biological replicates, each run being replicated in triplicate ± SE. t-Test revealed no significant mean differences between treatments at $p \leq 0.05$ (ns = not significant; t-Test).

**Figure 4 Genotype-specific changes of *XTH1* transcript abundance**

Relative changes in the transcript abundance of xyloglucan endotranshydrolases 1 (*ZmXTH1*) in response to an 8-d, 100-mM NaCl treatment. Measurements were based on reverse-transcribed highly purified maize poly$(A)^+$ RNA. The transcript for the ubiquitin-conjugating enzyme was used as the endogenous control (see Methods section). Effect of salt treatment on the relative transcript abundance with control as calibrator sample (+100 rel. expression = 2-fold up-regulation, -100 rel. expression = 2-fold down-regulation). Salt-sensitive Lector, white bar; salt-resistant SR03, black-spotted bar. Expression data correspond to means of three biological replicates, each being run in triplicate, ± SE.

**Figure 5 Changes in the β-expansin pattern in salt-affected leaves of salt-sensitive Lector**

For a specific labelling of the β-expansin isoforms, two-dimensional Western blot was performed in combination with an anti-peptide IgG antibody raised against a conserved 15 amino acid region shared by seven vegetatively expressed, β-expansin isoforms (anti-ZmExpB, see Material section). Proteins were two-dimensionally separated on a SDS-gel. Proteins < 40 kDa were electroblotted onto a PVDF-membrane that was subsequently used for the immunodetection. Gel fragments that contain proteins ≥ 40 kDa were used as loading control. (A) 2D Western blotting detection of β-expansin isoforms in expanding leaves of salt-

treated (100 mM NaCl) and control-treated (without NaCl) hybrids of the salt-sensitive Lector. Arrows, isoform that was not detected under saline condition. (B) Loading controls indicate equivalent level of proteins to be separated in all replicates. Coomassie-stained SDS-gels, Numbers (1-3) indicate three biological replicates.

**Figure 6 Western blot detection of β-expansin in the epidermal surface of expanding leaves**

The epidermal surface proteome from expanding leaves of the cultivar Lector was extracted and separated on a SDS-gel, and subsequently electro-transferred on a PVDF membrane. An anti-peptide antibody (anti-ZmExpB) was used for labelling the composite β-expansin proteins. (A) Coomassie-stained loading control indicates the appearance of several bands in a range spanning from 25 kDa and 35 kDa. To test whether unspecific signals were detected erroneously, the antibody was pre-incubated with the peptide that was used for antibody production. In case of a specific labelling of β-expansins, the label should be reduced by pre-incubation of the antibody with the peptide. (B) A molar ratio of antibody to added peptide of 2:1 almost completely blocks the labelling (signal intensity was 1513 density/$mm^2$-background). (C) A molar ratio of antibody to added peptide of 5:1 reduced the labelling (signal intensity was 4028 density/$mm^2$-background). (D) Under normal conditions, viz., a ratio of 1:0, signal intensity after exactly 2 minutes was 8413 density/$mm^2$-background. 1D Western blotting revealed the presence of a signal band between 25 kDa and 35 kDa. Upper black mark, 35 kDa; lower black mark, 25 kDa. In (B-D), blots were developed for exactly 2 min.

**Figure 7 Genotype-specific epidermal cells size under condition of NaCl-stress**

Effect of 8-d, 100 mM NaCl stress on the relative epidermal cell size. Since leaves were embedded in a histological sectioning-medium, epidermal cell size is referred as to “relative” because measurements were obtained with the inherent spatial inaccuracy resulting from the

embedding procedure. Epidermal cell size and width were quantified on basis of bright-field images using the scale bar provided by the imaging software. Cell area was calculated as a function of the pixel-per-area. (A) Relative cell length, (B) relative cell width, and (C) relative cell area. Light-grey, control; dark-grey, 100 mM NaCl. (D-G) Representative bright-field images demonstrating the leaf thickness in salt-treated (100 mM NaCl) and control-treated (without NaCl) hybrids of Lector and SR03. Sensitive hybrid, Lector; resistant hybrid, SR03. The data are means of four biological replicates, each run being carried out in triplicate ± SE. Asterisks indicate significant mean differences between salt treatment and control (*$p \leq 0.05$ and **$p \leq 0.01$; ns = not significant; t-Test).

**Figure 8 Genotype-specific effects of the NaCl-treatment in the leaf apoplastic pH**

*In planta* quantitation of apoplastic pH in expanding leaves that were challenged by an 8-d, 100 mM NaCl treatment. Leaf apoplastic pH at the adaxial face was discriminated within three apoplastic components, viz. in the stomatal cavity, in the epidermal apoplast and in the palisade apoplast. (A) Apoplastic pH as quantified for salt-sensitive Lector. (B) Apoplastic pH as quantified for salt-resistant SR03. Light-grey, control; dark-grey, 100 mM NaCl. (C-F) Representative ratio images show apoplastic pH in salt-treated (100 mM NaCl) and control-treated hybrids of Lector and SR03. Sensitive hybrid, Lector; resistant hybrid, SR03. Ratios were colour-coded on a spectral colour scale (see inset in D). Measurements were conducted on 45 different plants (n =45 biological replicates) with 5 regions of interest (n = 5 ROI) being quantified for each apoplastic sub-compartment (stomatal cavity, epidermal apoplast, and the palisade apoplast). Thus, each mean is based on 225 single data points (in total, Figure 8 is based on 2700 ROI). The data represent means ± SE. Asterisks indicate significant mean differences between salt treatment and control (*$p \leq 0.001$; ns = not significant; t-Test). t-Test was calculated based on de-logarithmized pH values, nevertheless, mean differences were indicated within the logarithmized pH representation.

## Figure Files

**Figure 1**

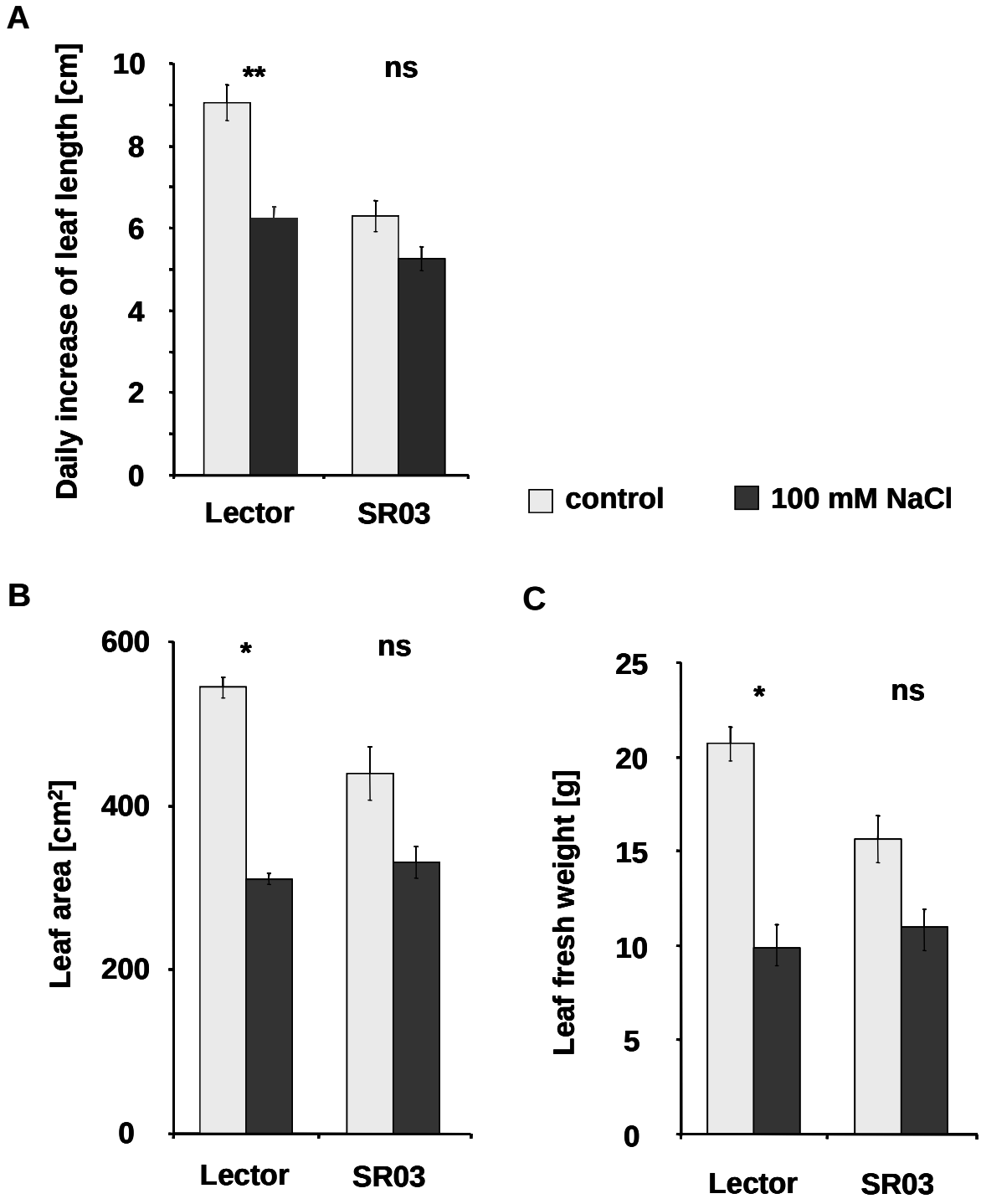

**Figure 2**

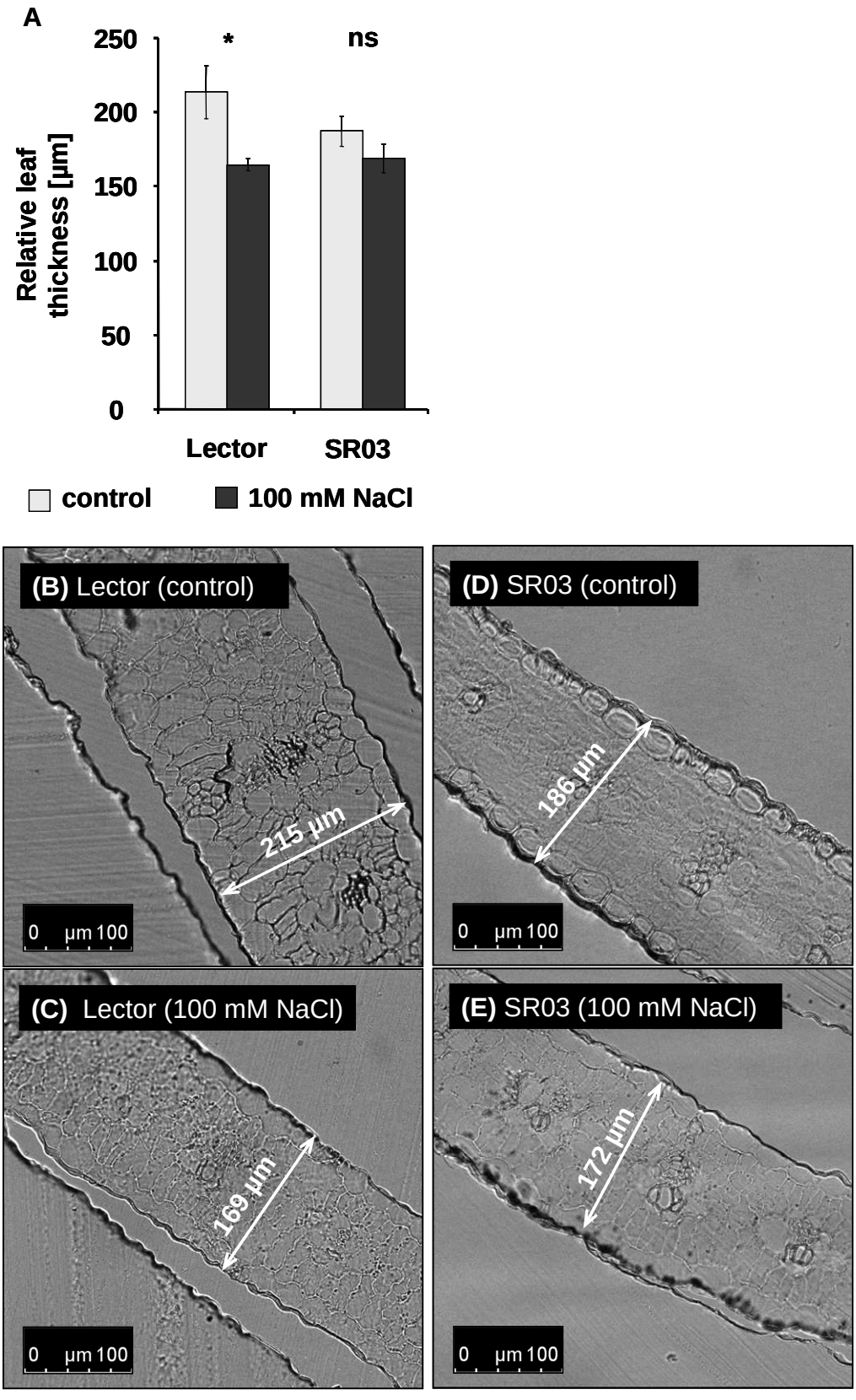
A
250
200
150
100
50
0
*
ns
Relative leaf thickness [µm]
Lector
SR03
control
100 mM NaCl
(B) Lector (control)
215 µm
(D) SR03 (control)
186 µm
(C) Lector (100 mM NaCl)
169 µm
(E) SR03 (100 mM NaCl)
172 µm
0 µm 100

**Figure 3**

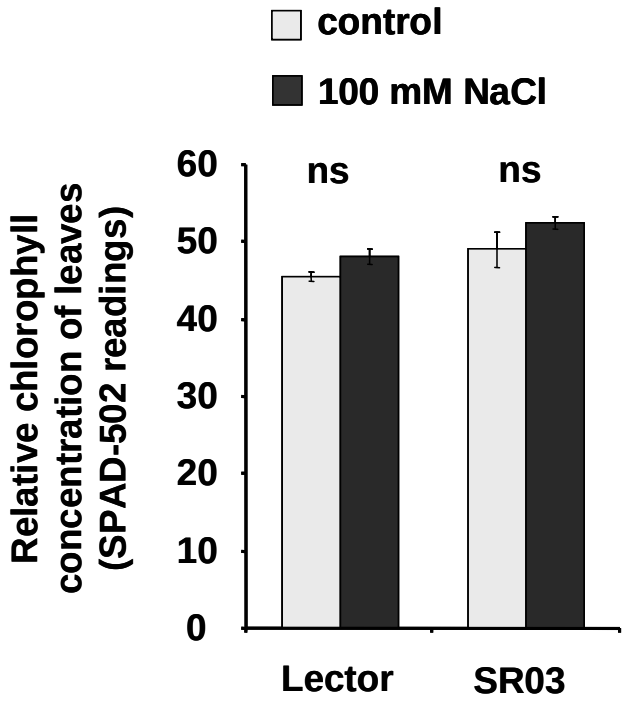


**Figure 4**

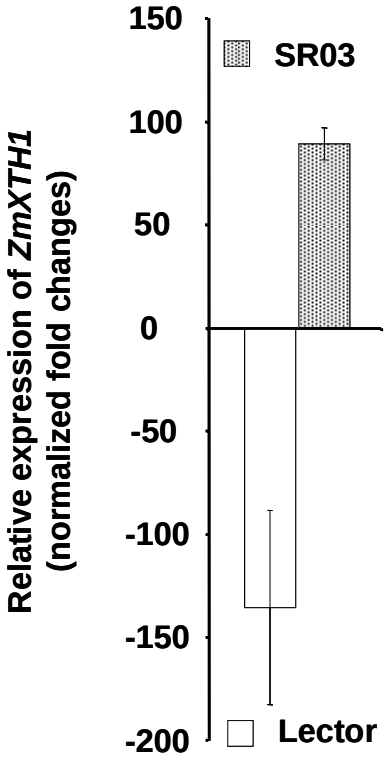

**Figure 5**

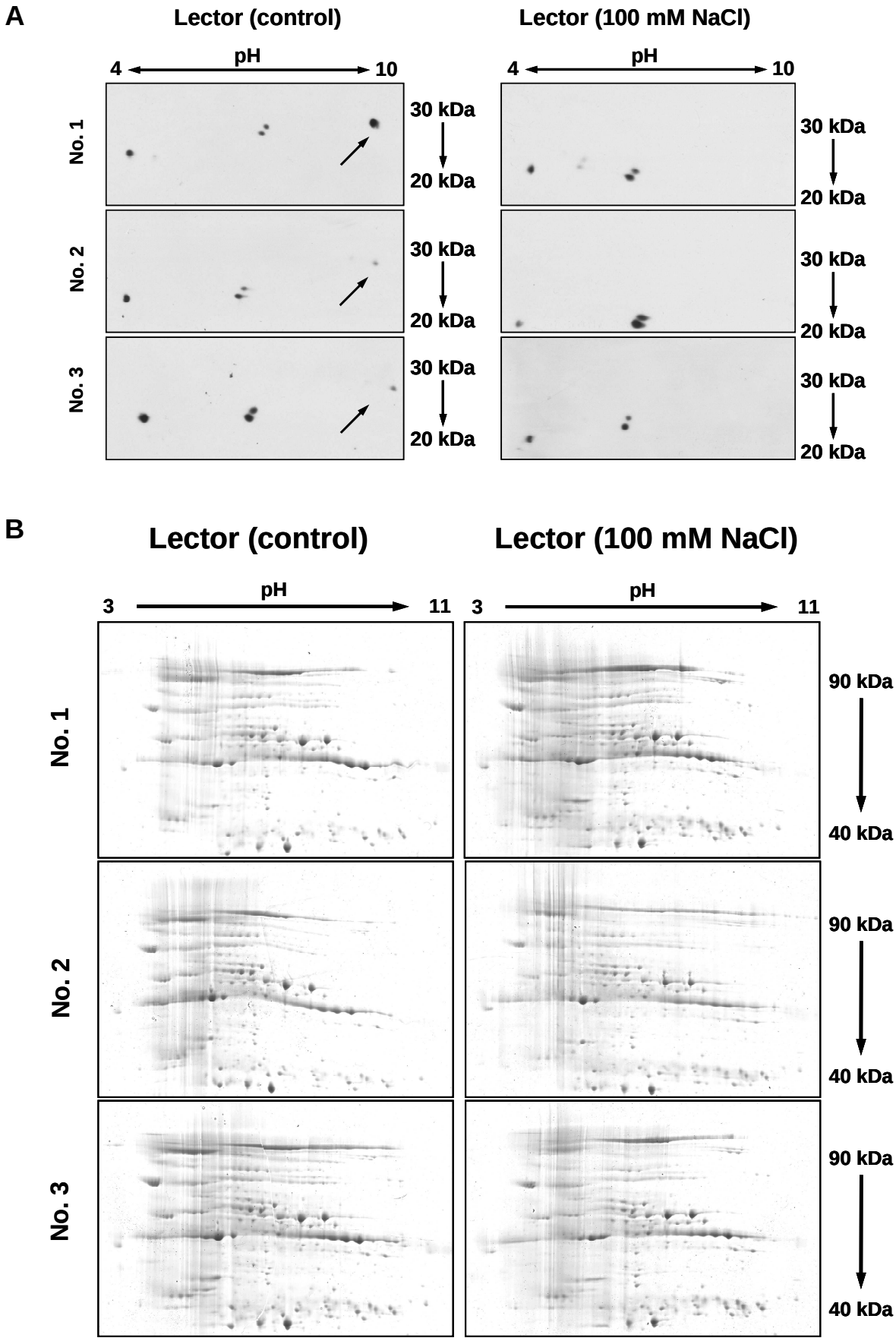
A
Lector (control)
Lector (100 mM NaCl)
pH
4
10
No. 1
No. 2
No. 3
30 kDa
20 kDa
B
Lector (control)
Lector (100 mM NaCl)
pH
3
11
No. 1
No. 2
No. 3
90 kDa
40 kDa

**Figure 6**

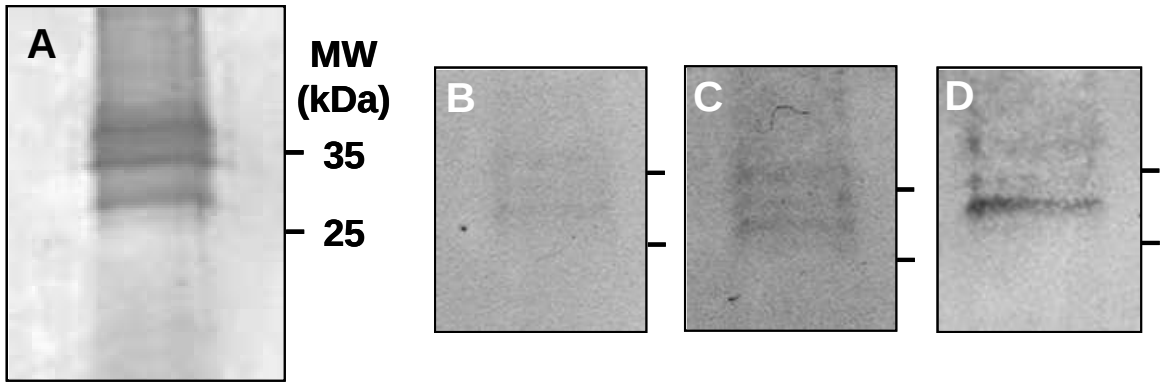

**Figure 7**

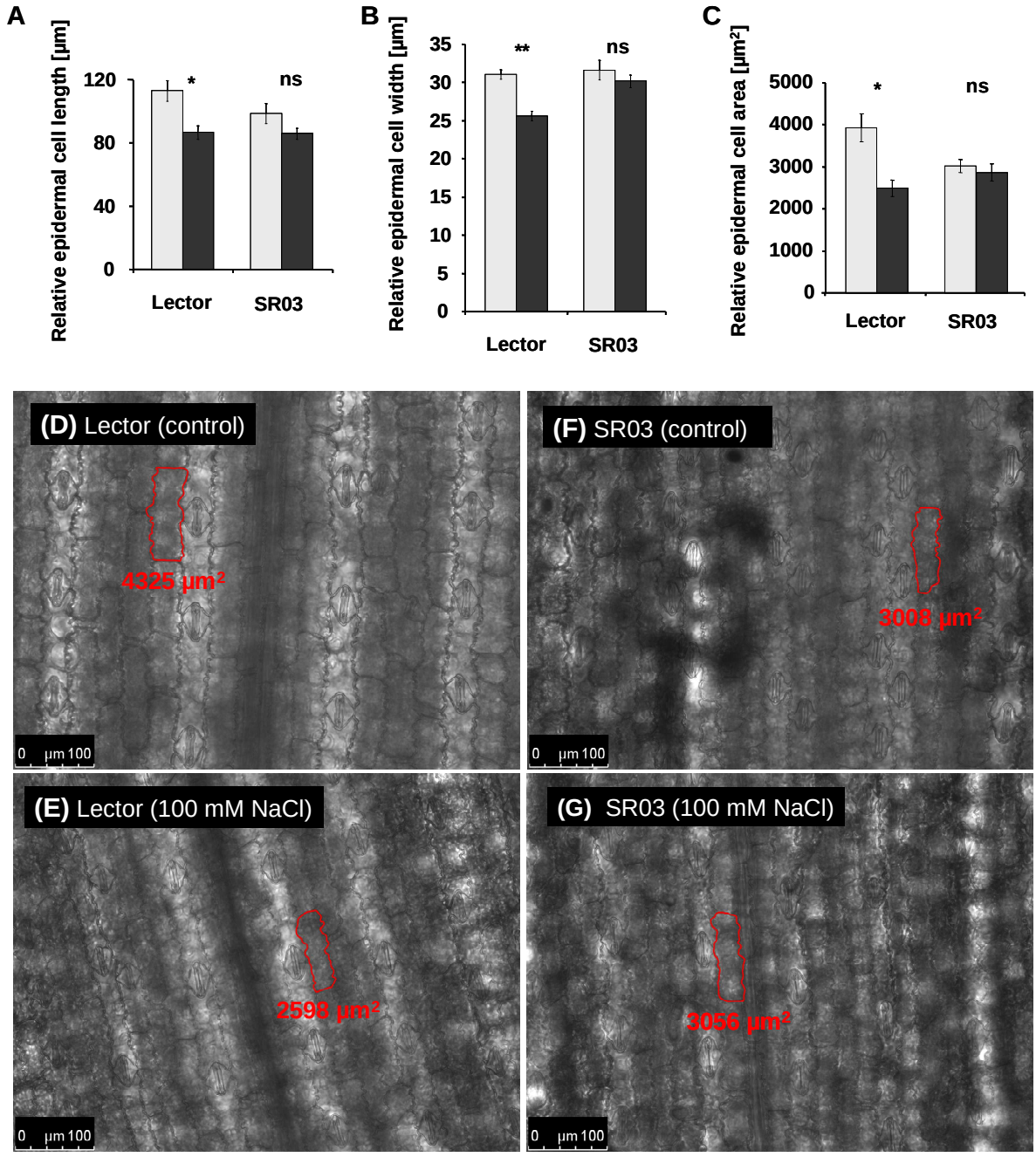
A
Relative epidermal cell length [µm]
120
80
40
0
*
ns
Lector
SR03
B
Relative epidermal cell width [µm]
35
30
25
20
15
10
5
0
**
ns
Lector
SR03
C
Relative epidermal cell area [µm²]
5000
4000
3000
2000
1000
0
*
ns
Lector
SR03
(D) Lector (control)
4325 µm²
0 µm 100
(F) SR03 (control)
3008 µm²
0 µm 100
(E) Lector (100 mM NaCl)
2598 µm²
0 µm 100
(G) SR03 (100 mM NaCl)
3056 µm²
0 µm 100

**Figure 8**

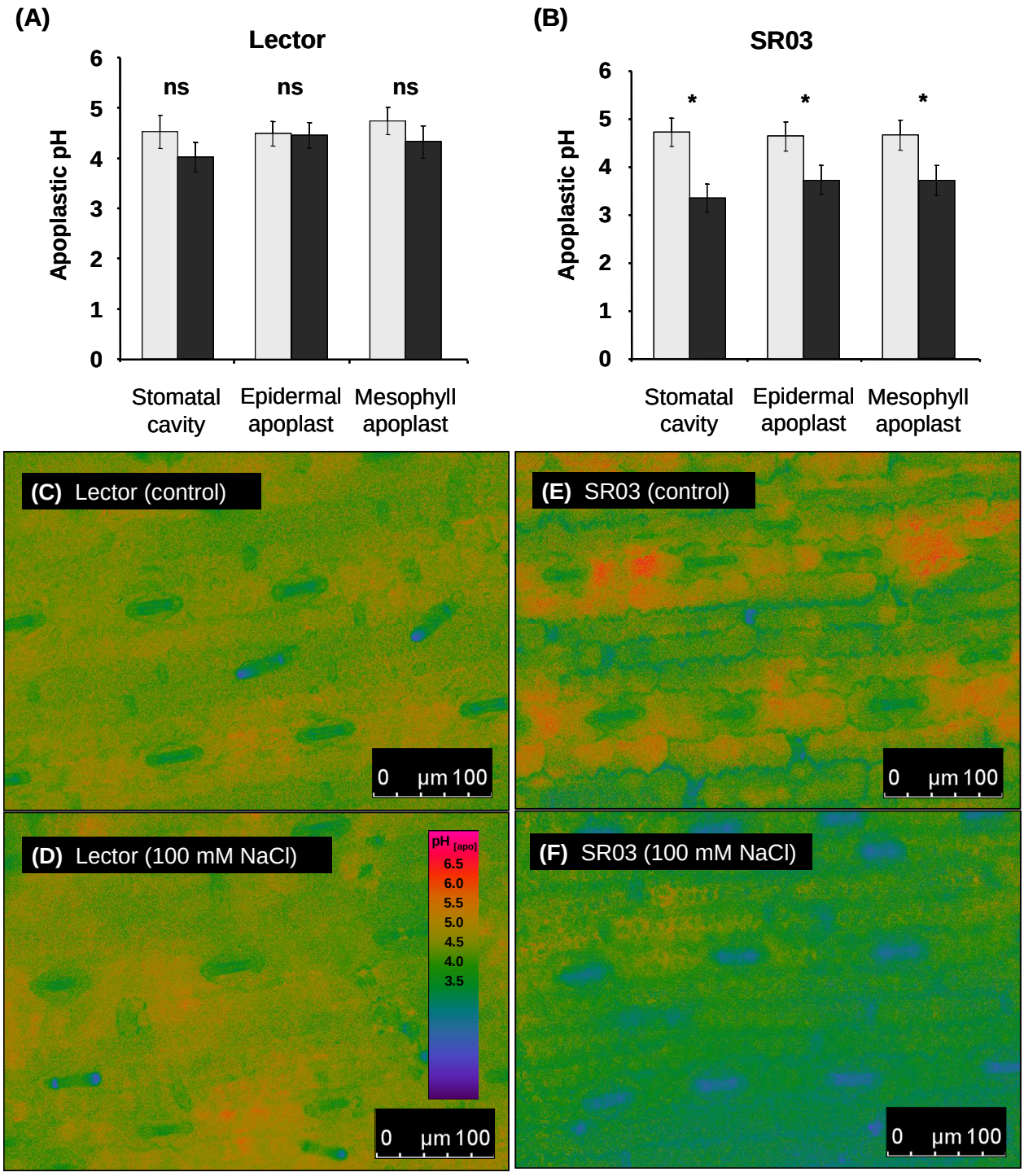
(A)
Lector
Apoplastic pH
ns
ns
ns
Stomatal cavity
Epidermal apoplast
Mesophyll apoplast
(B)
SR03
Apoplastic pH
*
*
*
Stomatal cavity
Epidermal apoplast
Mesophyll apoplast
(C) Lector (control)
(D) Lector (100 mM NaCl)
(E) SR03 (control)
(F) SR03 (100 mM NaCl)
pH [apo]
6.5
6.0
5.5
5.0
4.5
4.0
3.5
0 µm 100

## SUPPLEMENTARY

**Supplementary material 1** Real-time qRT-PCR primer pair used for analyzing transcript expression of *ZmXTH1*.

| Primer name | Accession number | Sequence of forward (f) and reverse (r) primers (5′–3′) | | Annealing temp. [°C] | Product size (bp) |
|---|---|---|---|---|---|
| *ZmXTH1* | NM_001111696.1 | f | CCGTCTCGTGCTTCTACCTC | 60.0 | 148 |
| | | r | TCGAACTGGTGCTCCTTCTT | | |

**Supplementary material 2**

Sequencing of the real-time qRT-PCR products demonstrates selectivity of the primer pair. Column 1 indicates the name of the primer pair. The corresponding DNA sequencing result is presented in column 2. The sequences were alignment against NCBI's reference mRNA sequences (refseq_rna; blastn). Search was limited to *Zea mays* L. (taxid:4577). Best Blast hit is presented in column 3 together with the respective Genbank accession number. Column 4 shows the resulting description of the Blast hits. Columns 5-7, Parameters for statistical quality of the hit.

| Primer pair | Sequencing summary of real-time quantitative RT-PCR products (using IUPAC base calls for wobbles) | Significant alignments of sequences (NCBI blastn on *Zea mays* L. [taxid:4577]; database: refseq_rna) | | | | |
|---|---|---|---|---|---|---|
| | | Accession number | Description | Max score/ Total score | Query coverag / Max ident (%) | E value |
| *ZmXTH1* | TTMGCACCACCGGCTGCCCGCTCGA GTTGCCCATGAACTCCATGTCGATCT CGTCGCGCC CGTCGCCGTCGCCGGAAGAGAGGTA GAAGCACGAGACGGACACGRMGT | NM_001111696.1 | Zea mays xyloglucan endo-transglycosylase/hydrolase (xth1), mRNA | 156/ 156 | 88/ 95 | 3e-38 |

**Supplementary material 3**

Visualization of the real-time qRT-PCR products demonstrates selectivity of the *ZmXTH1* primer pair. After quantitation, PCR products from both maize varieties were run on agarose gels. One single DNA appeared exhibiting the molecular size that was predicted by *in-silico* analysis (expected size = 148 bp). Numbers 1-3, biological replicates of the real-time qRT-PCR amplifications of Lector and SR03. 0.4 µg of ethidium bromide per mL gel.

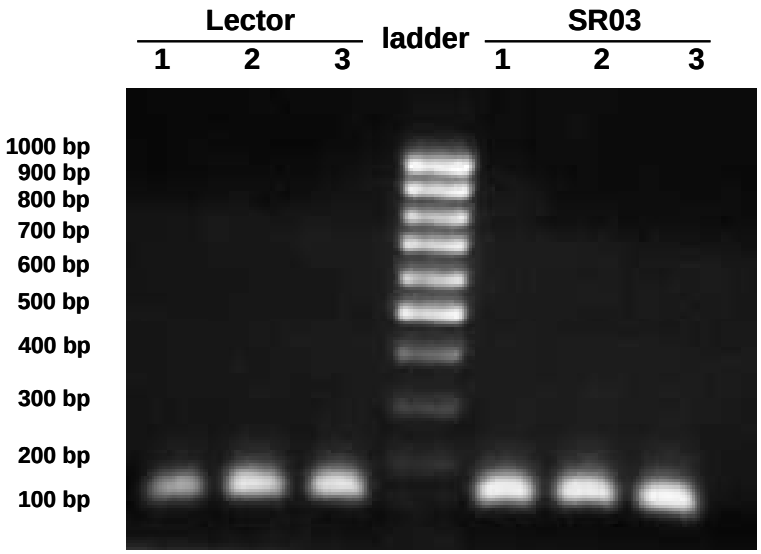

**Suppelemtary material 4**

Fluorescence image of the adaxial face an expanding leaf. Leaf apoplast was labelled with $H^+$-sensitive Oregon Green 488. The dye was excited at 495 nm (pseudo-green) and at 440 nm (pseudo-red) and fluorescence was collected at 535/25 nm-emission. Image represents an overlay of the ex 495 nm and the ex 440 nm images. The spatial resolution allows for discriminating the pH within three different compartments, viz., in the stomatal cavity, the epidermal apoplast and the palisade apoplast: (1) epidermal apoplast, (2-3) palisade apoplast, (4) stomatal cavity. (5) Areas that are not loaded with the dye do not exhibit background fluorescence (i.e. arising from cell wall, chloroplasts, or shot noise associated with image sampling). (6) adaxial epidermis cell, (7) stomatal apparatus, (8) palisade cell, (9) leaf hair.

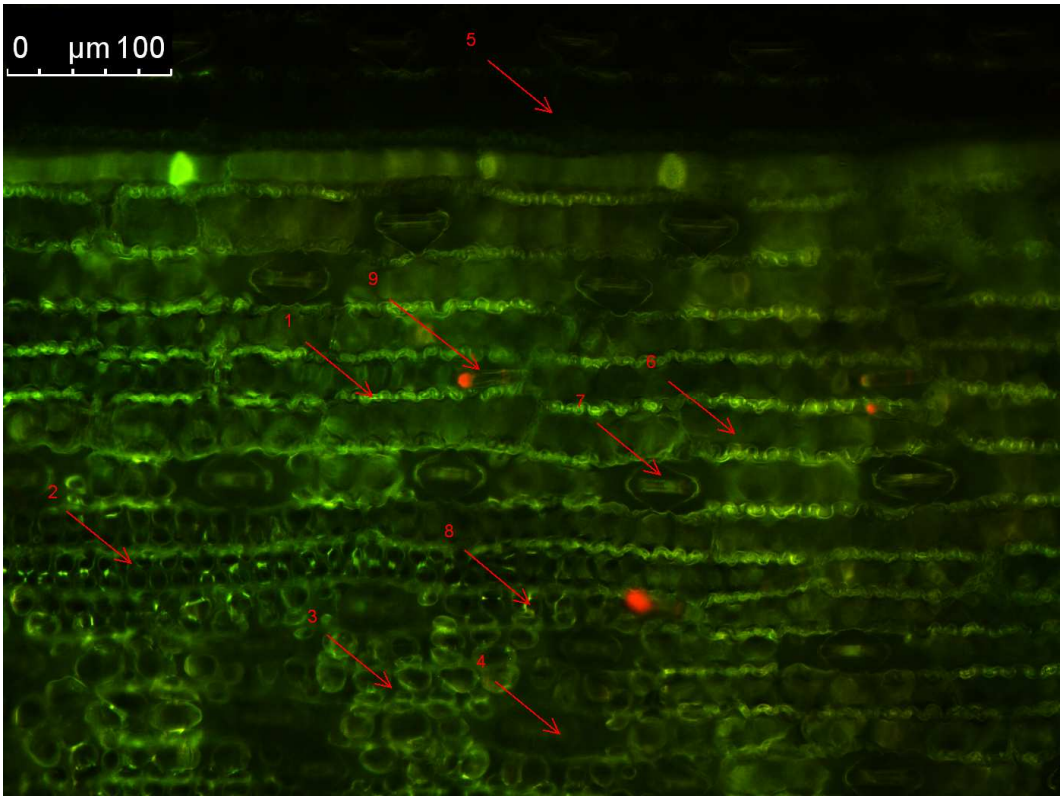

**Supplementary material 5**

In situ apoplastic pH calibration curve for Oregon Green 488 dextran fluorescence excitation ratio R(495ex/440ex; 525em). The Boltzmann fit was chosen for fitting sigmoidal curves to *in situ* calibration ratio data. Fitting resulted in an optimal dynamic range for pH measurements between 3.2 and 6.6 (corresponds to the ratios 0.95 and 2.15). *In situ* calibration was conducted on 4 different plants (n =4 biological replicates), each biological replicate was technically replicated in triplicate (n = 3 technical replicates.

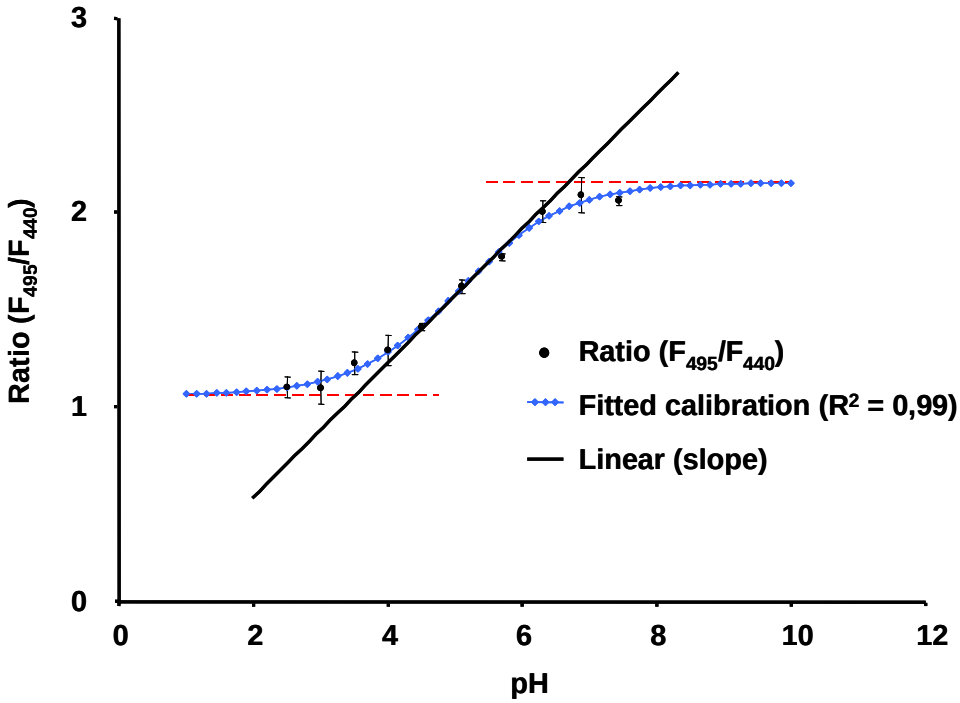

# Chapter 8

# General discussion

# 8. General discussion

An understanding of the growth responses of maize shoots to salinity is of great importance for a better understanding of plant resistance and for the eventual screening and smart breeding of stress-adapted crop plants.

This thesis was designed in order to identify and to characterize mechanisms involved in the growth responses of the shoots under saline conditions. For this purpose, shoot growth and shoot growth-related factors were compared between the salt-sensitive maize hybrid Lector and the highly salt-resistant hybrid SR03 (Schubert et al., 2009) under saline conditions. Such a comparative study of plants belonging to the same species but contrasting in their degree of salt resistance was undertaken because it might reveal contrasting features of physiological functions that may bear a causal relation to the differential response of the plants to salt (Epstein et al., 1980).

## 8.1 Salinity differentially affects shoot growth in resistant and sensitive maize hybrids

All measurements were based on expanding leaves (*Zea mays* L.) grown entirely under the influence of an 8-day 100 mM NaCl treatment. The tissue adequately revealed the effect of an 8-day salt treatment on growth-related processes. In order to avoid osmotic shock reactions, the plants were gently adapted to the full-strength treatment by stepwise increments in the NaCl concentration in the nutrient solution every 2$^{nd}$ day.

In the salt-sensitive hybrid Lector, the presence of 100 mM NaCl at the roots over a period of 8 days caused a significant biomass reduction of the growing shoots (chapter 2, fig. 1; chapter 7, fig 1C). This salinity-induced biomass depletion was attributable to a significant decrease in leaf area (chapter 7, fig 1B) and leaf thickness (chapter 7, fig. 2) and is generally known to occur in the first phase of salt stress, which is dominated by osmotic stress rather than sodium

toxicity (Sümer et al., 2004; Munns and Tester, 2008). Since (i) salinity inhibits the growth of young leaves via an inhibition of cell division and cell elongation (Mühling and Läuchli, 2002; Munns and Tester, 2008) and (ii) maize is considered to be a salt-sensitive plant (Maas et al., 1983), it is remarkable that, under saline conditions, the highly salt-resistant hybrid SR03 solely exhibits a minor reduction of the shoot biomass (chapter 2, fig. 1; chapter 7, fig 1C) and leaf growth (chapter 7, fig 1A). SR03 maize hybrids were originally developed and characterized as being highly salt-resistant showing nearly no harvest deficits under 10 dS $m^{-1}$ soil salinity (Schubert et al., 2009), whereas a soil conductivity of 6 dS $m^{-1}$ usually leads to a 50% reduced harvest of almost all recent maize hybrids (Doorenbos and Kassam, 1976). Thus, when compared with the salt-sensitive hybrid Lector, the unique highly salt-resistant maize hybrid SR03 provides an excellent tool for elucidating shoot growth-related differences possibly related to salt resistance.

## 8.2 Genotype-specific transcript expression of wall-loosening factors

Salinity has been described to inhibit the growth of young leaves via an inhibition of cell division and cell elongation (Munns and Tester, 2008). A modified capacity of cell walls to yield irreversibly has been suggested as the major growth-limiting factor contributing to the growth inhibition seen under salt stress (Cramer and Bowman, 1991). In accordance with this, extensometer-based measurements have revealed a decrease in wall extensibility to occur within both genotypes under conditions of salinity (chapter 3, tab. 2). However, the decrease in wall extensibility is more pronounced in size-reduced leaves of the salt-sensitive hybrid Lector compared with leaves of the salt-resistant SR03 that maintained growth. This implies that the physiological differences that contribute to the genotypic differences in the degree of the shoot growth depletion under salinity are possibly related to factors that alter the rheological properties of the wall.

In order to test this hypothesis, it was examined whether genotypic differences in leaf growth appear together with genotypic differences in transcript expression patterns of wall-loosening factors. For this, the transcript abundance of some wall-loosening factors was studied on the basis of purified poly(A)$^+$ RNA by using real-time quantitative reverse transcriptase-PCR (real-time qRT-PCR).

The xyloglucan endotranshydrolases (XTH) is an enzyme known to act as a wall-loosening factor. As summarized by Vissenberg et al. (2005), XTH can function in a transglucosylase (XET) mode, thereby cleaving and rejoining xyloglucan chains. This property makes XTH one of the most obvious candidates for wall loosening. In view of this, a genotype-specific effect of the 8-day 100 mM NaCl treatment on the *ZmXTH1* (chapter 7, fig 4) and *ZmXET1* (chapter 3, fig 2a) transcript abundance was demonstrated. Within the salt-affected and size-reduced shoots of the salt-sensitive hybrid Lector, a decrease in *ZmXTH1*and *ZmXET1* mRNA abundance was measured. This decrease possible contributed to the lower abundance of the corresponding enzyme within the cell wall of salt-stressed plants. In contrast, an increase of *ZmXTH1*and *ZmXET1* mRNA was detected in the salt-resistant SR03. This was indicative of a higher abundance of this protein in the shoots of the salt-resistant SR03 hybrids that maintained their growth under salinity. As Vissenberg et al. (2005) have described that ZmXTH facilitates the creep of cellulose microfibrils, the present results suggest that a higher XTH abundance (chapter 7, fig 4) improves wall extensibility in the salt-resistant hybrid SR03 under salt stress. This assumption is supported by the findings that XET activity is correlated positively with an increasing growth rate (Nishitani and Tominaga, 1992; Fry et al., 1992).

Expansin proteins are one of the best characterized cell-wall-loosening agents (Sella Kapu and Cosgrove, 2010) and are thought to intercalate within carbohydrate matrices in the cell wall, leading to the transient loosening of non-covalent interactions, and thus enhance the ability of these matrices to move relative to each other (Cosgrove, 2005). The transcript

abundance of the expansin isoforms *ZmEXPA1* (chapter 3, fig. 3a), *ZmEXPB2*, *ZmEXPB6*, and *ZmEXPB8* (chapter 2, fig. 3) appeared to be influenced in the same manner as demonstrated for *ZmXTH1* and *ZmXET1* under stress, viz. down-regulated in the salt-sensitive Lector but up-regulated in the salt-resistant SR03. In the salt-sensitive Lector, the down-regulation was correlated positively with a reduced shoot growth and reduced wall extensibility under stress. In contrast, the transcripts of the growth-mediating expansins *ZmEXPA1, ZmEXPB2, ZmEXPB6,* and *ZmEXPB8* were up-regulated in shoots of the salt-resistant SR03 that maintained shoot growth under saline conditions.

Hence, the transcripts of the wall-loosening factors *ZmXTH1* and *ZmXET1* and the transcripts of the growth-mediating expansin isoforms *ZmEXPA1, ZmEXPB2, ZmEXPB6,* and *ZmEXPB8* were differentially regulated in two maize hybrids contrasting in their degree of salt resistance. This genotype-specific transcript regulation is indicative of a role for these growth-mediating agents in processes that are related to salt resistance and thus to the maintenance of growth.

In contrast, the transcripts of the β-expansin isoform, viz. *ZmEXPB3, ZmEXPB5* and *ZmEXPB7* (chapter 2, fig. 3), the α-expansin isoforms *ZmEXPA3* and *ZmEXPA4* (chapter 3, fig. 3a) and the endoglucanase transcripts (chapter 3, fig. 2b) were equally regulated in both genotypes under stress. Thus, these wall-loosening agents are suggested not to contribute to the genotypic differences in terms of wall extensibility and shoot growth.

## 8.3 Genotype-specific protein abundance of β-expansins

The mRNA abundance as measured above is indicative of the abundance of the corresponding protein. However, discordance between mRNA and protein abundance attributable to diverse post-transcriptional regulatory processes is also known to occur (Waters et al., 2006; Scantland et al., 2011). For this reason, a test was undertaken to determine whether the above-

described genotype-specific regulation of the expansin transcript abundance also occurred at the level of the proteome. This is of importance, because it is not the expansin mRNA but the expansin protein that us the active molecule in terms of mediating wall-loosening.

Since β-expansins are more numerous and more abundantly expressed in maize tissue as compared to α-expansins (Wu et al., 2001), the abundance of vegetatively expressed β-expansin proteins was investigated in this study. This was achieved by using the technique of one-dimensional Western blotting (1D Western blotting) in combination with an anti-peptide antibody that labels β-expansins. This antibody does not specifically recognize single isoforms but labels a conserved amino acid region shared by all vegetatively expressed β-expansin isoforms. Therefore, by this 1D Western blotting approach, all β-expansins isoforms are marked as a composite signal.

The 1D Western blot confirmed that β-expansins were differentially affected in both genotypes under stress. (chapter 2, fig. 2B). In the shoots of salt-resistant SR03 maize, the β-expansin protein abundance was not affected by an 8-day 100 mM NaCl treatment. Since expansins are cell-wall-loosening agents that are thought to regulate cell wall enlargement in growing cells (Cosgrove, 2005), this unaffected abundance of vegetatively expressed growth-mediating β-expansin might be causally related to the maintenance of shoot growth in salt-resistant SR03 maize. Possibly, the β-expansin proteins remain to act as a wall-softening factor in the leaves of the salt-resistant SR03 maize under salinity. In contrast, the composite β-expansin protein abundance is down-regulated in size-reduced shoots of salt-sensitive Lector in response to the NaCl treatment (chapter 2, fig. 2B). This indicates that the growth depletion in Lector might be at least partially attributable to a quantitative reduction of the growth-mediating β-expansin. Possibly, growth in the shoots of the salt-sensitive Lector can only be mediated to a lower extent under saline conditions.

## 8.4 Improving the reliability of quantifiable 2D-Western blots

To test which particular protein isoform(s) accounted for the decrease of the composite β-expansin protein abundance in the size-reduced shoots of the salt-sensitive Lector (chapter 2, fig. 2B), a two-dimensional Western blotting (2D Western blot) procedure was performed.

However, this 2D-Western blot analysis was impaired by the bad reproducibility within the replicates. Such problems can arise because each electrophoresis and the subsequent immunoblotting cycle that is run for each replicate is performed under slightly different conditions. This is attributable to differences in, for example, the time of protein transfer onto the membrane, the strength of contact between the gel and membrane, the quality and dilution of antibodies or the detection of the signal (Aksamitiene et al., 2007). To achieve better reproducibility, the traditional 2D Western blotting procedure needed to be modified as described in chapter 4. Briefly, in the modified procedure, all biological replicates that belonged to an identical treatment were together two-dimensionally separated lying side by side on the same SDS gel (chapter 4, fig. 1A). If, for example, two treatments needed to be compared, two SDS gels were necessarily run. In a subsequent step, the proteins of the different treatments were electroblotted together onto the same blotting membrane. For this, the proteins from both SDS gels were cropped (indicated in chapter 4, fig. 2A) and positioned side by side onto the identical blotting membrane. After electrotransfer, the proteins were then incubated with the antibody and this was followed by the immunodetection. The reliability of this modified procedure was compared with that of the traditional 2D blotting procedure. For this traditional procedure, all biological replicates were each separated onto a different SDS gel (chapter 4, fig. 1B).

As a result, the improved 2D Western blotting procedure produced a more reliable spot pattern (chapter 4, fig. 4) and decreased the standard deviations (chapter 4, fig. 5) and the variation (chapter 4, tab. 1) of the data. This is probably because problems associated with

SDS gel heterogeneity have no effect in the modified procedure, because all replicates of one treatment are separated on an identical gel. Moreover, this modified procedure not only saves labour-costs (time), but also 2D-PAGE and immunoblotting reagents and costly antibodies.

## 8.5 One β-expansin protein isoform is less abundant in size-reduced leaves of the salt-sensitive hybrid

In control-treated plants of the salt-sensitive hybrid Lector, the improved 2D Western blot (chapter 4) revealed the presence of four vegetatively expressed β-expansin isoforms in expanding shoots (chapter 7, fig. 5A). However, under conditions of the 8-day 100 mM NaCl-treatment, one isoform was down-regulated (chapter 7, arrow in fig. 5A). The absence of this particular isoform possibly explains the decrease in the composite β-expansin protein abundance as demonstrated by the 1D Western blot (chapter 2, fig. 2B). *In-silico* analysis based on the molecular weight and the isoelectric point suggests that the isoform that is down-regulated in size-reduced leaves of the salt-affected hybrid Lector is one of the β-expansin ZmEXPB4, ZmEXPB6 or ZmEXPB8 (chapter 7, compare with tab. 1). Interestingly, the real-time qRT-PCR analysis confirmed that the mRNA of the isoforms *ZmEXPB6* and *ZmEXPB8* was down-regulated in salt-sensitive Lector under salinity (chapter 2, fig. 3). This in turn strengthens the idea that one of either ZmEXPB6 or ZmEXPB8 is down-regulated in response to salinity. The down-regulation of that particular β-expansin isoform might be in a causal relationship to the salinity-induced growth reduction in the salt-sensitive Lector. Growth is possibly reduced under saline conditions because the salinity at the roots somehow impairs the synthesis of this growth-mediating protein in size-reduced leaves of the salt-sensitive Lector.

## 8.6 Development of a method for *in planta* imaging of leaf apoplastic pH

In addition to growth-mediating molecules, apoplastic pH plays an important role in conferring cell wall loosening and growth (McQueen-Mason et al., 1993). For this reason, it is of interest to know whether genotypic differences in the apoplastic pH exist between hybrids that contrast in their degree of salt resistance. In this study, microscopy-based ratio imaging was used for the quantification of apoplastic pH in leaves of intact plants. However, ratiometric *in planta* analysis of the apoplastic pH are not straightforward. This is attributable to problems associated with gaining access to the intact leaf apoplast (Fricker et al., 1994). The major difficulty here is the development of loading protocols to insert the fluorescent ion indicator into the apoplast of a living plant. The traditional dye loading procedures, such as the transpiration-driven loading technique via the petiole or the pressure loading technique, do not allow the monitoring of ion concentrations in intact plants. In both cases, such monitoring is not possible because the leaves are detached from the plant. However, one aim of the present work was the measurement of apoplastic pH in the leaves of intact maize plants. For this reason, a new dye loading procedure was developed that allowed the ion indicator to be gently fed into the leaf apoplast of an intact plant without detachment of the leaf or the destruction of the cell membranes (chapter 5, figs. 1-3 and supplemental material 1). The development of this method was conducted on *Vicia faba* L., which is classified as being moderately salt-sensitive (Läuchli, 1984) and which is a model species that is frequently used in combination with microscopy-based studies. The new approach has been demonstrated to be suitable for the *in planta* visualization of leaf apoplastic pH dynamics in response to exogenously added NaCl to the roots or to the leaves (chapter 5, figs. 5 and 4). Moreover, the high spatial resolution of the camera-assisted imaging allowed the pH to be discriminated within three different apoplastic compartments within the leaf, viz. in the stomatal cavity, the

epidermal apoplast and the apoplast built by the palisade tissue (chapter 5, figs. 4A and 5A). With this improved technique, the salt-sensitive *Vicia faba* L. (not adapted to salt) could be demonstrated to show a transiently increased leaf apoplastic pH over a period of circa 1 h immediately after NaCl was added into the nutrient solution (chapter 6, fig. 3). The magnitude of this increase proved to depend on the intensity of the NaCl stress treatment (chapter 6, figs. 5 and 6). The transient nature of the observed pH increase and the finding that the pH response is triggered at the root site and is detectable in distant leaves are indicative for a role in the systemic signalling of the stress event. Such an interpretation of the function of the above-described pH dynamics agrees with that of Felle et al. (2008) who describe transient apoplastic alkalinizations that are similar in shape and magnitude and are thought to be a pH signal.

Hence, the suitability of this sophisticated dye loading approach was demonstrated for ratiometric quantification and visualization of the leaf apoplastic pH in living plants. This new tool allowed tests to be carried out for the detection of genotypic differences in the leaf apoplastic pH between the two maize cultivars that differ in salt-resistance.

## 8.7 Apoplastic pH appears to be involved in the genotype-specific growth reduction

Expansin proteins have an acidic pH optimum (Cosgrove, 2000). This observation gains in importance because, according to the acid growth theory, an auxin-mediated acidification of the leaf apoplast is the major requirement for increasing wall extensibility (Hager et al., 1971). The pH of the apoplast of growing cells is typically in a range in which acidification activates expansin activity (Cosgrove, 2005). The more sophisticated dye loading procedure (chapters 5) was used to quantify the leaf apoplastic pH in order to identify genotypic differences between the sensitive and the resistant maize hybrid. This was conducted so that

insights could be gained regarding the possible role of the apoplastic pH within processes related to leaf growth inhibition under salt stress. A leaf apoplastic acidification was demonstrated for the salt-resistant SR03 under salinity (chapter 7, fig. 8B, E, F): This low pH might be attributable to the fact that the transcript abundance of the plasma membrane proton pump (PM-$H^+$-ATPase) increased in response to salinity (chapter 3, fig. 3b). This is indicative for a higher abundance of the PM-$H^+$-ATPase. Under saline conditions, the $H^+$-pump possibly acidifies the leaf apoplast of the salt resistant hybrid SR03 by pumping protons from the cytosol into the apoplast. Taking into account that (i) enhanced growth rates are associated with increasing apoplastic acidification of maize leaves (Van Volkenburgh and Boyer, 1985), that (ii) a decreased cell wall pH is generally thought to promote the wall-loosening events necessary for growing cell enlargement (Rayle and Cleland, 1992) and that (iii) expansins exhibit reduced activity at the more alkaline pH (McQueen-Mason, 1995), this apoplastic acidification (chapter 7, fig. 8B, E, F) might provide one mechanism by which salt-resistant SR03 maize counteracts a growth reduction under salinity. In favour of this hypothesis, the apoplastic pH did not acidify in leaves of the salt-sensitive Lector in response to the 8-day 100 mM NaCl treatment (chapter 7, fig. 8A, C, D). These leaves exhibited a stronger reduction in the wall extensibility (chapter 3, tab. 2) and growth (chapter 3, fig. 1) as compared with leaves of the salt-resistant hybrid SR03 that acidified under salinity and maintained growth.

## References

Aksamitiene, E., Hoek, J.B., Kholodenko, B., Kiyatkin, A. (2007) Multistrip Western blotting to increase quantitative data output. *Electrophoresis.* 28(18), 3163-3173.

Cosgrove, D.J. (2000) Loosening of plant cell walls by expansins. *Nature.* 407, 321-326.

Cosgrove, D.J. (2005) Growth of the plant cell wall. *Nat Rev Mol Cell Biol*. 6, 850-861.

Cramer, G.R., Bowman, D.C. (1991) Kinetics of maize leaf elongation. I: Increased yield threshold limits short-term, steady-state elongation rates after exposure to salinity. *J Exp Bot.* 42, 1417-1426.

Doorenbos, J., Kassam, A.H. (1976) Yield response to water. In: *FAO irrigation and drainage paper*. Ed. FAO. p. 160. FAO, Rome.

Epstein, E., Norlyn, J.D., Rush, D.W., Kingsbury, R.W., Kelley, D.B., Cunningham, G.A., Wrona, A.F. (1980) Saline culture of crops: a genetic approach. *Science*. 210, 399-404.

Felle, H.H., Herrmann, S., Schäfer, P., Hückelhoven, R., Kogel, K.H. (2008) Interactive signal transfer between host and pathogen during successful infection of barley leaves by *Blumeria graminis* and *Bipolaris sorokiniana*. *J Plant Physiol.* 165, 52-59.

Fricker, M.D., Tlalka, M., Ermantraut, J., Obermeyer, G., Dewey, M., Gurr, S., Patrick, J., and White, N.S. (1994) Confocal fluorescence ratio imaging of ion activities in plant cells. *Scanning Microsc*. 8, 391-405.

Fry, S.C., Smith, R.C., Renwick, K.F., Martin, D.J., Hodge, S.K., Matthews, K.J. (1992) Xyloglucan-endotransglycosylase, a new wall-loosening enzyme activity from plants. *Biochem J.* 282, 821-828.

Hager, A., Menzel, H., Krauss, A. (1971) Versuche und Hypothese zur Primärwirkung des Auxins beim Streckungswachstum. *Planta*. 100, 47-75.

Läuchli, A. (1984) Salt exclusion: An adaptation of legumes for crops and pastures under saline conditions. In: *Salinity tolerance in plants - strategies for crop improvement*. Ed. RC Staple and GH Toenniessen. p. 171-188. Wiley and Sons, New York.

Maas, E.V., Hoffman, G.J., Chaba, G.D., Poss, J.A., Shannon, M.C. (1983) Salt sensitivity of corn at various growth stages. *Irr Sci*. 4, 45-57.

McQueen-Mason, S.J., Fry, S.C., Durachko, D.M., Cosgrove, D.J. (1993) The relationship between xyloglucan endotransglycosylase and in vitro cell wall extension in cucumber hypocotyls. *Planta.* 190, 327-331.

McQueen-Mason, S. (1995) Expansins and cell wall expansion. *J Exp Bot*. 46, 1639-1650.

Munns, R., Tester, M. (2008) Mechanism of salinity tolerance. *Annu Rev Plant Biol.* 59, 651-681.

Mühling, K.H., Plieth, C., Hansen, U.P., Sattelmacher, B. (1995) Apoplastic pH of intact leaves of *Vicia faba* as influenced by light. *J Exp Bot*. 46, 377-382.

Mühling, K.H., Läuchli, A. (2002) Effect of salt stress on growth and cation compartmentation in leaves of two plant species differing in salt tolerance. *J Plant Physiol.* 159, 137-146.

Nishitani, K., Tominaga, R. (1992) Endo-xyloglucan transferase, a novel class of glycosyltransferase that catalyzes transfer of a segment of xyloglucan molecule to another xyloglucan molecule. *J Biol Chem*. 267, 21058-21064.

Rayle, D.L., Cleland, R.E. (1992) The acid growth theory of auxin-induced cell elongation is alive and well. *Plant Physiol*. 99, 1271-1274.

Scantland, S., Grenon, J.P., Desrochers, M.H., Sirard, M.A., Khandjian, E.W., Robert, C. (2011) Method to isolate polyribosomal mRNA from scarce samples such as mammalian oocytes and early embryos. *BMC Dev Biol.* 11, 8.

Schubert, S., Neubert, A., Schierholt, A., Sümer, A. and Zörb, C. (2009) Development of salt resistant maize hybrids: the combination of physiological strategies using conventional breeding methods. *Plant Sci*. 177, 196-202.

Sella Kapu, N.U., Cosgrove, D.J. (2010) Changes in growth and cell wall extensibility of maize silks following pollination. *J Exp Bot.* 61, 4097-4107.

Sümer, A., Zörb, C., Yan, F., Schubert, S. (2004) Evidence of $Na^+$ toxicity for the vegetative growth of maize (*Zea mays* L.) during the first phase of salt stress. *J Appl Bot Food Qual*. 78, 135-139.

Van Volkenburgh, E., Boyer, J.S. (1985) Inhibitory effects of water deficit on maize leaf elongation. *Plant Physiol*. 77, 190-194.

Vissenberg, K., Fry, S.C., Pauly, M., Hofte, H., Verbelen, J.P. (2005) XTH acts at the microfibril-matrix interface during cell elongation. *J Exp Bot*. 56, 673-683.

Waters, K.M., Pounds, J.G., Thrall, B.D. (2006) Data merging for integrated microarray and proteomic analysis. *Brief Funct Genomic Proteomic.* 5(4), 261-72.

Wu,Y., Meeley, R.B., Cosgrove, D.J. (2001) Analysis and expression of the α-expansin and β-expansin gene families in maize. *Plant Physiol*. 126, 222-232.

# 9. Conclusion

Soil salinity poses a major threat to agriculture, since most crop plants will not grow in high concentrations of salt. During the osmotic stress phase, salt-sensitive crops such as maize (*Zea mays* L.) exhibit a strong and rapid growth reduction, mainly attributable to a decline in cell division and elongation. A modified capacity of cell walls to yield irreversibly has been suggested to be the major growth-limiting factor during the salinity-induced osmotic stress phase.

Elucidation of the way that salinity affects shoot growth is thus of great importance for a better understanding of processes that contribute to salt resistance. For this purpose, shoot growth and shoot growth-related factors have been compared between a salt-sensitive and a salt-resistant maize hybrid under saline condition. Such a comparative study of plants contrasting in their degree of salt resistance can reveal different features of physiological functions that might bear a causal relationship to the differential response of the plants to salt.

The treatment of maize plants that differ in their degree of salt-resistance to 100 mM NaCl over a period of 8–days has revealed genotype-specific differences regarding the ability of the young shoots to maintain growth. The salt-sensitive hybrid Lector exhibited a strong reduction in growth and biomass accumulation, as is known to occur in the first phase of salt stress. In contrast, the shoots of the salt-resistant hybrid SR03 were only marginally affected and maintained growth. The finding that, under saline conditions, the mRNA abundance of wall-loosening agents such as *ZmXTH1*, *ZmXET1*, *ZmEXPA1*, *ZmEXPB2*, *ZmEXPB6*, and *ZmEXPB8* was differentially regulated within both maize hybrids, viz. down-regulated in size-reduced shoots of the salt-sensitive Lector but up-regulated in shoots of salt-resistant SR03 that maintained growth under NaCl stress, is indicative of a role for these wall-

loosening agents in processes related to salt-resistance. The up-regulation of these wall-loosening factors within the expanding shoots of the salt-resistant hybrid SR03 might contribute to a mechanism for improving wall extensibility under stress and thus might counteract growth reduction as occurs, for example, in the salt-sensitive hybrid. In favour of this assumption, transcripts of the wall-loosening factors are down-regulated in the salt-sensitive Lector hybrid.

Genotypic-specific effects of the salt treatment on β-expansin mRNA were also confirmed to occur on the level of the proteome: salinity did not affect the abundance of the vegetatively expressed β-expansins in the shoots of the salt-resistant SR03. However, β-expansin proteins were down-regulated in size-reduced shoots of the salt-sensitive cultivar Lector. 2D-Western blotting revealed that one out of four isoform was down-regulated in size-reduced leaves of the salt-sensitive Lector. The finding that growth-mediating β-expansins were down-regulated in size-reduced leaves of the salt-sensitive maize but were not affected in leaves of the salt-resistant SR03 maize that maintained growth is indicative of a role for the β-expansins in maintaining growth and thus of their contribution to salt resistance. In the salt-sensitive Lector, growth might be reduced because salt stress possibly impairs the synthesis of this growth-mediating enzyme in expanding leaves.

After salt treatment, the apoplastic pH seemed to be differentially regulated between both hybrids. The leaf apoplast of the salt-resistant SR03 was acidified in response to salinity. The findings that (i) acidification of the leaf apoplast is a major requirement for increasing wall extensibility and that (ii) expansins are activated by an acidic pH, are both indicative that the observed acidification represents a mechanism possibly related to the maintenance of growth under saline conditions. In favour of this hypothesis, the leaf apoplast of the salt-sensitive Lector does not acidify but exhibits a strong reduction in its shoot growth.

A comparative study of plants that differ in their degree of salt resistance revealed contrasting physiological features in terms of cell wall-associated agents that mediate growth. Wall-loosening agents were impaired in size-reduced leaves of the salt-sensitive hybrid but not in leaves of the salt-resistant hybrid that maintained growth. This physiological difference is indicative for a role of these wall-loosening agents for salt-resistance and thus may be used for screening for salt-resistant plants.

# 10. Zusammenfassung

Bodensalinität stellt eine bedeutende Bedrohung für die Produktion landwirtschaftlicher Nutzpflanzen dar. Salzsensitive Pflanzen, wie Mais, reagieren mit einer ausgeprägten und schnell auftretenden Wachstumsreduktion auf das Salz, was hauptsächlich auf einen Rückgang in der Zellteilungsrate und Zellausdehnung zurückzuführen ist. Es wird vermutet, dass die Fähigkeit der Zelle sich während der osmotischen Stressphase irreversibel auszudehnen, beeinträchtig ist.

Für ein besseres Verständnis der Prozesse die zu Salzresistenz beitragen, ist es von großer Bedeutung aufzuklären, wie Salinität das Blattwachstum genau beeinflusst. Um dies zu erreichen, wurden das Blattwachstum sowie daran beteiligte Prozesse sowohl bei einem salzsensitiven als auch bei einem salzresistenten Maishybriden untersucht. Eine solche Vergleichsstudie mit Pflanzen, die sich im Ausmaß ihrer Salzresistenz unterscheiden, kann dazu beitragen, unterschiedliche physiologische Funktionen aufzudecken, die zu einer Salresistenz beitragen.

Die Behandlung der Maispflanzen mit 100 mM NaCl über einen Zeitraum von 8-Tagen deckte genotypische Unterschiede in Bezug auf die Aufrechterhaltung des Wachstums des jungen Sprosses auf. Der salzsensitive Hybrid Lector reagierte mit einer stark ausgeprägten Reduktion des Wachstums und der Biomassenbildung auf das Salz in der Nährlösung. Im Gegensatz hierzu war das Wachstum des salzresistenten SR03 Hybriden nur geringfügig beeinträchtigt. Vergleicht man die mRNA Abundanz von einigen zellwandauflockernden Substanzen, wie zum Beispiel *ZmXTH1*, *ZmXET1*, *ZmEXPA1*, *ZmEXPB2*, *ZmEXPB6* und *ZmEXPB8*, wird deutlich, dass die Abundanz der Transkripte zwischen beiden Hybriden durch die Salzbehandlung unterschiedlich beeinflusst wurde: In den Blättern von Lector lagen

die Transkripte geringer abundant vor, wohingegen die Transkripte in den Blättern von SR03, die das Wachstum beibehielten, hochreguliert wurden. Die Hochregulierung dieser wachstumsvermittelnden Faktoren in den expandierenden Blättern von SR03 trägt möglicherweise zu einem Mechanismus bei, der die Zellwandextensibilität unter Salinität verbessert und auf diese Weise einer Wachstumsreduktion, wie sie bei dem salzsensitivem Lector aufgetreten ist, entgegenwirkt. Für diese Annahme spricht, dass die Transkripte dieser wachstumsvermittelnden Faktoren in den wachstumsgehemmten Blättern von Lector geringer abundant vorliegen.

Genotypisch-spezifische Effekte der Salzbehandlung, wie sie für die β-Expansin Transkripte gezeigt wurden, konnten ebenfalls auf der Proteinebene gezeigt werden. Die Salzbehandlung hatte keinen Einfluss auf die Abundanz der β-Expansin in den wachsenden Blättern des resistenten SR03 Hybriden. Im Gegensatz hierzu erwiesen sich die β-Expansinproteine als geringer abundant in den Blättern der sensitiven Sorte. Mittels eines 2D-Western Blots konnte gezeigt werden, dass eine von vier Isoformen runterreguliert wurde. Die Tatsache, dass die wachstumsvermittelnden β-Expansinproteine in Blättern des salzsensitiven Hybriden, die ein vermindertes Wachstum zeigen, runterreguliert wurden, aber im Gegensatz hierzu, in den wachsenden Blättern des resistenten Hybriden nicht beeinflusst wurden, deutet auf eine Rolle der β-Expansine für die Beibehaltung des Wachstums und somit auf eine Rolle hinsichtlich einer Salzresistenz hin. Möglicherweise ist das Blattwachstum in dem salzsensitiven Lector verringert, weil Salinität die Synthese dieser wachstumsvermittelnden Enyzme in expandierenden Blättern beeinträchtigt.

Infolge der Salzbehandlung erwies sich der pH im Blattapoplasten beider Hybriden als unterschiedlich. Der Apoplast des salzresistenten Hybriden SR03 acidifizierte. Die Tatsachen, das (i) eine apoplastische Ansäuerung eine wichtige Voraussetzung für die Erhöhung der

Zellwandextensibilität darstellt und dass (ii) Expansine durch einen sauren pH aktiviert werden, deuten darauf hin, dass die beobachtete Ansäuerung einen Mechanismus darstellt, der möglicherweise zur Aufrechterhaltung des Wachstums des resistenten Hybriden unter salinen Bedingungen beiträgt. Zu Gunsten dieser Hypothese wurde gezeigt, dass der Blattapoplast des salzsensitiven Lector, dessen Blätter eine signifikante Wachstumsreduktion zeigen, nicht ansäuerte.

Eine vergleichende Untersuchung von Pflanzen die sich in ihrem Grad der Salzresistenz unterscheiden, zeigte gegensätzliche physiologische Merkmale hinsichtlich apoplastisch-lokalisierter, wachstumsvermittelnder Faktoren auf. Innerhalb der wachstumsgehemmten Blätter der sensitiven Sorte erwiesen sich einige zellwandauflockernde Faktoren infolge der Salzbehandlung als beeinträchtigt, wohingegen dies in den wachsenden Blättern des resistenten Hybriden nicht der Fall war. Dieser physiologische Unterschied deutet auf eine Rolle dieser zellwandauflockernden Faktoren hinsichtlich einer Salzresistenz hin und könnte zum Screening von salzresistenten Pflanzen verwendet werden.

# Danksagung

Mein Dank gilt meinem Doktorvater Herrn Prof. Dr. Karl Hermann Mühling der es ermöglicht hat, dass ich diese Arbeit durchführen konnte. Für jede Unterstützung während der Konzeption der Arbeit, der Erstellung der Manuskripte, der Dissertation und der Tagungsvorträge danke ich herzlich. Ich bin sehr dankbar für das entgegengebrachte Vertrauen, die stete Motivation sowie die Förderung.

Herrn PD Dr. Christian Zörb danke ich für die Einführung in verschiedene experimentelle Techniken die substantiell für die Entstehung dieser Arbeit waren. Ich danke auch für die Diskussionsbereitschaft, die vielen konzeptionellen Beiträge und die Hilfe während der Manuskripterstellung.

Indem Prof. Dr. Sven Schubert das SR03 Saatgut bereitgestellt hat, hat er wichtige Teile dieser Arbeit erst ermöglicht. Recht herzlichen Dank!

Herrn Prof. Dr. Dietrich Ober und Herrn PD Dr. Hartwig Lüthen danke ich für die Kooperation in diesem Projekt. Mir hat die Arbeit in diesem Team immer sehr viel Freude bereitet.

Ohne meine Doktorandengeschwister wäre die alltägliche Arbeit sicherlich etwas weniger bunt gewesen. Genauso wie Dorothee, verabschiedete sich leider auch das gemeinschaftliche Büro mit Fördeblick. Vielen Dank an Christina für die Hilfsbereitschaft und den Beitrag zu dieser Arbeit. Ich danke Mehmet, Shahzad, Jan-Reent, Nicole, Sajid und Marcus für die Atmosphäre!

Ohne die TAs und die Institutsverwaltung wären viele Teile dieser Arbeit nicht möglich gewesen. Einen besonderen Dank an Steffi thor Straten, Annegret Thiessen, Martina Bach und Anne Putbrese. Ich danke der gesamten Stammbesatzung für die freundliche Aufnahme im Kieler Institut. Ich habe mich in diesem Kreis der Kollegen immer sehr herzlich aufgenommen, betreut, beraten und unterstützt gefühlt. Herrn Dr. Reiner Krähmer dient mein Dank für die eine oder andere Lektion im Diskutieren. Auch Erwin Danklefsen war immer ein hilfsbereiter Kollege!

Christina Neuhaus und Tim Hansen danke ich für die tolle Laborarbeit und die Unterstützung beim Abrunden der Arbeit mit zusätzlichen Daten.

Der Friedrich-Ebert-Stiftung danke ich herzlich für die finanzielle und ideelle Förderung in dieser Zeit!

Meiner Schwester Marie Christine, meinen Eltern und meiner Freundin Theresa danke ich für die mannigfaltige Unterstützung. Ich bin Euch sehr dankbar!

Inka, Fairy und Finja danke ich für die vielen Spaziergänge und die stets kritische Diskussionsbereitschaft fachlich-komplexer, teils hoch-theoretischer Sachverhalte.

# Schriftenreihe des Instituts
## Neuere vorrätige Titel

**Band 69** **Wibke Markgraf (2006):** Microstructural changes in soils rheological investigations in soil mechanics. (//e-diss.uni-kiel.de/diss_1882)

**Band 70** **Dorota Agnieszka Dec (2006):** Thermal properties in Luvisols under conventional and conservation tillage treatment (//e-diss.uni-kiel.de/diss_1904)

**Band 71** **Emilia Jasinska (2006):** Management effects on carbon distribution in soil aggregates and its consequences on water repellency and mechanical strenght (//e-diss.uni-kiel.de/diss_1706)

**Band 72** **Rainer Horn, Heiner Fleige, Stephan Peth (2006):** Soils and Landuse Management Systems in Schleswig-Holstein (Germany) - Guide of ISTRO Excursion 2006

**Band 73** **Jürgen Lamp, Hans-Jürgen Hess und Götz Reimer (2007):** Technik- und Feldführer zur Veranstaltung „Präziser Landbau / Precision Farming im Dienst für Landwirtschaft und Umwelt

**Band 74** **Julia Krümmelbein: (2007):** Influence of various grazing intensities on soil stability and water balance of a steppe soil in Inner Mongolia, P.R. China

**Band 75** **Stephan Gebhardt (2007):** Wasserhaushalt und Funktionen der Böden im Grundwasserabsenkbereich des Wasserwerkes Wacken in Schleswig-Holstein

**Band 76** **Imke Janßen (2008):** Landnutzungsabhängige Dynamik hydraulischer und mechanischer Bodenstrukturfunktionen in Nassreisböden

**Band 77** **Ying Zhao (2008):** Grazing effects on hydraulic, thermal and mechanical soil properties at multiple scales – a case study in Inner Mongolia grassland

**Band 78** **Hans-Peter Blume & Rainer Horn (Hrsg.):** Persönlichkeiten der Bodenkunde I Vorträge der Arbeitsgruppe Geschichte der Bodenkunde im Rahmen der Jahrestagung der Deutschen Bodenkundlichen Gesellschaft im September 2007 in Dresden

**Band 79** **Britta Pitann (2008):** Einfluss der Plasmalemma-ATPase-Aktivität und des apoplastischen pH-Wertes auf das Blattwachstum und die Proteinexpression von salzempfindlichen und salzresistenten Maisgenotypen

**Band 80** **Peter Hartmann (2008):** Bodenphysikalische Eigenschaften, Benetzbarkeiten und Wasserhaushalt von Waldböden unter Flugascheeinfluss

**Band 81** **Kristine Bolte (2008):** Untersuchungen zur feuchteabhängigen Dynamik des bodenspezifischen Erosionswiderstandes bei Bewindung unter Windkanalbedingungen

**Band 82** **Limeng Zhang (2008):** Effect of nitrogen fertilizer on yield formation and nitrogen uptake of aerobic rice in North China

**Band 83** **Ruirui Chen (2009):** A study on apparent added nitrogen interactions and priming effects of soil organic matter using stable isotopes

**Band 84** **Alexander Zink (2009):** Bodenstabilität und Auswirkungen dynamischer Lasteinträge auf physikalische Eigenschaften von Ackerböden unter konservierender und konventioneller Bodenbearbeitung

**Band 85** **Hans-Peter Blume & Rainer Horn (Hrsg.):** Persönlichkeiten der Bodenkunde II Vorträge der Arbeitsgruppe Geschichte der Bodenkunde im Rahmen der Jahrestagung der Deutschen Bodenkundlichen Gesellschaft im September 2009 in Bonn

**Band 86** **Mehmet Senbayram (2010):** Greenhouse gas emission from soils of bioenergy crop production systems and regulating factors

**Band 87** **Nicole Fanselow (2010):** Soil nitrogen - plant interactions as affected by grazing and water availability in semiarid grassland of Inner Mongolia

**Band 88** **Dorothee Steinfurth (2010):** Storage protein quality, metabolite composition, and baking quality of winter wheat as affected by late sulfur fertilization

**Band 89** **Dörthe Holthusen (2010):** Fertilization induced changes in soil stability at the microscale revealed by rheometry

**Band 90** **Agnieszka Reszkowska (2010):** Grazing effects on soil mechanical strength and physical functions in Inner Mongolia, China